Stockholm University

Master Thesis

Degree Project in
Geology 30 hp

Episyenite along the Stockholm Bypass

Etienne Lindborg Bordenave

Stockholm 2021

Department of Geological Sciences
Stockholm University
SE-106 91 Stockholm

Episyenite along the Stockholm Bypass

Description of a drill core from south Lovön

Etienne Lindborg Bordenave

Abstract

Episyenite, a quartz-leached granitoid, has been encountered during tunnel excavation for the Stockholm Bypass. In drill core 19A373sk, drilled at Lovön, the core showed episyenite altered granitoids. The sections that have been altered are porous and depleted in quartz, have a strong red colour, and are in places soft and weathered. The porosity corresponds with the grain-size in the sections. The episyenite altered parts are mostly made up by k-feldspar and sericitisied plagioclase with minor biotite. Most of the biotite is black and shows exsolution of Fe-Ti oxides. Biotite is also broken down to a green-yellow coloured clay mineral. The vugs are formed by leaching of quartz and are now mostly filled with secondary minerals such as fine-grained red-stained albite, tooth-shaped k-feldspar and a mixture of clay minerals. Episyenite alteration is found in three different grain-size types: fine, medium, and coarse (pegmatitic). In fine grained samples quartz minerals are still present while in medium and coarse grained they are absent. All sections have high increased concentrations of K_2O+Na_2O especially the medium- and coarse- grained samples.

Keywords:

Episyenite, XRF, Thin Section, Core logging, SEM.

Mineral abbreviations

Mineral abbreviations used in this thesis are based on Whitney and Evans (2010).

Symbol	Mineral Name
Adl	adularia
Ab	albite
Afs	alkali feldspar
Aln	allanite
Bt	biotite
Chl	chlorite
Ep	epidote
Gth	goethite
Ms	muscovite
Opq	opaque mineral
Pl	plagioclase
Qz	quartz
Ser	sericite
Ttn	titanite
V	vug
Zrn	zircon

Contents

Introduction

The Stockholm Bypass project (Fig. 1) is a large infrastructural project developed to relieve the heavily trafficked Essingeleden. This is done by redirecting traffic that is not going into the city by connecting Akalla in the northern part to Kungenskurva in southern part of the city with the new motorway. The new traveling time is estimated to be 15 minutes. Of the 21-km new road that will be constructed, 18 of those km will be in tunnels. The new tunnels will pass Lovön, a small island in Mälaren, at about 60 m depth below surface. The work with the new main tunnels started here in the autumn of 2018. During the excavation of the tunnels zones of heavily altered bedrock were discovered. These altered zones contained a high porosity rock with low strength, significant enough to affect tunnel production. These rocks which are rich in alkali-feldspar and depleted in quartz are interpretated of have undergone episyenite alteration.

Episyenite

Episyenite is a hydrothermally altered granitic rock that has undergone dissolution and leaching of the primary quartz leaving the rock with a porous framework (Möller et al., 2003). These pores are usually referred to as vugs. When the rock has undergone episyenite alteration the magmatic texture is preserved and the new geochemical composition of the rock now resembles syenite hence the name episyenite (Petersson and Eliasson, 1997). The name has primary been used in Europe for describing these types of vuggy granitoids. The vugs in the rock have the corresponding shape and size of the absent quartz (Cathelineau, 1986). The episyenite rock is left with a porous feldspar-rich framework and the magmatic texture remains preserved if no further deformation occurs (Cathelineau, 1986) i.e., quartz leached in brittle conditions (Petersson et al., 2014). Episyenite alteration is commonly related to alkali metasomatism (sodium and or potassium (Suikkanen and Rämö, 2019). Two types of episyenite are commonly described in the literature; the deep red coloured e.g., from the Central Iberian Massif (Recio et al., 1997) and white coloured e.g., from Forsmark (Petersson et al., 2012).

Cathelineau (1986) grouped three types of episyenite alteration; type I, involves quartz leaching ± vug infill, type II, quartz leaching + albitization, and type III, quartz leaching + potassic alteration. In the first step leaching of the quartz is accompanied by alkali metasomatism (e.g., albitisation of primary plagioclase) in some cases followed by a second hydrothermal event where the vugs gets mineralised by secondary infill minerals. Common infill minerals are authigenic albite, adularia, phengite, chlorite, Fe-Ti oxides and carbonates (Cathelineau, 1986) and white mica, Illite, pyrite and quartz (Hecht et al., 1999). Some of the episyenite altered rocks are associated with mineral deposits. Most prominent uranium mineralisation such as those from the Variscan belt e.g., (Leroy and Cathelineau, 1982; Poty et al., 1986; Turpin et al., 1990; Dolníček et al., 2014; Eglinger et al., 2014). Other important mineralization types are Au (Jébrak, 1991), Sn-W-Mo (Cheilletz and Giuliani, 1982; López-Moro et al., 2019), Pb-Zn-Cu mineralisation (Recio 1997), and Rare Earth Elements deposits in New Mexico (McLemore, 2012).

Episyenite forms inside the host granites (sensu lato) e.g., (Cathelineau, 1986; Recio et al., 1997) or related to shear zones as “cloud-shape” bodies (Turpin et al., 1990) or in relation to faults or active fracture zones as irregular pipe-like bodies e.g., (Fraipont, 1982; Poty et al., 1986; Turpin et al., 1990; Recio et al., 1997). The episyenite bodies can be 100 meters long and a few meters wide (Recio et al., 1997). The contact between the unaltered granite (host rock) and the episyenite altered body is usually sharp or just a few cm wide (Cathelineau, 1986). The episyenite altered zone is not bound by lithological contacts but is more commonly continuous over neighbouring rocks. Hercynian granites that have been subject of episyenitisation show similar characteristics regardless of location of formation and lithology e.g., (Leroy, 1978; Cathelineau, 1985). Studies from Hercynian granites indicate that the episyenite formed after the emplacement of the granites by circa 25 Ma. Hot meteoric water caused the alteration driven by crustal extension due to the intrusion of dykes (Turpin et al., 1990). Studies made on Bohus granite show that the vugs were filled with minerals circa 670 Ma after the episyenite framework was already developed. The mineral infill occurred at the same time the development of the Oslo Rift (Petersson et al., 2001). The origin of hydrothermal fluids has been interpreted through fluid inclusion studies and most studies describe aqueous fluids of most likely meteoric origin with low salinity from 0 to maximum 12 eq. wt.% NaCl and temperature from 250 to 450 °C and pressure 500 bar (Turpin et al., 1990). Cathelineau (1986) showed fluids with 0 to 10 eq. wt.% NaCl and temperature from 250 to 400 ◦C and pressure varying from 300 to 1800 bar. Other fluid inclusion studies have given 2-6 eq. wt.% NaCl (Leroy, 1978) and 0-7 eq. wt. % NaCl (Martin, 1981) and similar temperatures of 300-380 °C with a meteoric origin of the fluids (Turpin, 1984).

The trigger to dissolve primary quartz is controlled by the amount dissolved silica in the fluid. Silica oversaturated fluid rapidly becomes silica unsaturated when the temperature changes from 450 to 360 °C or going from 250 to 360 °C (Cathelineau, 1986). When the water-rock ratio is high then this become an effective way to dissolve a high amount of magmatic quartz in the rock (Cathelineau, 1986). Other authors have proposed a high temperature late magmatic fluid (deuteric alteration) as the source for episyenitisation e.g., (Dempsey et al., 1990; Recio et al., 1997; Hecht et al., 1999).

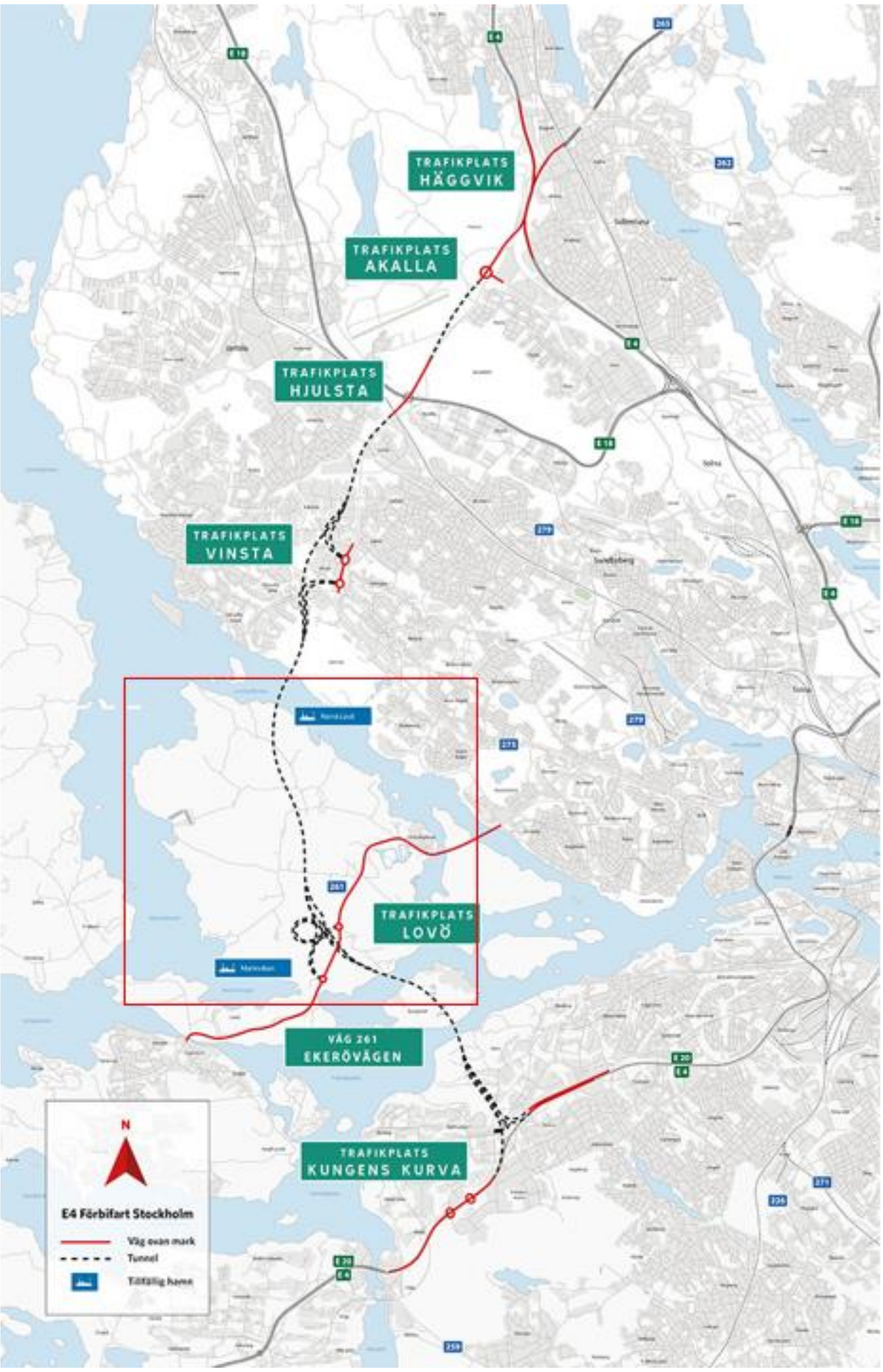

Figure 1 overview map of the Stockholm Bypass. Red square is the location of Lovön. Map modified from Trafikverket (2020) webpage.

Geological setting

Lovön island is located west of Stockholm (Fig. 1). The region belongs to the Bergslagen lithotectonic unit that evolved and underwent metamorphism during the Svecokarelian orogeny (2850-1870 Ma). The Stockholm region is dominated by supracrustal and intrusive rocks that dates to circa 1900 Ma (Wahlgren et al., 2018). In the north and western part is dominated by felsic intrusive rocks such as, granites, granodiorite and tonalite (Fig. 2). Younger grey or red coloured granites that occur as irregular or elongated bodies are also present (Wahlgren et al., 2018). These granites are called "stockholmsgranit" and are equigranular fine to medium grained granites that partly can show foliation (Persson et al., 2001) they have been dated at Frescati to be circa 1803 Ma (Ivarsson and Johansson, 1995). To the northeast, there are lanes of dolerite dykes with northwest-southeast strike. Dating of "Mackmyradiabasen" in Gästrikland have shown an age of 1260 Ma e.g., (Söderlund et al., 2006). This could be corresponding with the age of the dykes at Lovön.

On the western part of the island, small irregular bodies of metabasite exist. They have not been further divided into subgroups between gabbro, diorite or amphibolite. To the south and east on the island metasedimentary rocks are encountered, dominated by metagreywacke and mica schist that locally show migmatisation (Persson et al., 2001). The quartz- and felspathic metagreywacke are usually more preserved than the mica-rich metasedimentary rocks that show migmatisation more frequently (Wahlgren et al., 2018). Hosted in the metasedimentary rocks occur small bodies or dykes of granite and pegmatite. Brittle and plastic deformation lines with a strike in northwest-southeast direction are dominated. But also, deformation lines with strike in east-west and southwest-northeast exist. On the north shore mylonite have been observed indicating a northwest-southeast deformation zone that formed ductile (Wahlgren et al., 2018) and then later reactivated in brittle regime as a dextral strike-slip fault (Vass, 2012). The area has been subject for metamorphism at (700 ◦C and 4 kbar) (Stalhos, 1969). The drilling site (fig. 1) is located in the southern part adjacent to the outcrops of metagreywacke and mica schist.

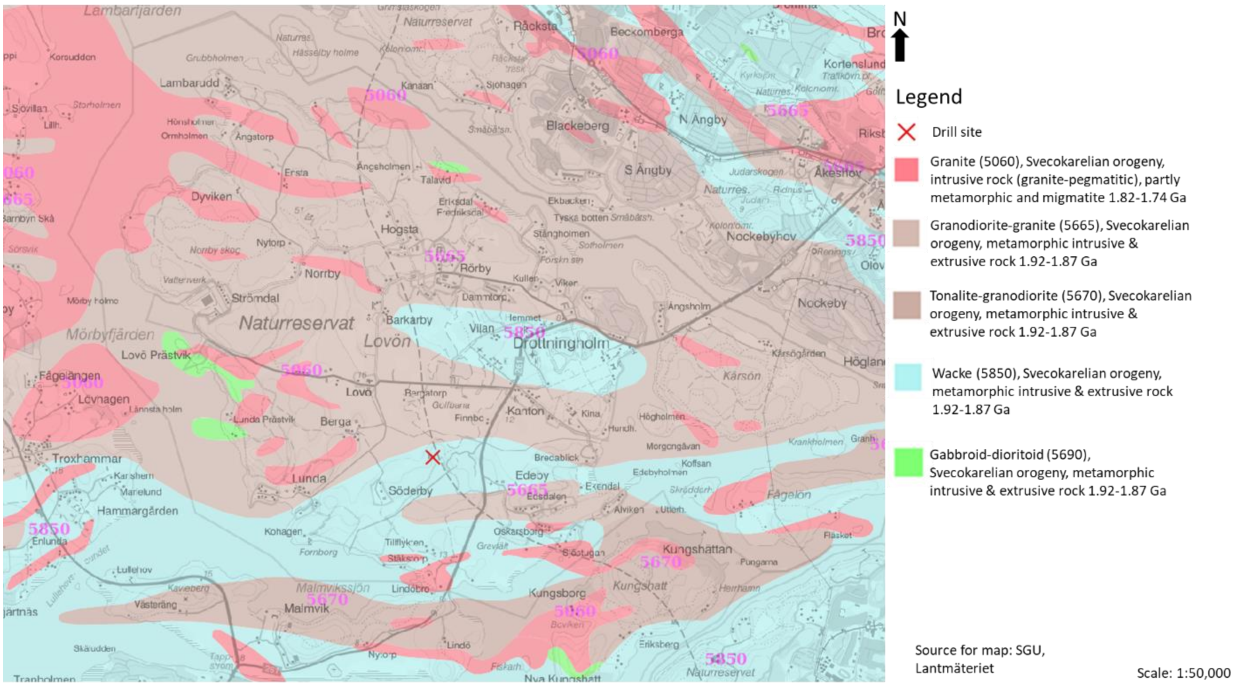

Figure 2 Geological and property map of Lovön. The red cross is the site where the drill core was taken from.

Aim of the study

The aim of this study is to investigate, describe and classify the drill core 19A374sk, focusing on the alteration of the rock. The study describes the mineralogy and whole rock geochemistry and evaluates where the alteration can be classified as episyenitisation. This study will also focus on the cause of the red staining, clay alteration and the composition of infill minerals in the vugs.

The main hypothesis that will be tested is that the increased porosity in sections of the rock is caused by leaching of quartz, which is the central process of episyenite alteration, meaning that the porous areas should be quartz and silica poor.

Sampling and Method

The episyenite alteration was identified in the drill core 19A374SK, that was drilled on south Lovön (WGS84 dec coordinate: 59.313397°, 17,851061°) in a vertical shaft with inclination 85° to the south. The core recovers rock from (-8 to -61) m below surface. Core logging was carried out at the Department of Geological Sciences at Stockholm University. The core was logged visually with only the aid of a hand lens (x10). The core was divided into lithological units based on mineralogy and textures. The core was divided up into three major rock type units: *felsic intrusive rock, quartzofeldspathic gneiss* and *mafic intrusive rock.* These rocks were further subdivided based on grain size and textures. Four subdivisions were recognised: *Gneiss, Fine Grained Granitoid, Medium Grained Granitoid and Coarse Granitoid*. The episyenite alteration has occurred in the felsic intrusive rock creating zones of high porosity. The size of the vugs is corresponding to the size of the mineral grains in the different sections. Vugs range from less than mm in size to cm scale. For quartzofeldspathic gneiss and mafic- or intermediate intrusive rock, only one type was recognised. *Gneiss* respective *diabase.*

Sampling drill core

A total of 22 samples were taken from the core covering the variation in lithologies but also focusing on the granitoid rocks containing the vugs (i.e., episyenite). A set of 13 samples were also collected for whole-rock geochemistry from the vuggy granitoids, which are the focus for this study. A total of four samples for thin-section preparation and for whole-rock geochemistry were taken from the fine grained granitoid section (30.4-33.98) m. The purpose of taking the four samples was to follow the increasing of porosity in the fine grained granitoid. A total of five samples for thin-section preparation and whole-rock geochemistry were taken from the coarse (pegmatitic) granitoid. Two of the samples were taken at 15.35 and 15.55 m. Between these two sample sites, a transition in porosity occurs going from high to low.

Three more samples were taken at (30.15-30.7) m. Porosity varies from low to medium in this section. A total of three samples for thin-section preparation and whole-rock geochemistry were taken from the medium grained granitoid. One at 30.9 m with high porosity sits in a transition from a pegmatitic granitoid that have medium porosity to a fine grained granitoid that have low porosity. The one at 39.8 m sits on the boundary from gneiss to granitoid. The one at 41.95 m is taken after the pegmatitic granitoid in a section of high porosity and medium sized grain. Two samples of gneiss were also collected for whole-rock geochemistry and thin-section preparation. From the other sections only samples for thin-section preparation were taken. See table 1 for more information.

Table 1. samples, where on the core they were collected, and analysis done to the samples.

Nr	Sample id	Meter	Porosity	Box	Analysis
1	374sk14.5	14.5	low	2	thin section
2	374sk15.35	15.35	high	2	thin section/chemistry
3	374sk15.55	15.55	low	2	thin section/chemistry
4	374sk19.8	19.8	non	3	thin section/chemistry
5	374sk21.4	21.4	non	3	thin section
6	374sk21.8	21.8	non	3	thin section
7	374sk24.5	24.5	non	4	thin section
8	374sk26.3	26.3	non	4	thin section/chemistry
9	374sk30.15	30.15	low	5	thin section/chemistry
10	374sk30.5	30.5	Medium	5	thin section/chemistry
11	374sk30.7	30.7	Medium	5	thin section/chemistry
12	374sk30.9	30.9	high	5	thin section/chemistry
13	374sk31.4	31.4	low	5	thin section/chemistry
14	374sk33.3	33.3	increasing	5	thin section/chemistry
15	374sk33.6	33.6	increasing	5	thin section/chemistry
16	374sk33.85	33.85	increasing	6	thin section/chemistry
17	374sk39.8	39.8	high	6	thin section/chemistry
18	374sk41.85	41.85	high	7	thin section/chemistry
19	374sk41.95	41.95	high	7	thin section/chemistry
20	374sk43.2	43.2	non	7	thin section
21	374sk47.75	47.75	non	8	thin section
22	374s53.75	53.75	non	9	thin section

Thin sections

The selected positions on the drill core were cut out with a rock cutting saw into pieces for the making of thin section. The cut rock pieces were scanned with an Epson perfection 2400 photo scanner before sent to Vancouver BC, Canada for manufacturing of polished thin section made by Vancouver Petrographics LTD. The examination of thin section was done at the Department of Geological Sciences at Stockholm University using a petrographic Microscope. Photos of thin section was taken with an iPhone 7 camera. Overview Images scanning of the thin sections was done with a Nikon super cool scan 9000 ED thin section scanner.

Crushing to rock powder.

The rock pieces were crushed in a BB 200 Jaw Crusher (Retsch®) into fragments. The fragments where further made into a powder in a Vibratory Disc Mill Type RS 200 (Retsch®). The disc mill ran for 59 second at 900 rpm. The powder was transferred to a plastic bag and sealed.
Between each sample all the equipment were thoroughly cleaned with compressed air and alcohol (95%).

Loss On Ignition

Loss On Ignition (LOI) was done on the rock samples before melting the rock into a glass disc for performing XRF. This is done to dehydrate the samples (i.e., removal of bounded OH ion in minerals and other volatiles in the samples). First the crucible (c) was weighed (W) empty and noted, then about

10 g of rock powder was added to the crucible and the total weight was noted (c+s). The crucible where set in the oven which ran 10 hours over the night. The oven had a temperature increase of 3 C^{o}/minute to 1000 C^{o} which it held for 2 hours before starting to cool down to about 30-25 C^{o} before new weighing was performed on the dry samples (-1000). Calculating the LOI (wt.%) was done using equation 1.

$$LOI\ (wt\%) = \left(\frac{W_{c+s} - W_{-1000}}{W_{c+s} - W_{c}}\right) * 100 \qquad (1)$$

XRF

The preparation of the samples consisted of two grams (±0.0002 g) of the dried rock sample which were added to a platinum-gold alloy (Pt-5Au%) crucible and 5 g (±0.0002 g) of flux. The flux used were a mix of 66% lithium-tetraborate ($Li_2B_4O_7$) and 34% lithium-metaborate ($LiBO_2$). The dry rock powder and the flux were gently mixed before placed in the autofuser (Phoenix, VFD 4000). The autofuser ran a pre-recorded recipe (B). The molten rock was added to molds for cooling down into glass discs. The XRF analyses were performed on the glass discs with a Rigaku ZSX primus. Twenty-four international reference standards were used for calibration of the instrument. The internal standards used were AGV-2, BRC-2, RGM-1 and they were used for every 10th sample to confirm instrument accuracy. The results for major elements are presented as weight percentages (wt %) of oxides.

Point counting

A Petrographic microscope was used for identifying the minerals in the samples and the software for operating the count was PelaconPointCounter9. This means that larger grains in the samples were counted multiple times and that smaller grains/vugs could fall between step counts due to the steps being too big. The coarse-grained sample was performed with a step length of 2 mm (the maximum step length in the point counter) while the medium- and fine- grained were carried out with a step length of 1 mm. Even with this configuration it is possible that the larger grains in the samples were counted multiple times and that smaller grains/vugs could fall between step counts. The point count was done parallel with the length of the sample and at each end the sample was moved one step on the width corresponding to the step length i.e., 2 mm for coarse- and 1 mm for medium- and fine- grained samples. Table 2 summarise the count chart that was used. Vug + infill means that an area that clearly was an empty pore is now filled with a secondary mineral e.g., goethite would count to this group. Secondary minerals (SM) would be other minerals that have not necessarily filled a pore space but are not primary minerals e.g., minerals in veins. Other minerals (OM) would be the rest e.g., muscovite, opaque minerals, titanite.

Table 2. point counting codes used.

key nr.	code
1	Kfs
2	Pl
3	Vug
4	Vug+infill
5	Bt
6	Chl
7	Qz
8	SM
9	OM

Scanning Electron Microscopy (SEM)

SEM is a non-destructive method used to get a qualitative result of the chemical composition in individual mineral grains. The analysis was carried out at Naturhistoriska riksmuseet, Stockholm. Four samples were selected out (samples: 374sk15.55, 374sk30.15, 374sk31.4, 374sk33.95). These were representative of the different granitoid types. The samples were carbon coted. The instrument a FEI Quanta FEG 650 SEM with Oxford instruments, X-MAX 80 mm2 energy dispersive spectroscopy (EDS) detector. Voltage 20.00 kV, spot size 4 µ, working distance 10 mm. Results from the SEM are incorporated with thin section results. i.e., not presented in its own category.

Results

Core logging

Felsic Intrusive Rock

Fine grained granitoid (Fig. 3a): is seen in section (30.9-35.7) m. and is a felsic rock with a brick-red colour. The section is dominated by fine grained minerals (up to 3 mm) with a massive texture and no foliation or fabric to the minerals. The most common minerals are feldspars, commonly darker pink orthoclase and rarer paler coloured feldspars presumably plagioclase. Micro fractures or thin veins filled with quartz or a dark red mineral exist in the section. Brecciation occurs locally (35.3-35.7) with secondary felsic minerals and red matrix (Fig 3b). Vugs in the section are very fine (grain size 1 mm) and hard to distinguish as they have an infill of dark minerals (presumably chlorite). They appear throughout the rock and are estimated to make up approximately 5 to 8 % of the core surface but locally it can be from 5 to 35 %.

Medium grained granitoid (Fig. 3c): seen in section (28-29.5, 35.7-36.7, 39.9-41.1, 43.6-45) m. is a felsic rock that has a brick-red colour. The section is dominated by medium to coarse grained minerals (up to 5 mm) with a phaneritic texture. The most common minerals are feldspars, commonly darker pink orthoclase and rarer paler coloured feldspars presumably plagioclase. Vugs in the section are fine to medium (1-5 mm) and are estimated to make up approximately from 3 to 10 % of the surface. Some of the vugs have secondary dark or pale green mineral infill presumably chlorite and epidote. Some of the larger vugs have a dusty mineral coating on the inside which is orange in colour.

Coarse grained granitoid (Fig. 3d): seen in section (15.1-15.9, 29.75-30.9, 41.1-41.9) m is a felsic rock with a brick-red colour. The sections are in places extremely fractured and the core surface appears to be weathered. The most common minerals are feldspars, commonly Pegmatitic (cm size) darker pink orthoclase with dark red rim. Micro fractures or thin veins filled with a dark red mineral occur in the section. The vugs in the section are large (up to 1.5 cm) and irregular shape. Some of the vugs has a secondary green mineral infill presumably chlorite and epidote. The vugs are estimated to make up approximated 5 to 10 % of the surface but are more locally assembled then even spread out over the section. An orange-coloured dusty mineral coating occurs on the inside of some of the vugs.

Gneissic granitoid (Fig. 3e): seen in sections (12.95-15.1, 15.9-18.7, 38.7-39.9, 42.3-43.6, 50-52.4, 57-61.35) m. The rock has a gneissic texture with dark-green coloured bands. The dark bands have a foliated green-black mineral matrix, presumably containing chlorite and mica minerals. The bands fold around porphyroblasts or ellipse shaped lithic fragments of the granitoid material with mostly quartz and potassium feldspars in whitish pink to red colour. Sulphide minerals are present with the green mineral foliation. Micro fractures or thin veins filled with dark red mineral occur in the section. Parts of the sections appear weathered and have vugs adjacent to the potassium feldspar minerals. The vugs are large (up to 1 cm) and elongated. The wall surface in some of the vugs are covered by very fine yellow-orange mineral with sugary or clay texture. The vugs covers locally a couple of percent of the core surface in the sections.

Quartzofeldspathic gneiss

Gneiss (Fig. 3f,g,h,i): occurs in section (18.7-28, 45-50) m. The section is heterogeneous and display variation in texture, mineral composition and grain sizes. The rock is partly foliated and contains more homogenous dark coloured, fine grained (< 1mm) area with a shiney lustre, presumably mica minerals, and pale coloured quartz-rich areas. Vugs in these sections are negligible. From (18.7-28) meters this section has strong foliation texture (Fig. 3f). The foliation wraps around lithic eyes of felsic materials such as quartz and feldspars (cm size). The section has very few vugs (< 1 mm in size) on the core surface. Continuing down, core black foliated sections increase in thickness and spotty sub-angular grains of pale pink k-feldspar up to 5 mm in size occur on fracture surfaces.

At circa 22 m of the section (Fig. 3g) a local change in the texture of the rock occurs circa one meter wide. It does not show any foliation and instead displays a homogenous texture, fine grained (1 mm size), black coloured with metallic lustre due to the high mica content. Sulphide minerals are also seen and red and white feldspars (3 mm size) as well as quartz. Thin veins filled with black mineral are also prevalent. Continuing even further down core to 23.1 meter (Fig. 3h), the rock has a grey-white colour and pegmatitic texture with quartz and white coloured feldspars minerals. Red fragments of gneissic textured rock that can be up to 2 cm in size occur and spotty sub-angular pink feldspars that are up to 5 mm in size are also present. Micro fractures or thin veins filled with dark green or yellow-orange mineral are found in the section. In section (45-50) m (Fig. 3i). The rock shows a pervasive foliation and a deformed gneissic texture with coarse lithic fragments. The fragments are grey-white or dark red in colour. The grey-white is most likely made up of quartz and feldspars and the dark red of potassium feldspars. The thin foliation bands wrap around lithic eyes or porphyroblasts of dark red feldspars and crosscuts the white mineral patches. Sulphide minerals can be seen in the dark foliation bands.

Mafic or Intermediate Intrusive Rock

Diabase (Fig. 3j): seen in sections (52.4-55.6, 56.2-57) m. Intermediate rock, green coloured with white coloured fold bands that contain red stains. The rock is fine grained. The most common minerals are green minerals presumably amphiboles and or chlorite minerals. Some spotty fine grains of white feldspars and light green mineral, presumably epidote, can be seen. Spotty blood red stains of iron oxide minerals can also be seen. Micro fractures filled with calcite occur in the section as well as micro fractures or thin veins filled with quartz or white feldspars occur. The section is crosscut by 20 cm width pegmatite vein. Vugs are negligible in this section.

Figure 3 photo of the different rock and texture-types that was identified in the drill core.

Thin sections

Fine grained granitoid

Main mineralogy: Kfs (29%), Pl (21%), Qz (11%), Bt (5 %)

The general appearance for the fine grained granitoid (Fig. 4), is that it is fine grained with homogenous texture and feldspar grains varying from (1-4) mm and where alkali-feldspars grains are bigger compared to other minerals. The rock is weathered and contains sporadically placed vugs which increase in intensity going down the section to 33.85 m. Parallelly to this, quartz decreases in concentrations.

The most common mineral in the rock is k-feldspar. It occurs as well-preserved, subhedral grains with tartan twinning, perthite unmixing or as grains with no visible twinning. Some of the grains, especially those with perthite unmixing, have been interpreted as microclines. The grains have inclusions of sericite. On some edges of the k-feldspars towards the vugs albitisation have occurred. Plagioclase (albite) is the next most abundant mineral and is strongly altered to sericite and stained with fine grained Fe-oxide. Within the areas of most intense sericitisation are coarser muscovite grains. In some plagioclase grains lamellae twinning can clearly be observed while in others its barley seen. Quartz (Fig. 5) forms patches or veins with recrystalised subgrains of variable size and shape. They do not display undulose extinction. Biotite (Fig. 7) in the sample has a dark appearance and are not fully biotite minerals anymore. Exsolution of Fe-Ti oxides have occurred forming Ti-oxides inside the grains of the biotite. Muscovite can be observed as tiny grains inside or next to several of the biotite grains. Accessory minerals are opaque minerals, titanite, Ti-oxides, apatite (fluorapatite), bastnäsite and zircon. Other secondary mineral is a is a green-yellow coloured anhedral clay mineral with no pleochroism or cleavage and 2nd order birefringence. Inside these minerals tiny opaque minerals occurs. These minerals are found close to vugs and biotites giving the indication that they have formed as a result of the breakdown of biotite grains in the rock (Fig. 7).

The rock contains a small abundance of vugs (Fig. 8) that have variable size and shape. On the vugs wall a tooth-shaped mineral overgrowth the adjacent k-feldspars. This mineral are geochemically k-feldspars and presumed to be adularia.

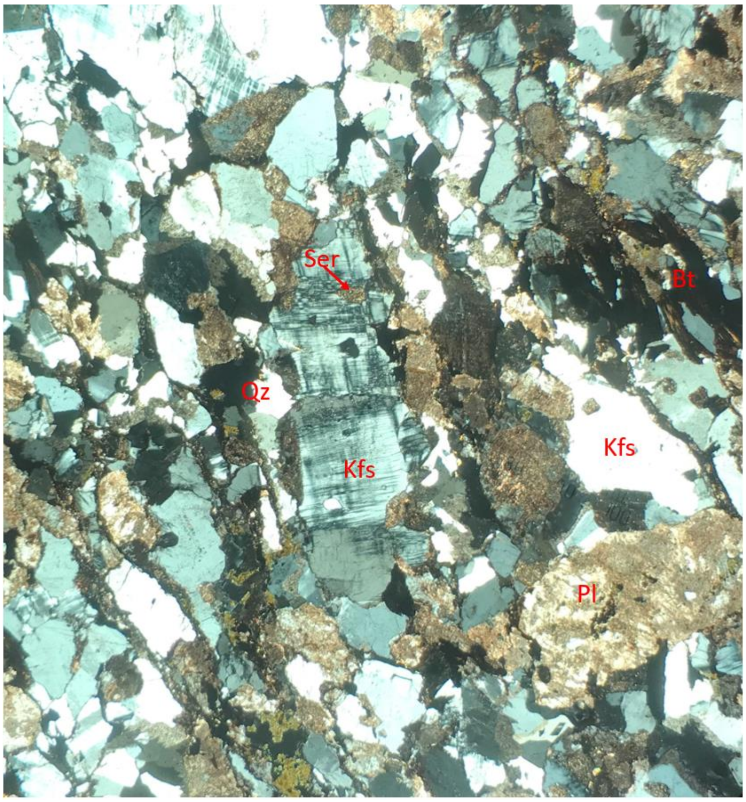

Figure 4 Photo (X2.5) general mineralogy of the rock.

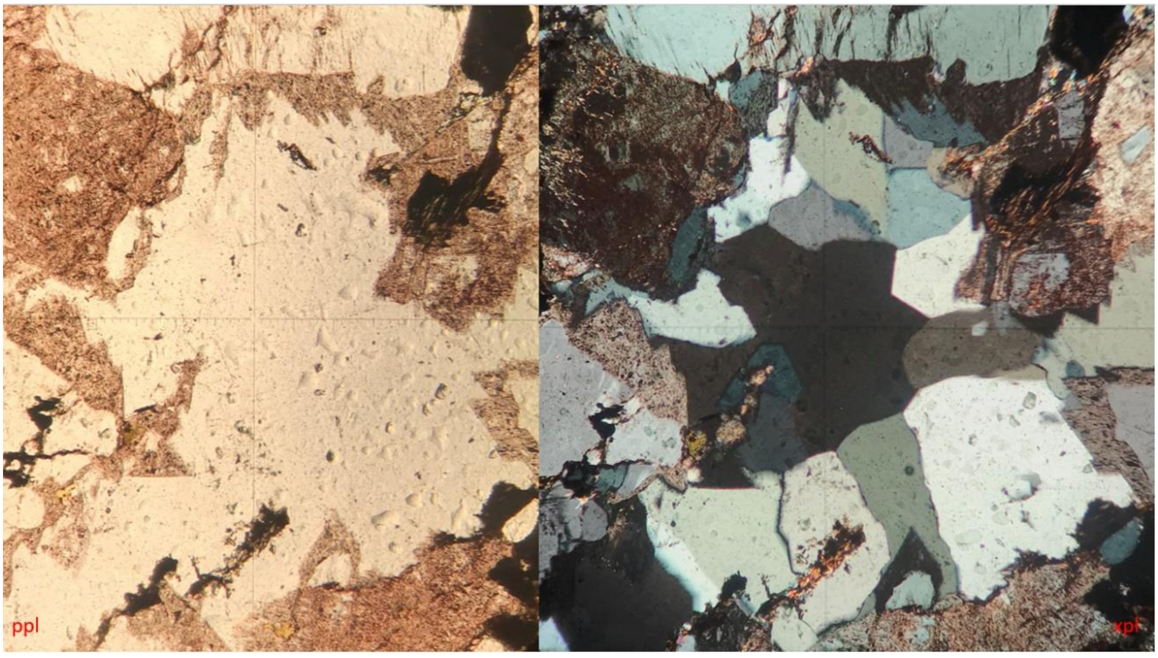

Figure 5 Photo (X10) of quartz patch with recrystalised grains of variable size and shape with no undulose extinction.

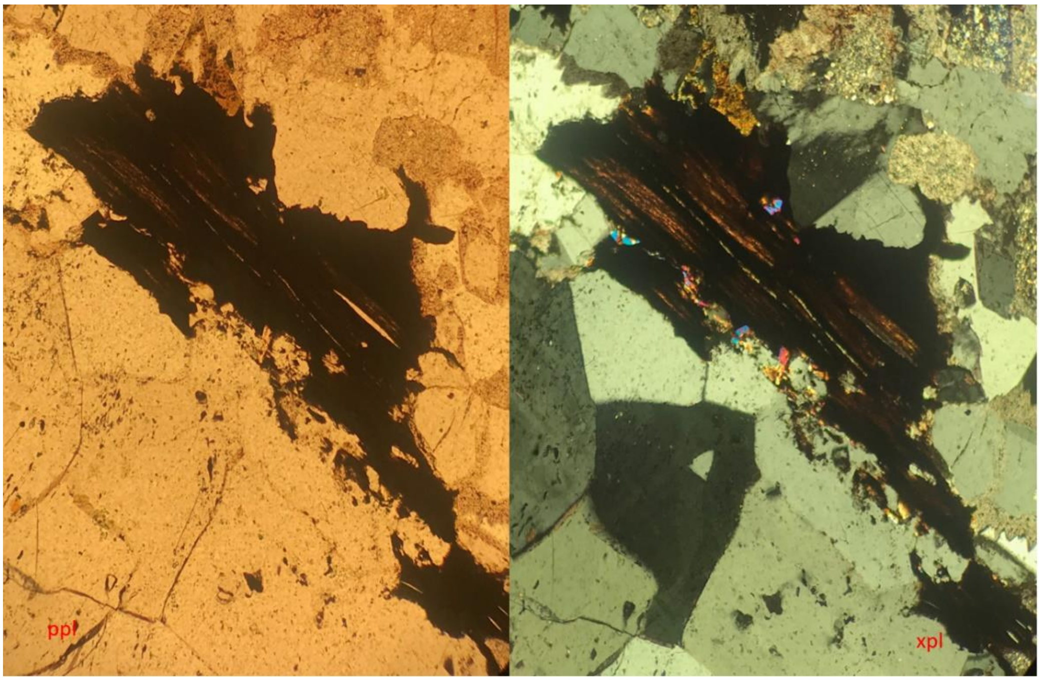

Figure 6 photo (X2.5) dark biotite in sample with tiny muscovite grains present.

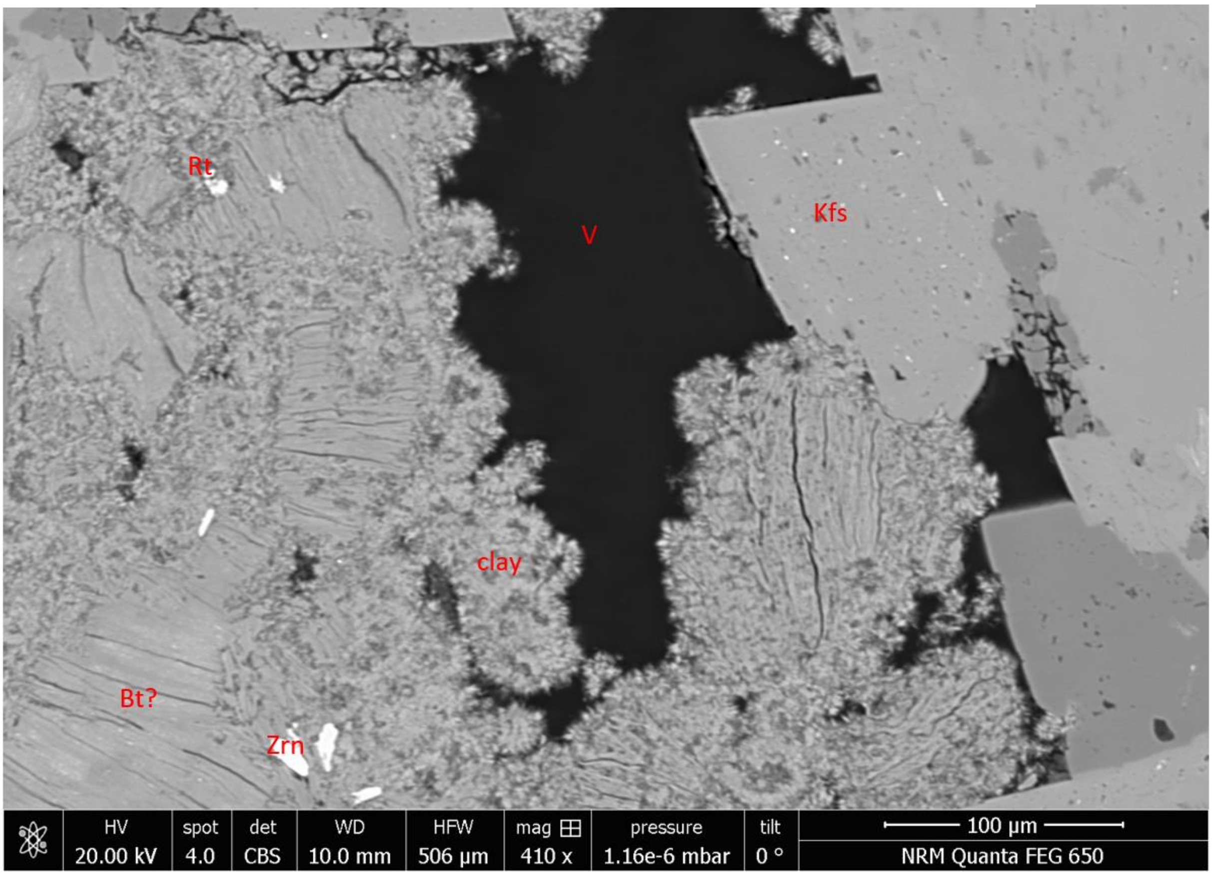

Figure 7 Backscatter electron image from the SEM showing a vug partially infilled by euhedral k-feldspar and biotite that is breaking down to clay minerals

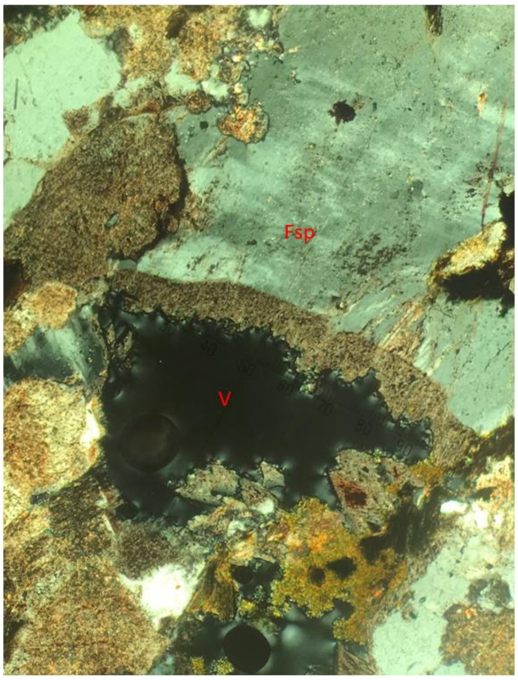

Figure 8 photo (X10) in centre a vug that is partly field with secondary minerals and the vug wall on top shows a feldspar with overgrowth of adularia.

Medium grained granitoid

Main mineralogy: Kfs (44%), Pl (35%), Bt (7%), Qz (1%).

The rock (Fig. 9) has an inequigranular texture with felspars between 5-10 mm wide. It is heavily weathered and fractured and contains proportions of vugs in variable size and shape, which of variating degree are infilled with secondary minerals.

The most common mineral in this sample is k-feldspar which occur well-preserved, subhedral to anhedral grains with tartan twinning or without visible twinning. The grains have inclusions of sericite. Plagioclase is the next most abundant mineral that is either strongly altered to sericite or more preserved with clear lamellae twinning. Within the areas of most intense sericitisation, coarser muscovite grains are seen. Plagioclases tend as well to be stained with Fe-oxide. Biotite is minor and forms anhedral grains that are spread out in the rock. Most of the grains are dark or green and only show weak pleochroism. Commonly exsolution have occurred forming Ti-oxides inside the biotite grains. Tiny muscovite grains are commonly seen around or inside blacker parts of the biotites. Accessory minerals are quartz, Ti-oxides, apatite, zircon and opaque minerals.

The sample contains a large abundance of vugs (Fig. 10) that have irregular shape, and several contain secondary mineral infill or mineral growth on the vug walls. The most common secondary mineral is fine grained albite that have a dark red brown colour and tabular form, occurring commonly in aggregates. Tooth shaped colourless low birefringence mineral also fill the vugs rim. These commonly have twinning and exsolution lamellae and are k-feldspars. The shape of the grains indicate that they are secondary and grew into space once the vugs had been developed. Chlorite minerals forming aggregates are also seen as infill in fractures.

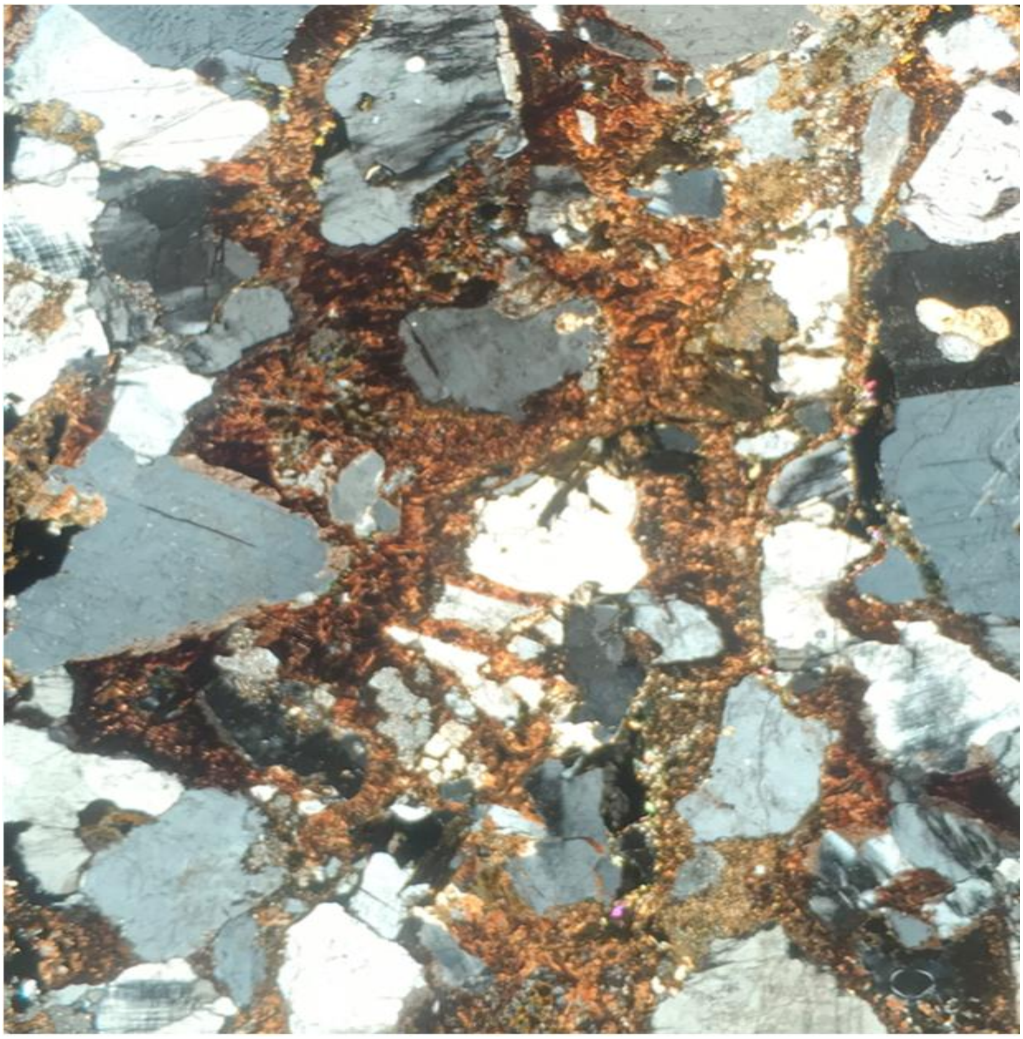

Figure 9 photo (X2.5) of a section of the thin section. Larger grains of feldspars and finer "matrix" or mostly red brown clay, but also muscovite, biotite, and chlorite.

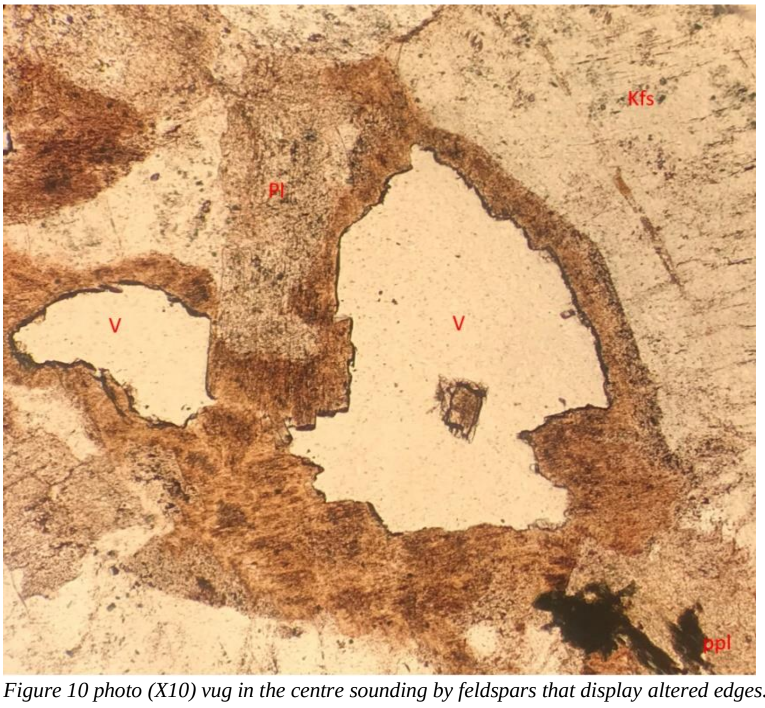

Figure 10 photo (X10) vug in the centre sounding by feldspars that display altered edges. Presumably, albites.

Coarse grained granitoid

Main mineralogy: Kfs (58%), Pl (21%)

The rock is very coarse grained (Fig. 11), pegmatitic texture with feldspars up to 1.5 cm wide. It is heavily weathered and fractured and contains large proportions of vugs, which are commonly infilled with a red brown dusty mineral.

The most common mineral in this rock is k-feldspar which occurs as well-preserved, subhedral to anhedral grains with tartan twinning, pericline twinning or perthite unmixing. The grains have inclusions of sericite and are stained with Fe-oxides. Plagioclase is the next most abundant mineral and is strongly altered to sericite. Within the areas of most intense sericitisation are coarser muscovite grains. Lamellae twinning can barely be observed in the grains. Biotite in the rock is minor and it forms aggregates adjacent to larger vugs. Most of the biotite has undergone some sort of breakdown. Chlorite in the rock are few and they form larger aggregates. Accessory minerals are muscovite, Ti-oxides minerals, apatite, zircon, opaque minerals.

The rock contains a large abundance of vugs that have irregular shape and contain secondary mineral infill. The most common secondary mineral is clay minerals (Fig. 12), possible formed from the breakdown of feldspars. Tiny albite grains that have a dark red brown colour and tabular form and occurring commonly in aggregates. Tooth shaped colourless low birefringence mineral also fill the vugs. These commonly have twinning and exsolution lamellae and are k-feldspars. The shape of the grains indicate that they are secondary and grew into space once the vugs had been developed. Other secondary infill mineral is a dark yellow coloured, clay mineral with no pleochroism and II-order birefringence. These are interpreted as formed from the breakdown of biotite grains.

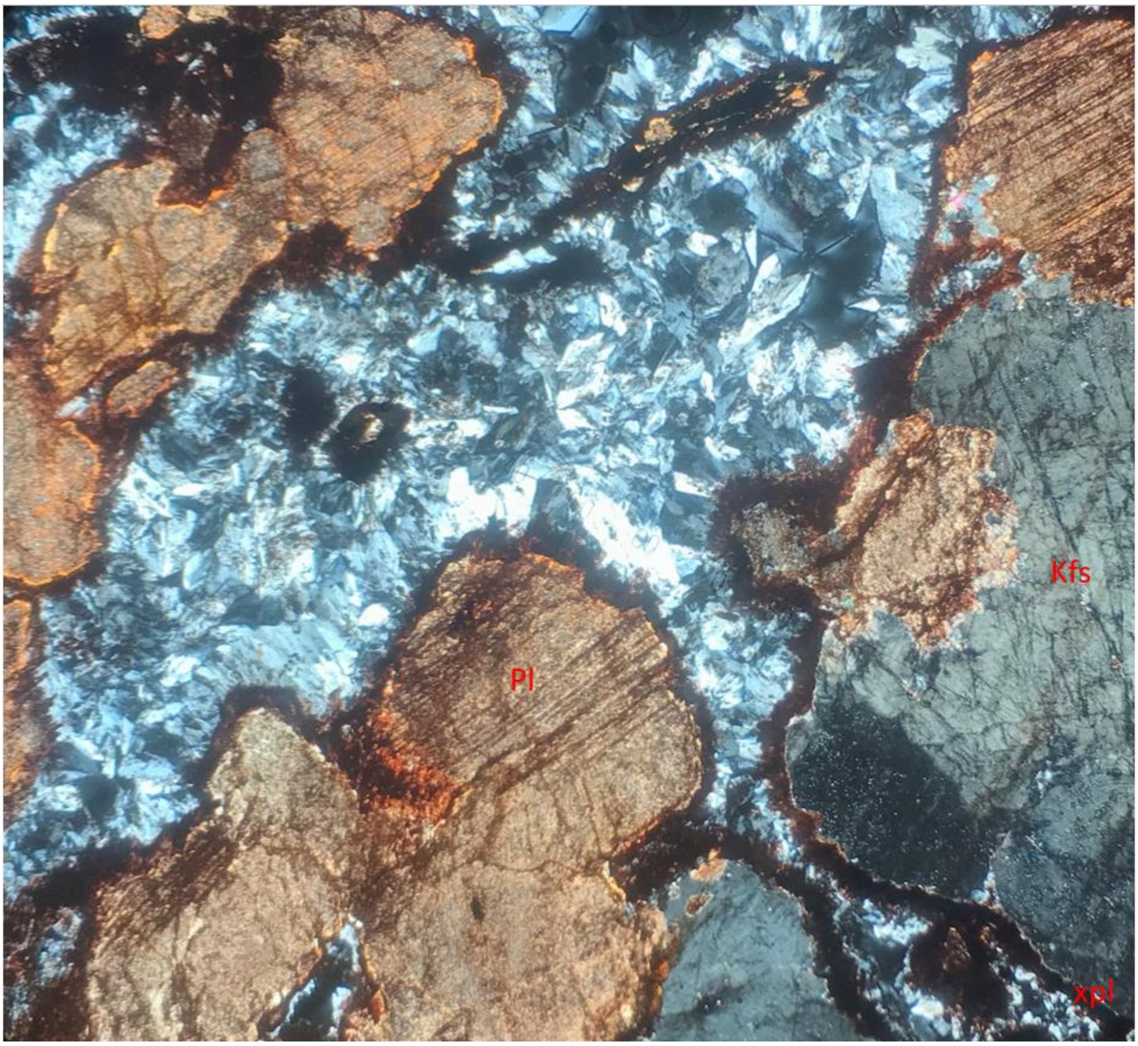

Figure 11 photo (X2.5) central in the photo a vug that has been filled with fine-grained secondary feldspar.

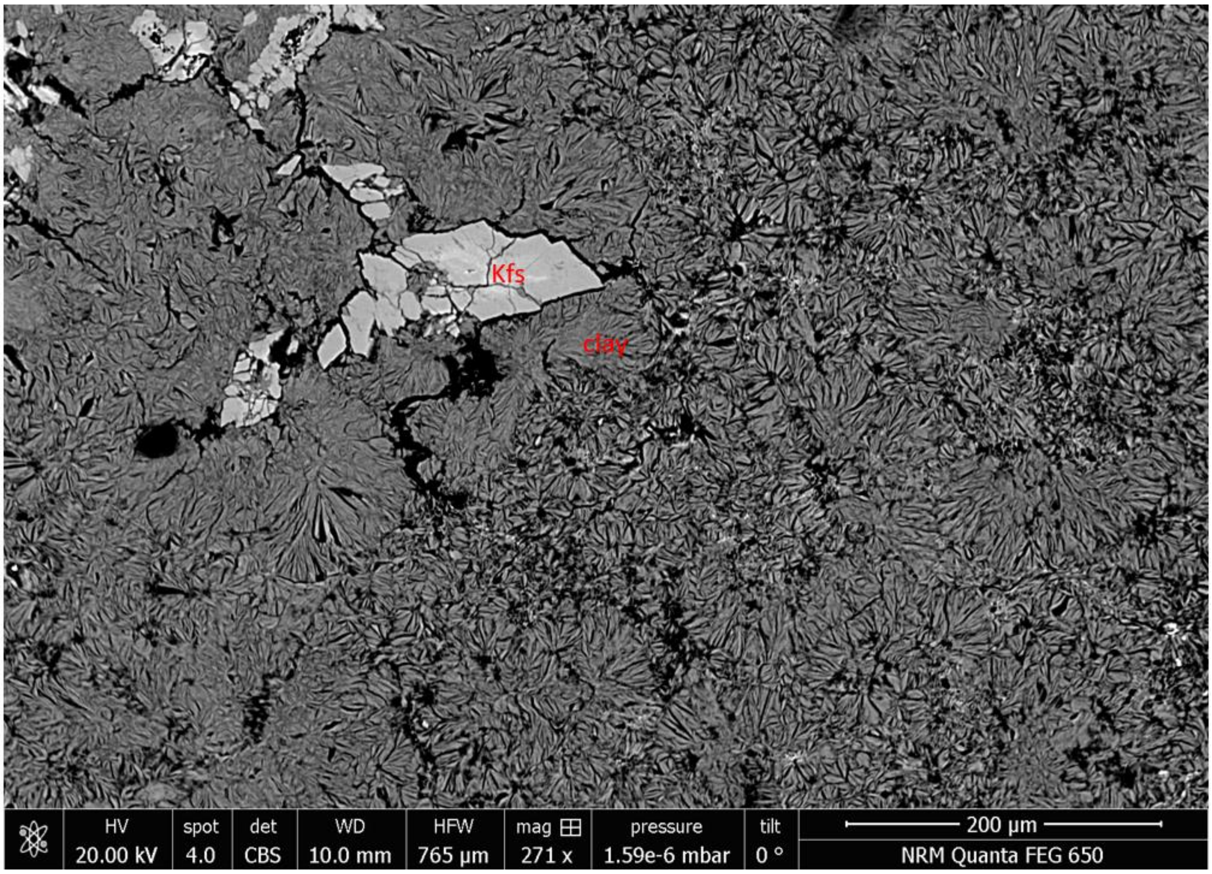

Figure 12 Backscatter electron image from the SEM showing part of a vug that is filled with a mix clay mineral.

Gneissic granitoid

Main mineralogy Kfs (35%), Pl (18%), Bi/Chl (13%)

The rock (Fig. 13) is medium grained with feldspars up to 5 mm wide. It has irregular foliation bands of biotite/chlorite and it is heavily weathered and fractured and contains sporadically placed vugs. These are commonly infilled with a red brown dusty mineral. The most common mineral in this sample is k-feldspar which occurs as better-preserved, subhedral to anhedral grains with tartan twinning or perthite unmixing. The grains have inclusions of sericite. Plagioclase is the next most abundant mineral and is strongly altered to sericite. Within the areas of most intense sericitisation are coarser muscovite grains. Lamellae twinning cannot or barely be observed in the grains. Larger plagioclases are stained with Fe-oxides. The majority of the biotite have been altered to chlorite. They form aggregates of bands. Within the grains they have turned opaque. Inside biotite grains zircon grains are found. The sample contains a large abundance of vugs that have irregular shapes and contain secondary mineral infill. The most common secondary mineral seems to be tiny albites that have a dark red brown colour and tabular form occurring commonly in aggregates. Tooth shaped colourless low birefringence k-feldspars also fill the vugs. The shape of the grains indicate that they are secondary and grew into space once the vugs had been developed. An additional secondary mineral is a green-yellow coloured anhedral mineral with no pleochroism or apparent cleavage, II- order birefringence interpreted has a clay mineral formed after the break down of biotite grains. Other secondary minerals include opaque minerals, micas (including muscovite).

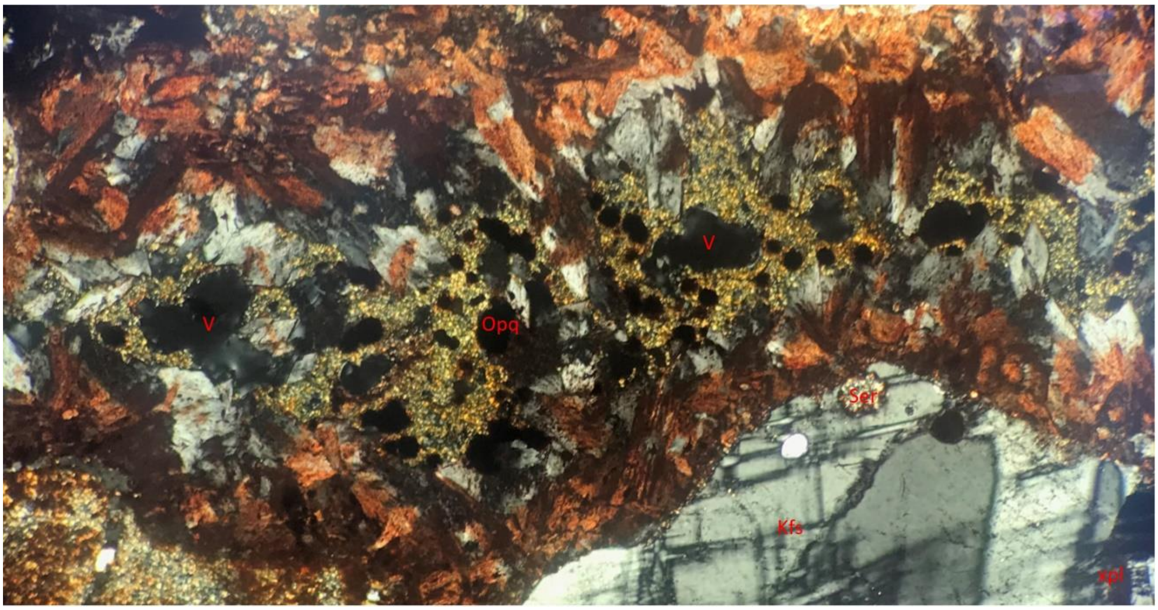

Figure 13 photo over part of a thin section. in the middle vugs that partly infilled with secondary clay mineral and k-feldspars and albite.

Quartzofeldspathic gneiss

Minerology: Qz (33%), Pl (25%), Kfs (21%), Bt (14%), Chl (6%)

The rock has heterogenous texture, it is partly foliated (Fig 14) and has feldspars (plagioclase) porphyroclast which are between 5-10 mm wide. Feldspars in the sample are weathered and fractured and quartz has been plastically deformed (Fig 15). The foliation bands are made up by biotite and chlorite minerals.

The most common mineral in this rock is quartz which occurs as elongated patches or aligned bands of recrystallised subgrains with variable shape and size as well as with undulose extinction. Quartz grains occur as well as single grains with undulose extinction. Plagioclase is the next most abundant mineral, and it forms porphyroclast in the foliation. Where foliation is less, they form larger subhedral to anhedral interlocking grains. They are partly heavily sericitisied. Within the areas of most intense sericitisation are coarser muscovite grains and even epidote can be seen. Lamellae twinning are preserved in most grains and grains are common stained with Fe-oxides. Enclaves of dark coloured area of the section where plagioclase appears in two different forms. The first type is an anhedral, colourless mineral with first order interference colours which are strongly altered to sericite. Within the areas of most intense sericitisation, larger patches of sericite forms.

The second type forms subhedral grains with clear lamellae twinning and they appear less weathered and only moderately altered to sericite. K-feldspar occurs as larger or clusters of smaller grains that are well-preserved, subhedral to anhedral grains with tartan twinning or perthite unmixing. The grains have inclusions of sericite. Biotite occurs of varying intensity locally it can dominate the minerology forming large foliation aggregates where in other areas it is just single grains. Many of them have inclusions of dark deep red Ti-bearing minerals and several have been chloritised. In the more foliated sections chlorites form thin aggregates of align bands between quartz bands. Within the chlorite bands inclusions of elongated recrystalised subgrains of quartz exist. Here muscovite and red-brown clay minerals also form thin bands adjacent to the thicker chlorite bands. Accessory minerals are epidote, muscovite, opaque minerals, Ti-oxide minerals.

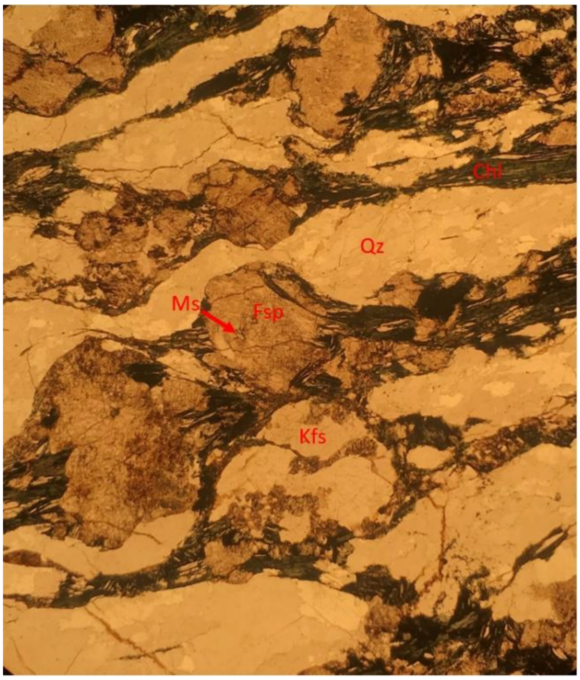

Figure 14 photo (X2.5) of a part of the thin section, displaying foliation of quartz and chlorite and larger phenocryst of feldspars (plagioclase).

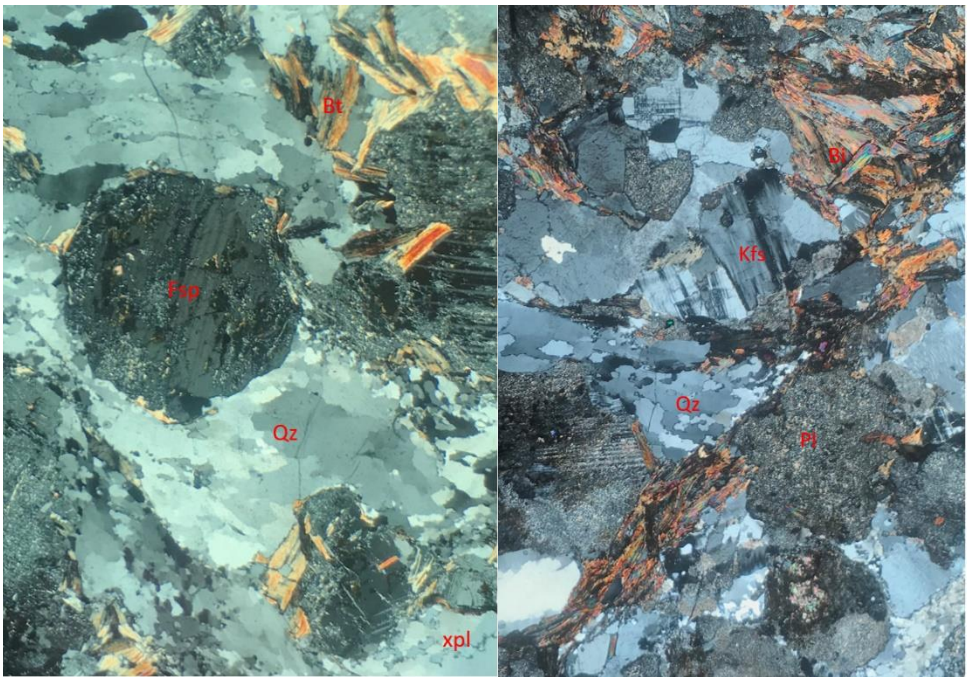

Figure 15 photo (X2.5) L. large fsp surrounded by deformed and recrystallized quartz. H. general minerology.

Diabase

The rock is fine grained (Fig. 16) with grains up to 2 mm wide. It is heavily weathered and deformed with grains displaying interlocking boundaries. The most common minerals in this rock are green minerals. Amphiboles are extremely weathered and most of the grains has been altered to chlorite. Chlorites appear both as alteration from amphibole minerals and as euhedral minerals. Plagioclases are complete sericitisied, and some plagioclases are stained with Fe-oxides. Quartz veins are crossing the rock and they consist of subgrains with undulose extinction. Accessory minerals are epidote, calcite, apatite, Ti-oxides, titanite and opaque minerals.

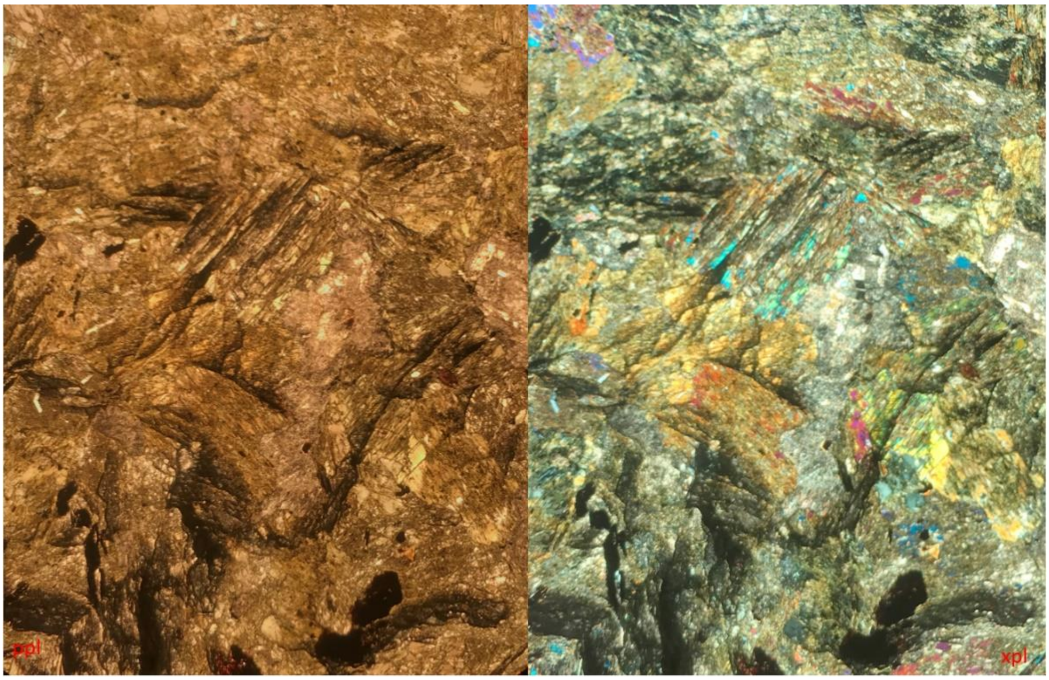

Figure 16 photo (X10) displaying the general minerology in the sample. Left photo in ppl right photo in xpl.

Point counting data

A correlation between the decrease in quartz and the increase of vugs can be seen in the fine-grained samples (Fig. 17). Lower percentage vugs in the samples correspond with higher percentage quartz grains. Vugs in the samples range from 6 to 18 %. Empty vugs without any infill made up less than 6 % of the sample with the highest amount of vugs. The sample with the least amount of vugs had less than 1 % empty vugs. A source for error here is that it can be difficult to distinguish between some white feldspars and quartz. The thin section is attached to a metal stand to stay in line and not to move freely and in some cases, this could be an obstacle to fully determine the type of grain. For medium- and coarse-grained samples, this correlation is not as clear. Here none of the samples have quartz regardless of the vug percentage (Fig. 18). The vug percentage of these samples can be difficult to represent due to the large grain size. One single feldspar grain can make up 75 % of the thin section and in other cases vugs can make up 50 % of the thin section. For medium- and coarse-grained samples most of the vugs have secondary mineral infill to them and less than 10 % of the vugs where empty.

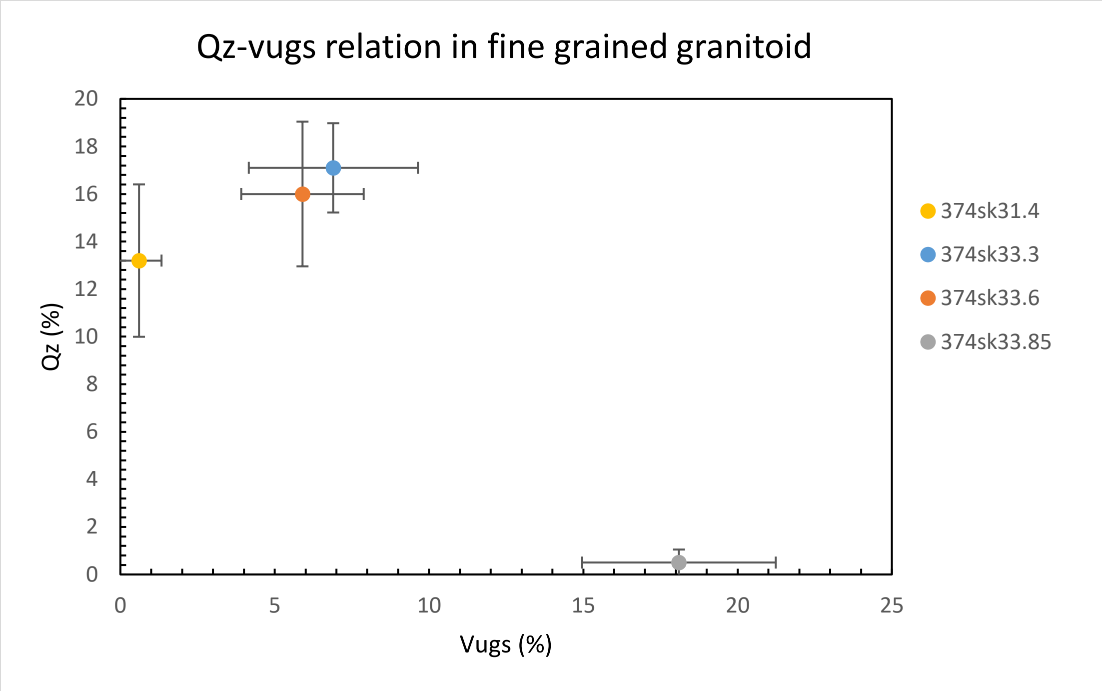

Figure 17 Graph showing the correlation between quartz and vugs in three different samples from the section containing fine grained granitoid.

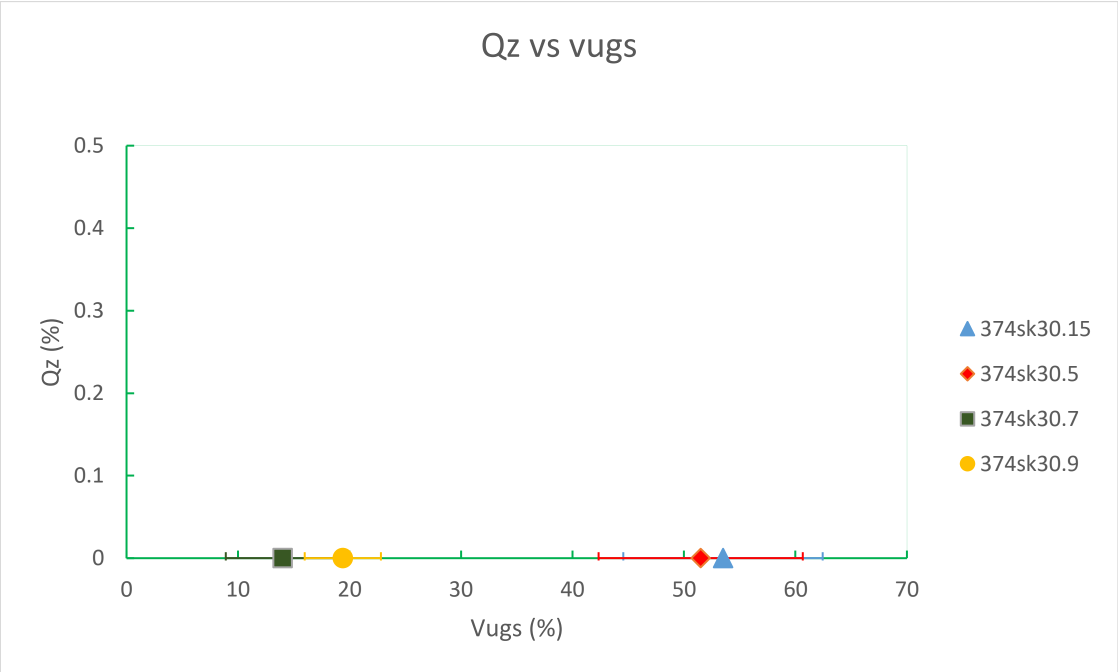

Figure 18 medium- and coarse- grained granitoid samples. Quartz vs vugs. The samples contain no visible quartz. The change in vug percentage is rather affected by the size of the grains in the sample and sizes of vugs.

XRF

From the XRF analysis (table 3) for the least altered fine grained granitoid, the major elements concentrations show for SiO_2 a concentration of 67.49 wt%. For Al_2O_3 the concentration is 14.8 wt% of the sample. The Na_2O concentration is 2.45 wt% and for K_2O it is 7.90 wt%. The concentration of Fe_2O_3 is 5.46 wt%, for MgO it is 1.02 wt% and for the rest of the major elements it is under one wt%. (CaO = 0.33, MnO = 0.02, P_2O_5 =0.08, TiO_2 = 0.46) wt%. Plotting the data of major oxides SiO_2 vs K_2O+Na_2O in a TAS diagram (Fig. 18) based after Cox et al., (1979) shows that the least altered low porosity granitoid plots in the granite field. When porosity increases in the fine grained granitoid the concentration of SiO_2 decreases. For the samples with most porosity the SiO_2 decreases to 62.1 wt%. Other oxides that also decrease in concentration are Fe_2O_3 that decreases to 5.1 wt% and MnO which decreases to zero. On the contrary, there are oxides which increase in concentration due to the increase in porosity. Such as Al_2O_3 which has a relative concentration increase to 18.1 wt%. For the alkali ions, the concentration has increased with Na_2O to 3.4 wt% and with K_2O to 8.4 wt%. The concentrations of TiO_2 increased to 0.7 wt% and MgO increased in concentration to 1.7 wt%. CaO increased to 0.4 wt%. Plotting the data from the samples with increased porosity in the TAS diagram shows they plot in the syenite field.

All the medium grained samples have a high amount of porosity. SiO_2 concentration are ranging between 62.2-61.46 7 wt% which are lower compared with the fine grained least altered sample. The fine-grained sample that had the highest amount of porosity had a SiO_2 concentration of 62.1 wt%. The relative Al_2O_3 concentration is ranging from 19.54-19.19 wt% which is higher than in the fine-grained samples. This could be the effect of the high porosity in these samples. Concerning the alkali ions in the samples, they show a higher concentration compared with the fine -grained samples. For K_2O have concentrations ranging between 9.59-10.13 wt% and 3.61-4.26 wt% for Na_2O. Fe_2O_3 concentrations are lower in the medium grained samples compared with the fine-grained. Here the concentrations range between 3.99-2.34 wt% for Fe_2O_3. Plotting the data in the TAS diagram shows the samples ending up in the syenite field or just above it due to the relatively high amount of alkali ions in the samples.

The coarse (pegmatitic) grained samples are varying in porosity, ranging from samples with low to high porosity. Even with the variation in porosity the SiO_2 concentrations of the samples do not show a large range, 63.7-62.03 wt%. Comparing these concentrations with the fine-grained samples show that the coarse-grained samples have concentrations close to the fine-grained sample with high porosity. The Al_2O_3 concentration is ranging from 19.03-20.76 wt%. The increase in Al_2O_3 compared with fine-grained samples can be an effect of relative concentration changes due to porosity increase. The alkali ions (K_2O+ Na_2O) in the samples demonstrate a much higher concentration compared with the fine -grained samples. The concentration of K_2O is higher in the coarse-grained samples compared with the fine-grained. The concentrations are ranging between 9.43-13.27 wt% and for Na_2O the concentration is ranging between 2.02-4.21 wt%, which for the low values are lower than the concentrations in the fine-grained sample. Fe_2O_3 concentrations are lower in the coarse-grained samples compared with the fine-grained. Here the concentrations range between 2.98-1.53 wt% for Fe_2O_3. When plotting the data in the TAS diagram the samples end up on the border to the syenite field or above it due to the relative high amount of alkali ions in the samples.

Table 3. Geochemical analyses of the episyenite granitoids.

Analyses	Major elements, Anhydrous normaliazed											
	Fine grained				Coarse grained					Medium grained		
Sample No.	374sk31.4	374sk33.3	374sk33.6	374sk33.85	374sk15.35	374sk15.55	374sk30.15	374sk30.5	374sk30.7	374sk30.9	374sk39.8	374sk41.95
SiO2 (wt%)	67.49	65.52	64.89	62.1	62.43	63.03	62.57	63.95	63.7	61.46	63.26	63.20
Al2O3	14.80	15.72	15.81	18.1	19.57	20.76	19.34	19.09	19.3	19.25	19.19	19.54
CaO	0.33	0.40	0.41	0.4	0.19	0.19	0.19	0.19	0.2	0.33	0.23	0.22
MgO	1.02	1.55	1.53	1.7	0.36	0.35	0.63	0.20	0.4	1.20	0.73	0.52
MnO	0.02	0.03	0.03	0.0	0.01	0.01	0.01	0.00	0.0	0.01	0.01	0.01
P2O5	0.08	0.13	0.13	0.1	0.01	0.01	0.01	0.01	0.0	0.06	0.03	0.02
Fe2O3	5.46	5.41	5.74	5.1	2.06	1.91	2.98	1.53	2.2	3.99	2.34	2.47
Na2O	2.45	2.48	2.36	3.4	2.02	4.27	3.42	3.36	4.1	3.61	3.89	4.26
K2O	7.90	8.10	8.45	8.4	13.27	9.43	10.68	11.61	10.1	9.62	10.13	9.59
TiO2	0.46	0.67	0.67	0.7	0.08	0.05	0.19	0.05	0.1	0.47	0.20	0.17
LOI	1.34	1.69	1.74	2.0	1.11	1.27	1.20	0.63	0.9	1.82	1.04	0.94

Standards: The best fitted standards in term of accuracy and precision were AGV-2. It gave values for Mg and Mn within ± 3 % and for K within ± 2 % and for the rest of the elements within ± 1 % accuracy.

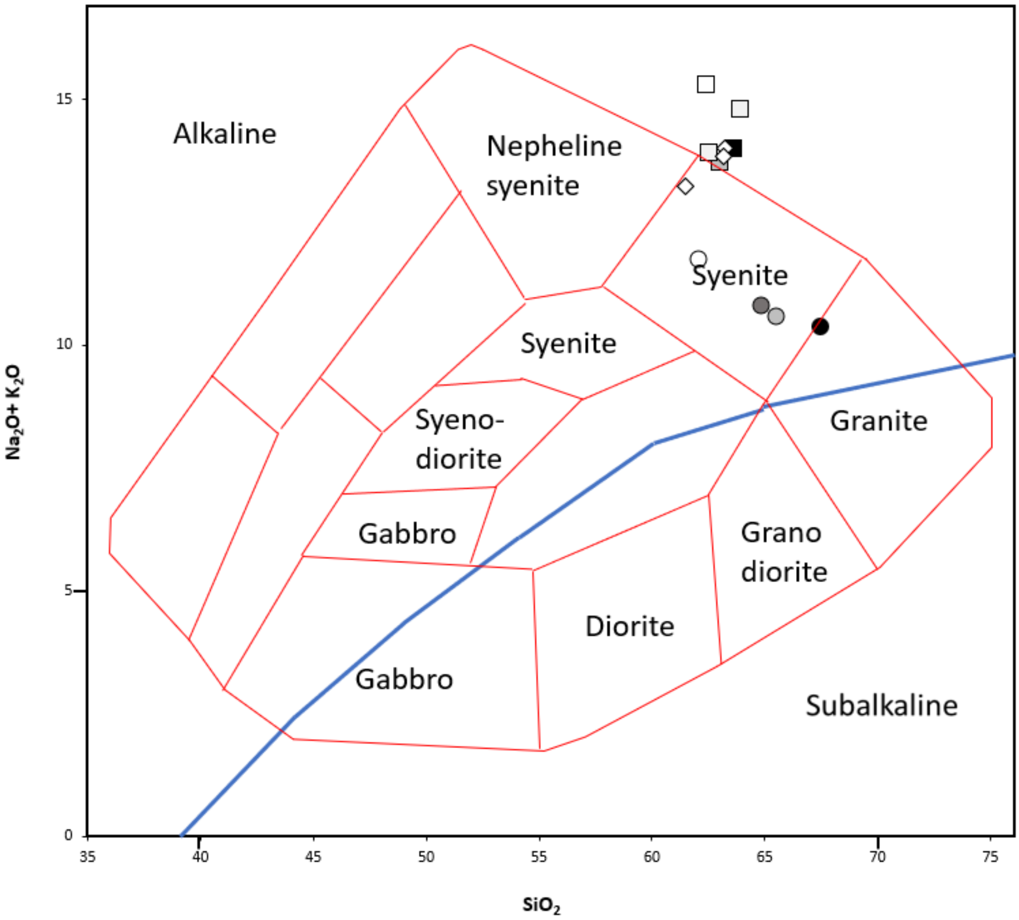

Figure 19 TAS diagram for rock classification, based after Cox et al., (1979).

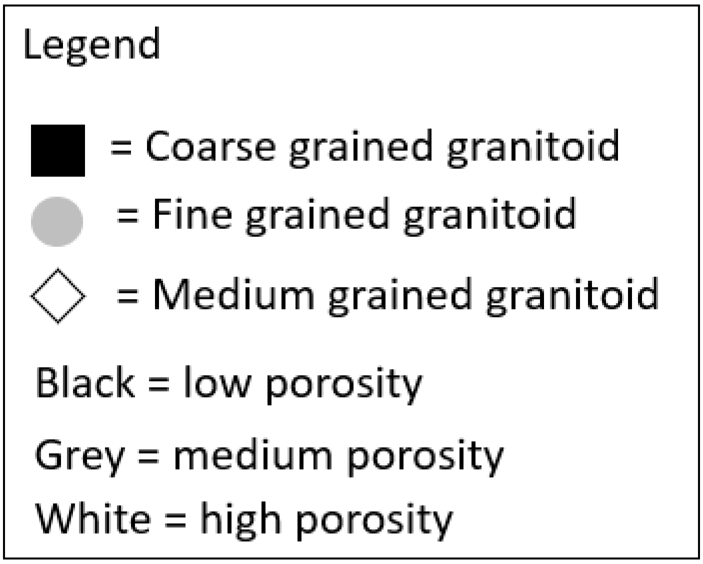

Discussion

Episyenite alteration

Based on the study carried out, it is clear that our samples of granitoids have the characteristics of episyenite, with its red colour, porous felspathic framework consisting of albite and microcline, a lack of quartz and the vugs with mineral infills that can be seen both in the drill core and in the thin sections.

Figure 19 shows that in the fine-grained granitoid, the least altered sample with lowest porosity plots in the granite field and as porosity increases SiO_2 decreases and Na_2O+K_2O increase pushing samples into the syenite field. Point counting data (Table 4) show that k-feldspar dominates the samples followed by plagioclase regardless of vug percentage. The samples generally had a low amount of vugs and as well as less infill minerals to them. In fine-grained samples infill minerals were not as abundant and had more diversity between albite, k-feldspars, and clays, with a fair amount of quartz grains still present in the samples. All this together keeps the fine-grained samples in moderate concentrations of Na_2O+K_2O compared with the other samples.

A similar but less clear trend can be observed in the coarse grained granitoid (Fig. 19). From point counting data sets (table 5.), coarse-grained samples are totally dominated by k-feldspars and plagioclase. Considering that most of the vugs have infill minerals to them, and that the most common infill minerals are albite and k-feldspars, this helped push the high concentrations of Na_2O+K_2O seen in figure 19 and with no visible quartz in the samples, the relatively low SiO_2 content follow. It is likely that the vugs in the coarse-grained samples were originally quartz grains even if no quartz is seen today in the samples. Only highly porous samples of the medium grained samples were preserved in the core, but it is likely that their least altered protoliths would have higher SiO_2 and lower Na_2O+K_2O and plot towards the granite field in the TAS diagram (Fig. 19). Only one medium-grained sample were point counting preformed on (table 5). The sample show a clear dominance of k-feldspar minerals followed by plagioclase. Vugs with infill minerals dominate the sample. The infill minerals are commonly albite and k-felspar as in the coarse samples which helped increase the concentrations for Na_2O+K_2O.

Table 4. point counting for fine-graine samples.

Sample	374sk31.4		374sk33.3		374sk33.6		374sk33.85	
	%	± 2σ	%	± 2σ	%	± 2σ	%	± 2σ
Kfs	35.7	4.5	26.6	3.2	29.1	3.8	31	3.6
Pl	27.4	4.2	18.8	2.8	21.3	3.4	23.3	3.3
Vug	0.2	0.4	2.9	1.2	2.1	1.2	5.7	1.8
Vug + infill	0.4	0.6	4	1.4	3.8	1.6	12.4	2.6
Bt	4.3	1.9	5.8	1.7	2.4	1.3	6.2	1.9
Chl	0	0.0	0	0.0	0	0.0	0	0.0
Qz	13.2	3.2	17.1	2.7	16	3.0	0.5	0.5
Secondary minerals	9.4	2.8	11.3	2.3	14.8	2.9	11	2.4
Other minerals	9.4	2.8	13.5	2.5	10.7	2.6	9.8	2.3
Total vugs in samples	0.6	0.7	6.9	1.9	5.9	2.0	18.1	3.1

Table 5. point counting data. The three fist samples from left were coarse-grained samples. The last is from a medium-grained sample.

Sample	**374sk30.15**		**374sk30.5**		**374sk30.7**		**374sk30.9**	
	%	± 2σ	%	± 2σ	%	± 2σ	%	± 2σ
Kfs	15.3	5.7	13.2	5.8	85	5.1	44.6	4.1
Pl	26.1	7.0	35.3	8.2	2.1	2.1	11.1	2.6
Vug	7	4.1	3.7	3.2	2.1	2.1	5	1.8
Vug + infill	46.5	8.0	47.8	8.6	11.9	4.7	14.4	2.9
Bt	0	0.0	0	0.0	0	0.0	1.9	1.1
Chl	5.1	3.5	0	0.0	0	0.0	0	0.0
Qz	0	0.0	0	0.0	0	0.0	0	0.0
Secondary minerals	0	0.0	0	0.0	0.5	1.0	19	3.2
Other minerals	0	0.0	0	0.0	0	0.0	4.1	1.6
Total vugs in samples	53.5	8.9	51.5	9.2	14	5.1	19.4	3.4

Comparison with other studies

To interpret the geochemical data of the granitoid samples the major oxides were plotted in a Harker diagram (Fig. 20) together with compositions of other metagranite and episyenite samples from Forsmark (Petersson et al., 2004) which has the closest documented episyenite alteration to the Stockholm area. Geochemical data from granites in the Stockholm area (Geijer, 1913) are also plotted in order to have a geochemical comparison between other granites in Stockholm area and our samples. It is likely that the episyenite in Stockholm formed under similar conditions to those from Forsmark. They both belong to the Bergslagen lithological unit, and both the areas developed and evolved during the Svecokarelian orogeny and the belonging metamorphism that occurred. The geochemical data from Forsmark is taken from a drill core where 3 samples that were identified as episyenite although one of them had been resilicified. The rest of the samples were classified as metagranite-granodiorite. The geochemical data from Stockholm area (Svälnäs, Alby, Edeby, Vasastaden) were done by Holmquist (1910) found in Geijer (1913).

For the samples analysed in this study, similar trends can be observed in the Harker diagrams in Figure 20 as are shown in the TAS diagram in Figure 19 such as increasing K_2O and Na_2O with decreasing SiO_2 as porosity increases. The compositions of the samples from this study are different to those from the other areas such as Forsmark, but some of the same trends can be observed (Fig. 20). For example, Na_2O concentrations increase as SiO_2 decreases in episyenite samples from Forsmark compared to the least altered granites (Fig. 20). For our fine-grained samples K_2O trends are stable and do not show a clear trend of increased K_2O as SiO_2 decreases. But K_2O concentrations are higher in our samples than the samples of Forsmark.

For Al_2O_3 which is considered to be an immobile element, there is a slight increase in content with decreasing SiO_2. This is most likely due to passive enrichment of Al_2O_3 due to removal of SiO_2 from the rocks. Similar trends can also be observed for TiO_2 and MgO (Fig. 20) which is also an immobile element.
For CaO all episyenite altered samples show a decrease in concentrations compared with non-altered samples. CaO loss is common during albitization of plagioclase (Suikkanen and Rämö, 2019).

Looking closer to the alkali for our episyenite samples and plotting them in a Q_1-F_1 diagram (Fig. 21) based after Cathelineau, (1986) the samples plot on the k-metasomatism side indicating that they would be subject of a type III alteration (Cathelineau, 1986). However, we were not able to do a proper mass balance to see if this is really metasomatism or rather the granites are slightly enriched in K^+ from formation. The alteration vector in figure 21 rather move vertical down indicating a loss in silica of the granites compared with the other granites from Stockholm area. Then increment in K^+. Compared with

Forsmark is considered to be a type II alteration (Petersson et al., 2012). Petersson et al., (2012) suggested that the episyenite in Forsmark had formed in brittle regime (< 300 ˚C) at circa 1800-1700 Ma, after peak metamorphism and that the fluid that had caused the alteration had a higher temperature then 300 ˚C. Other studies from Hercynian granites have shown that fluids would had have a temperature of circa 250-450 ˚C and a pressure of 500 bar and a low to moderate salinity 0-12 eq. NaCl (Turpin et al., 1990) and that the hydrothermal fluids was caused by the intrusions of dykes in the area.
The process of forming episyenite based on the observations in SiO_2 decreases and Na_2O+K_2O this study is:

1) dissolution of quartz
2) Secondary feldspar precipitation (both albite and k-feldspar)
3) A later fluid-rock interaction event possibly with meteoric fluid that precipitates new minerals inside or on the walls of the formed vugs. This event also causes clay alteration and precipitation of feldspar and biotite

This sequence of events is similar to that presented by Petersson and Eliasson, (1997). Our samples have a deep red colour and the vugs are partly filled with tiny red grains of albite that forms larger aggregates. Between grain boundaries extremely small iron-oxides could be present causing the deep-red colour of rock. Eliasson, (1993) have shown that the red colour in granites from Stipa was caused by haematite and Fe-oxyhydroxide along grain boundaries and microfractures. Suikkanen and Rämö, (2019) concluded that the red colour in episyenite was caused by fine films of haematite along grain boundaries. From Äspö the deep red colour in granites was caused by a late-stage low temperature prosses (150-200 ˚C) forming fine-grained Fe-oxyhydroxide/hydroxides (Eliasson, 1993).

Rock mass stability

Rock stability is affected by episyenitisation which increases the porosity of the rock. When constructing tunnels in rocks, geologists can use a geological strain index (GSI) (Sonmez and Ulusay, 1999) chart as aid. Based on the visible observation in the rock GSI generates a number based on criteria that engineers can use for determining the proper measures to take while construction the tunnel. In the case of episyenite it would obtain the lower values in the chart. Because episyenite being a high porosity rock groundwater flow may be affected (Petersson et al., 2012), possibly leading to water leaking in which could affect the constructions.

Clay alteration

Most of the plagioclase in the samples have undergone sericite alteration. This is a common alteration type. Sericite can form from hydrothermal fluids that are slightly acid. At temperatures around 200-250˚C fine-grained sericite forms (Thompson et al., 1996). Clay mixes was recognized as a mineral in some of the vugs. Geochemical they were not pure, but a qualified guess would be it is kaolinite and Illite that can form from weathering of feldspars in the present of meteoric waters close to the surface. These minerals are non-swelling ones. They can also be formed by hydrothermal alteration under low temperatures.

Adjacent to the biotite grains in the different samples a green-yellow coloured clay mineral where present. It is believed to have been formed from the weathering or alteration of the biotite in presumably later event after the episyenite was formed. Clay minerals forms by interaction with H_2O at relatively low temperatures where as episyenite would have had higher temperature fluids. This clay chemistry does not clearly correspond to any of the known clay groups associated with biotite alteration. One reason for this can have to do with the fact that there is a pre-stage of clay or rather a mix of different clay types. A clay group that are formed from alteration of biotite is vermiculite. These minerals are swelling in contact with H_2O and could therefore be considered as a potential risk for rock stability when constructing the tunnel.

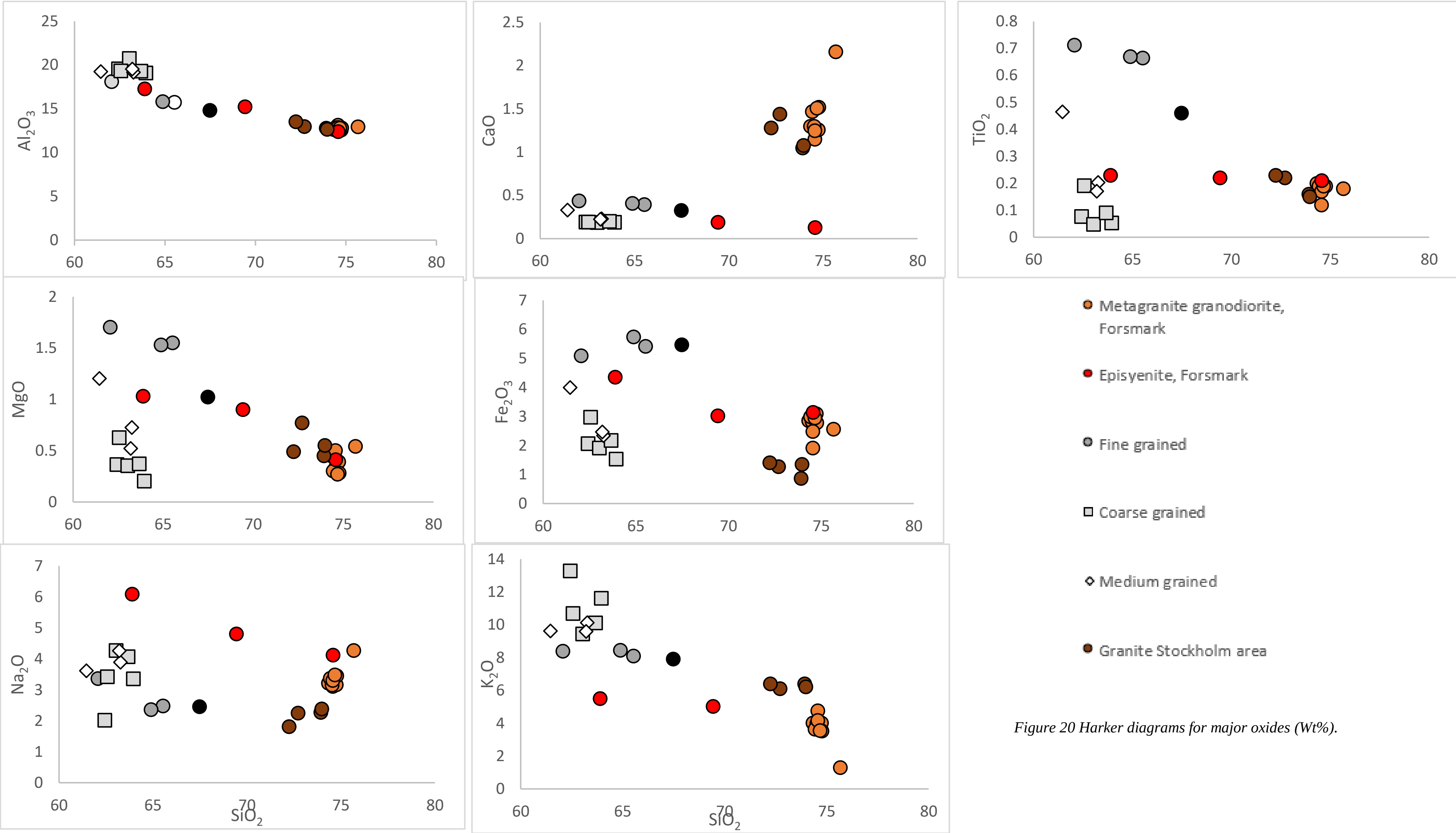

Figure 20 Harker diagrams for major oxides (Wt%).

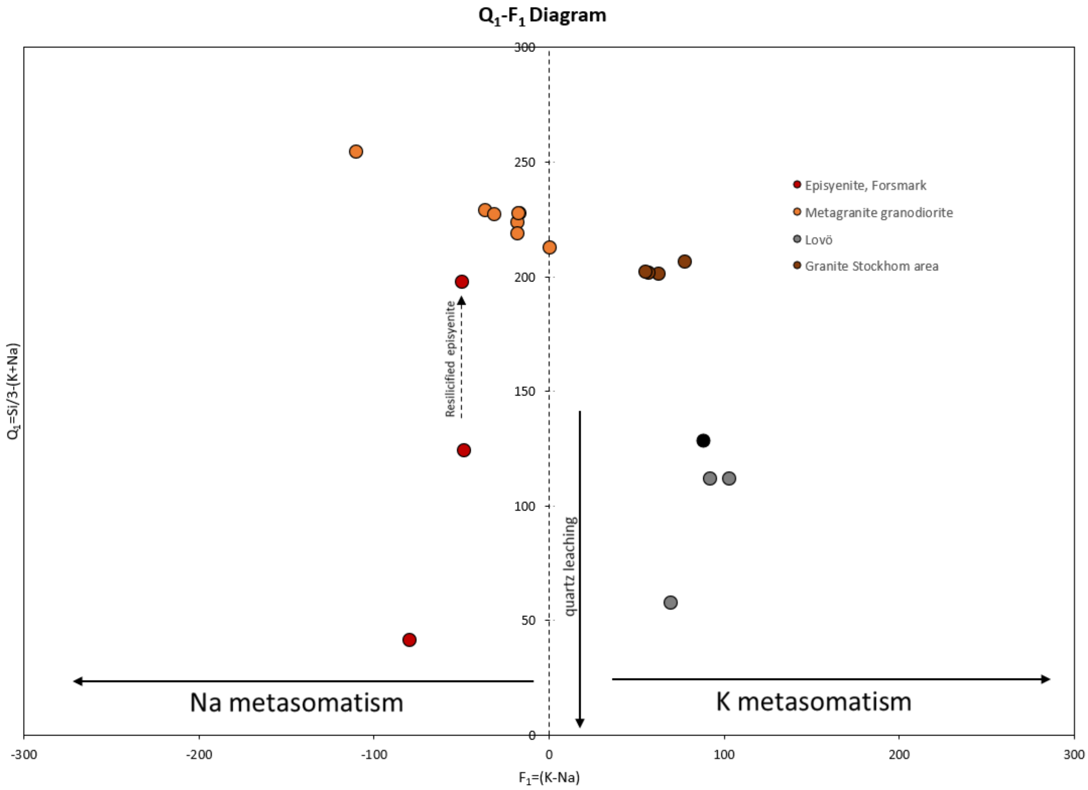

Figure 11 Q_1-F_1 plot of samples of fine-grained granitoid from Lovön (. Plus comparing samples from Forsmarks Metagranite-granodiorite and granites from Stockholm.

Conclusions

The following conclusion can be drowned from the study of the drill core 19A374sk from Lovön.

- Vuggy granitoids occur in three different grain-sizes, fine, medium, and coarse. They are all mainly constructed of plagioclase and k-feldspar and minor biotite.
- The fine-grained rocks still contained larger amounts of quartz grains compared with medium and coarse-grained rocks that contain low or no visible quartz.
- The rocks are rich in potassium and the vugs are partly or fully infilled with secondary minerals. The rocks have the characteristics of a type-III episyenitisation.
- Most common infill minerals are albite, k-feldspar, and other clay types of minerals.
- No uranium or other types of metal-bearing mineralisation has been found in the vugs.

Acknowledgments

I would like to thank AFRY who financed this project. I would like to thank my main supervisor Iain Pitcairn (SU) who helped me through the project and my co-supervisor Felix Makowsky from AFRY who proposed this thesis project. I would also like to thank Victoria Pease (SU) for helping with the XRF analysis and Andreas Karlsson (NRM) for helping with SEM analysis.

References

Cathelineau, M., 1985, Quartz leaching and hydrothermal alkali metasomatism in granites: J Petrol.

Cathelineau, M., 1986, The hydrothermal alkali metasomatism effects on granitic rocks: Quartz dissolution and related subsolidus changes: Journal of Petrology, v. 27, p. 945–965.

Cheilletz, A., and Giuliani, G., 1982, Role de la D�formation du Granite dans la Gen�se des Episy�nites Feldspathiques des Massifs de Lovios-Geres (Galice) et des Zaer (Maroc Central): Mineralium Deposita, v. 17.

Dempsey, C. S., Meighan, I. G., and Fallick, A. E., 1990, Desilication of Caledonian granites in the Barnesmore complex, Co. Donegal: The origin and significance of metasomatic syenite bodies: Geological Journal, v. 25, p. 371–380.

Dolníček, Z., René, M., Hermannová, S., and Prochaska, W., 2014, Origin of the Okrouhlá Radouň episyenite-hosted uranium deposit, Bohemian Massif, Czech Republic: Fluid inclusion and stable isotope constraints: Mineralium Deposita, v. 49, p. 409–425.

Eglinger, A., Tarantola, A., Durand, C., Ferraina, C., Vanderhaeghe, O., André-Mayer, A. S., Paquette, J. L., and Deloule, E., 2014, Uranium mobilization by fluids associated with Ca-Na metasomatism: A P-T-t record of fluid-rock interactions during Pan-African metamorphism (Western Zambian Copperbelt): Chemical Geology, v. 386, p. 218–237.

Eliasson, T., 1993, Mineralogy, geochemistry and petrophysics of red coloured granite adjacent to fractures.:

Fraipont, P. D., 1982,Approche multiscalaire de la fracturation du massif granitique de Saint Sylvestre, Télédétection et analyse tectonique appliquées aux gisements d'uranium de la division de la Crouzille (Cogema) Limousin, Massif Central français: Uni. Strasbourg.

Geijer, P., 1913, Zur petrographie des stockholm-granites: Gff, v. 35, p. 123–150.

Hecht, L., Thuro, K., Plinninger, R., and Cuney, M., 1999, Mineralogical and geochemical characteristics of hydrothermal alteration and episyenitization in the Konigshain granites, northern Bohemian Massif, Germany: International Journal of Earth Sciences, v. 88, p. 236–252.

Ivarsson, C., and Johansson, Å., 1995, U-Pb zircon dating of Stockholm granite at Frescati: GFF, v. 117, p. 67–68.

Jébrak, M., 1991, Une épisyénite à or dans la ceinture archéenne de l'Abitibi (Québec): Comptes rendus de l'Académie des sciences. Série 2, Mécanique, Physique, Chimie, Sciences de l'univers, Sciences de la Terre, v. 313, p. 1031–1037.

Leroy, J., 1978, The Margnac and Fanay uranium deposits of the La Crouzille District (western Massif Central, France); geologic and fluid inclusion studies: Economic Geology, v. 73, p. 1611–1634.

Leroy, J., and Cathelineau, M., 1982, Les mineraux phylliteux dans les gisements hydrothermaux d'uranium. I. Cristallochimie des micas herites et neoformes.: Bulletin de Mineralogie, v. 105, p. 99–109.

López-Moro, F. J., Romer, R. L., Rhede, D., Fernández, A., Timón-Sánchez, S. M., and Moro, M. C., 2019, Early uranium mobilization in late Variscan strike-slip shear zones affecting leucogranites of central western Spain: Journal of Iberian Geology, v. 45, p. 223–243.

Martin, S., 1981,Episyênitisation et minéralisation dans le leucogranite d'Hyvernersse (Nord Millevaches, M.C.E1.): Univ. Clermont II.

McLemore, V. T., 2012, Rare earth elements (REE) deposits in New Mexico: 2012 SME Annual Meeting and Exhibit 2012, SME 2012, Meeting Preprints, p. 707–713.

Möller, C., Snäll, S. ., and Stephens, M. B., 2003, Forsmark site investigation Dissolution of quartz, vug formation and new grain growth associated with post-metamorphic hydrothermal alteration in KFM02A:, accessed at https://www.researchgate.net/publication/268353981%0AP-03-77.

Petersson, J., and Eliasson, T., 1997, Mineral evolution and element mobility during episyenitization (dequartzification) and albitization in the postkinematic Bohus granite, southwest Sweden: Lithos, v. 42, p. 123–146.

Petersson, J., Whitehouse, M. J., and Eliasson, T., 2001, Ion microprobe U-Pb dating of hydrothermal xenotime from an episyenite: Evidence for rift-related reactivation: Chemical Geology, v. 175, p. 703–712.

Petersson, J., Berglund, J., Danielsson, P., Wängnerud, A., Tullborg, E., and Ab, T., 2004, P-04-103 Forsmark site investigation:

Petersson, J., Stephens, M. B., Mattsson, H., and Möller, C., 2012, Albitization and quartz dissolution in Paleoproterozoic metagranite, central Sweden - Implications for the disposal of spent nuclear fuel in a deep geological repository: Lithos, v. 148, p. 10–26.

Petersson, J., Fallick, A. E., Broman, C., and Eliasson, T., 2014, Imprints of multiple fluid regimes on episyenites in the Bohus granite, Sweden: Lithos, v. 196–197, p. 99–114.

Plas, L. v. d., and Tobi, A. C., 1965, A chart for judging the reliability of point counting results: American Journal of Science, v. 263, p. 87–90.

Poty, B., Leroy, J., Cathelineau, M., Cuney, M., Friedrich, M., Lespinasse, M., and Turpin, L., 1986, Uranium deposits spatially related to granites in the French part of the Hercynian orogen:

Recio, C., Fallick, A. E., Ugidos, J. M., and Stephens, W. E., 1997, Characterization of multiple fluid-granite interaction processes in the episyenites of Avila-Béjar, Central Iberian Massif, Spain: Chemical Geology, v. 143, p. 127–144.

Söderlund, U., Elming, S.-Å., Ernst, R. E., and Schissel, D., 2006, The Central Scandinavian Dolerite Group—Protracted hotspot activity or back-arc magmatism? Precambrian Research, v. 150, p. 136–152.

Sonmez, H., and Ulusay, R., 1999, Modifications to the geological strength index (GSI) and their applicability to stability of slopes: International Journal of Rock Mechanics and Mining Sciences, v. 36, p. 743–760.

Stalhos, G., 1969, Beskrivning till stockholmstraktensberggrund (P. H. . Lundegårdh, Ed.): Stockholm, Norstedt, 190 p.

Suikkanen, E., and Rämö, O. T., 2019, Episyenites—Characteristics, Genetic Constraints, and Mineral Potential: Mining, Metallurgy and Exploration, v. 36, p. 861–878.

Thompson, A. J. B., Thompson, J. F. H., Allen, R. L., Barrett, T. J., Browne, P. R. L., Clemson, J. E., Dunne, K. P. E., Ettlinger, A. D., Gibson, H. L., Groat, L. A., Hannington, M. D., Hawke, M. M., Jowett, E. C., Lang, J. R., et al., 1996, Atlas of Alteration: A Field and Petrographic Guide to Hydrothermal Alteration Minerals: p. 119.

Trafikverket, 2020, Våren 2020: det här händer i E4 Förbifart Stockholm, Trafikverket (https://www.trafikverket.se/nara-dig/Stockholm/vi-bygger-och-forbattrar/Forbifart-stockholm/Aktuellt/2020/2020-03/varen-2020-det-har-hander-i-e4-forbifart-stockholm/).

Turpin, L., 1984, Altérations hydrothermales et caractérisation isotopique (OHC) des minéraux et des fluides dans le massif uranifère de Saint-Sylvestre-extension à d’autres gisements intragranitiques d’uranium français: Extension à d’autres gisements intragranitiques d’uranium français. Géol Géochim Uranium, Mém. Nancy, v. 6, p. 290.

Turpin, L., Leroy, J. L., and Sheppard, S. M. F., 1990, Isotopic systematics (O, H, C, Sr, Nd) of superimposed barren and U-bearing hydrothermal systems in a Hercynian granite, Massif Central, France: Chemical Geology, v. 88, p. 85–98.

Vass, A., 2012,Structural Model of the Lambarfjärden Area from Surface and Subsurface Data in Connection with the E4 Stockholm Bypass Structural Model of the Lambarfjärden Area from Surface and Subsurface Data in Connection with the E4 Stockholm Bypass Structural Model: Uppsala universitet: 59 p.

Wahlgren, C.-H., Schoning, K., and Hansen, L. M., 2018, Stockholmsområdets berggrund, jordarter, geologiska utveckling och erfarenheter från infrastrukturprojekt:

Whitney, D. L., and Evans, B. W., 2010, Abbreviations for names of rock-forming minerals: American Mineralogist, v. 95, p. 185–187.

Appendix

Core log

In the core log shown in the figure below. The first column from left represents the lithology with 3 main rock types based on the colour - felsic intrusive (red colour), sedimentary (white colour), mafic or intermediate intrusive (green colour). The second column shows the vug percentage (ranging from 0 to 30 percent) of the lateral surface of the core. The size of the vugs is shown by the colour; black is large vugs (>5 mm) and blue is fine vugs (<2 mm). The third column has a short description of textural properties of the core. The fourth column shows the alteration mineralogy dominant for the specific section. The fifth column shows were the samples for thin-section and chemical analysis was taken.

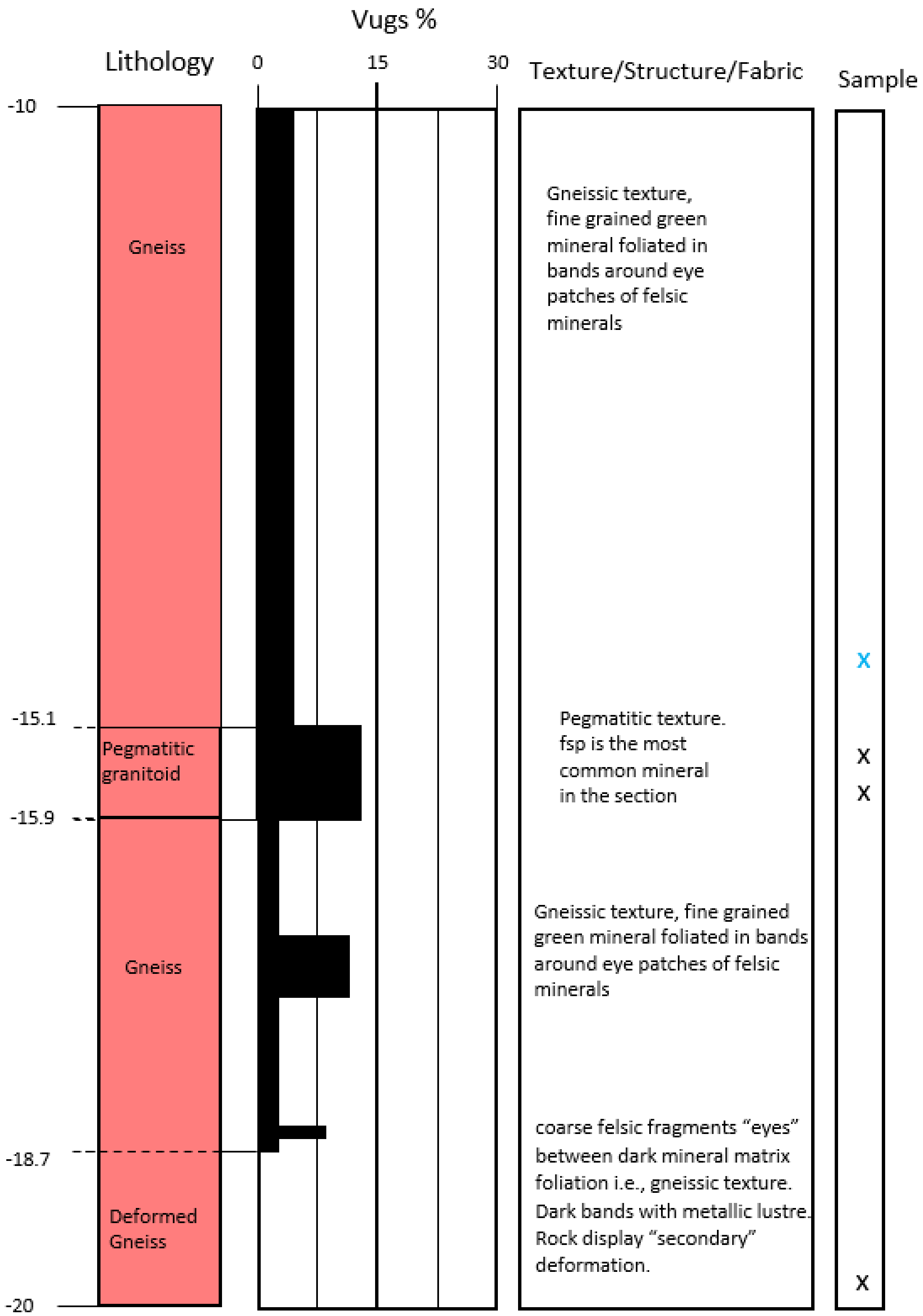

Vugs %
Lithology
0
15
30
Texture/Structure/Fabric
Sample
-10
Gneiss
Gneissic texture, fine grained green mineral foliated in bands around eye patches of felsic minerals
X
-15.1
Pegmatitic granitoid
Pegmatitic texture. fsp is the most common mineral in the section
X
X
-15.9
Gneiss
Gneissic texture, fine grained green mineral foliated in bands around eye patches of felsic minerals
-18.7
Deformed Gneiss
coarse felsic fragments "eyes" between dark mineral matrix foliation i.e., gneissic texture. Dark bands with metallic lustre. Rock display "secondary" deformation.
X
-20

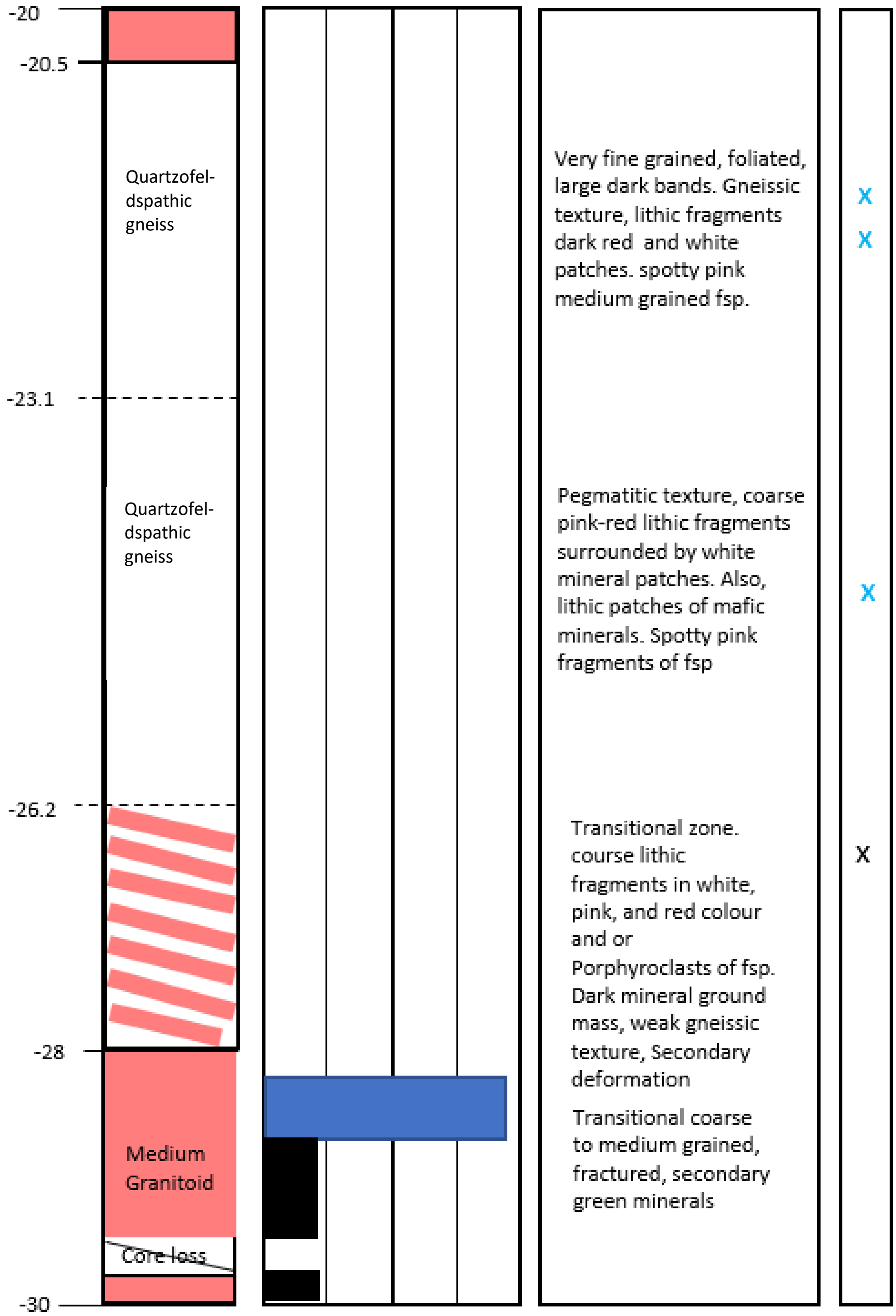
-20
-20.5
Quartzofel-dspathic gneiss
-23.1
Quartzofel-dspathic gneiss
-26.2
-28
Medium Granitoid
Core loss
-30
Very fine grained, foliated, large dark bands. Gneissic texture, lithic fragments dark red and white patches. spotty pink medium grained fsp.
Pegmatitic texture, coarse pink-red lithic fragments surrounded by white mineral patches. Also, lithic patches of mafic minerals. Spotty pink fragments of fsp
Transitional zone. course lithic fragments in white, pink, and red colour and or Porphyroclasts of fsp. Dark mineral ground mass, weak gneissic texture, Secondary deformation
Transitional coarse to medium grained, fractured, secondary green minerals
X
X
X
X

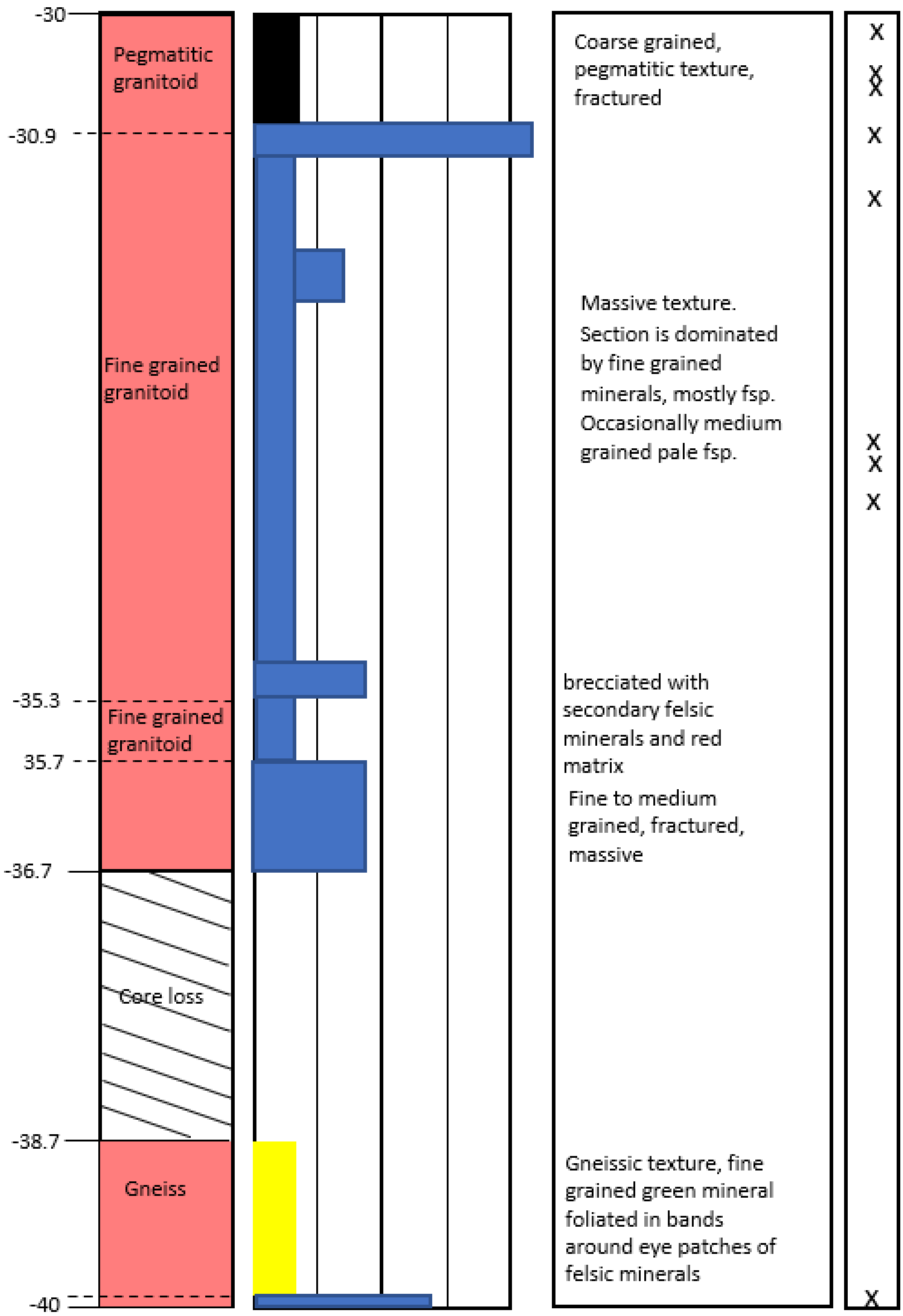
-30
-30.9
-35.3
35.7
-36.7
-38.7
-40
Pegmatitic granitoid
Fine grained granitoid
Fine grained granitoid
Core loss
Gneiss
Coarse grained, pegmatitic texture, fractured
Massive texture. Section is dominated by fine grained minerals, mostly fsp. Occasionally medium grained pale fsp.
brecciated with secondary felsic minerals and red matrix
Fine to medium grained, fractured, massive
Gneissic texture, fine grained green mineral foliated in bands around eye patches of felsic minerals

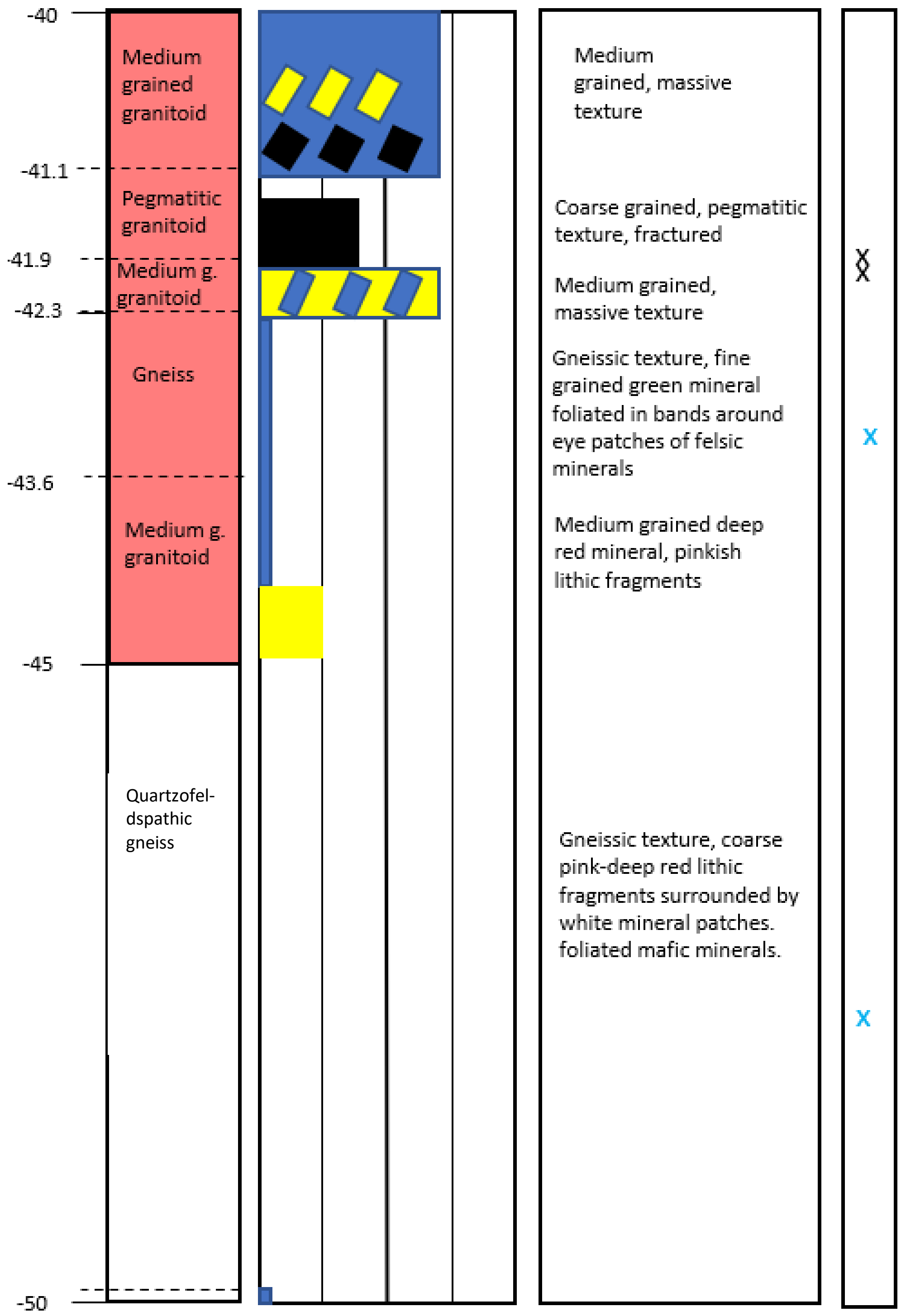
-40
-41.1
-41.9
-42.3
-43.6
-45
-50
Medium grained granitoid
Pegmatitic granitoid
Medium g. granitoid
Gneiss
Medium g. granitoid
Quartzofel-dspathic gneiss
Medium grained, massive texture
Coarse grained, pegmatitic texture, fractured
Medium grained, massive texture
Gneissic texture, fine grained green mineral foliated in bands around eye patches of felsic minerals
Medium grained deep red mineral, pinkish lithic fragments
Gneissic texture, coarse pink-deep red lithic fragments surrounded by white mineral patches. foliated mafic minerals.
X
X

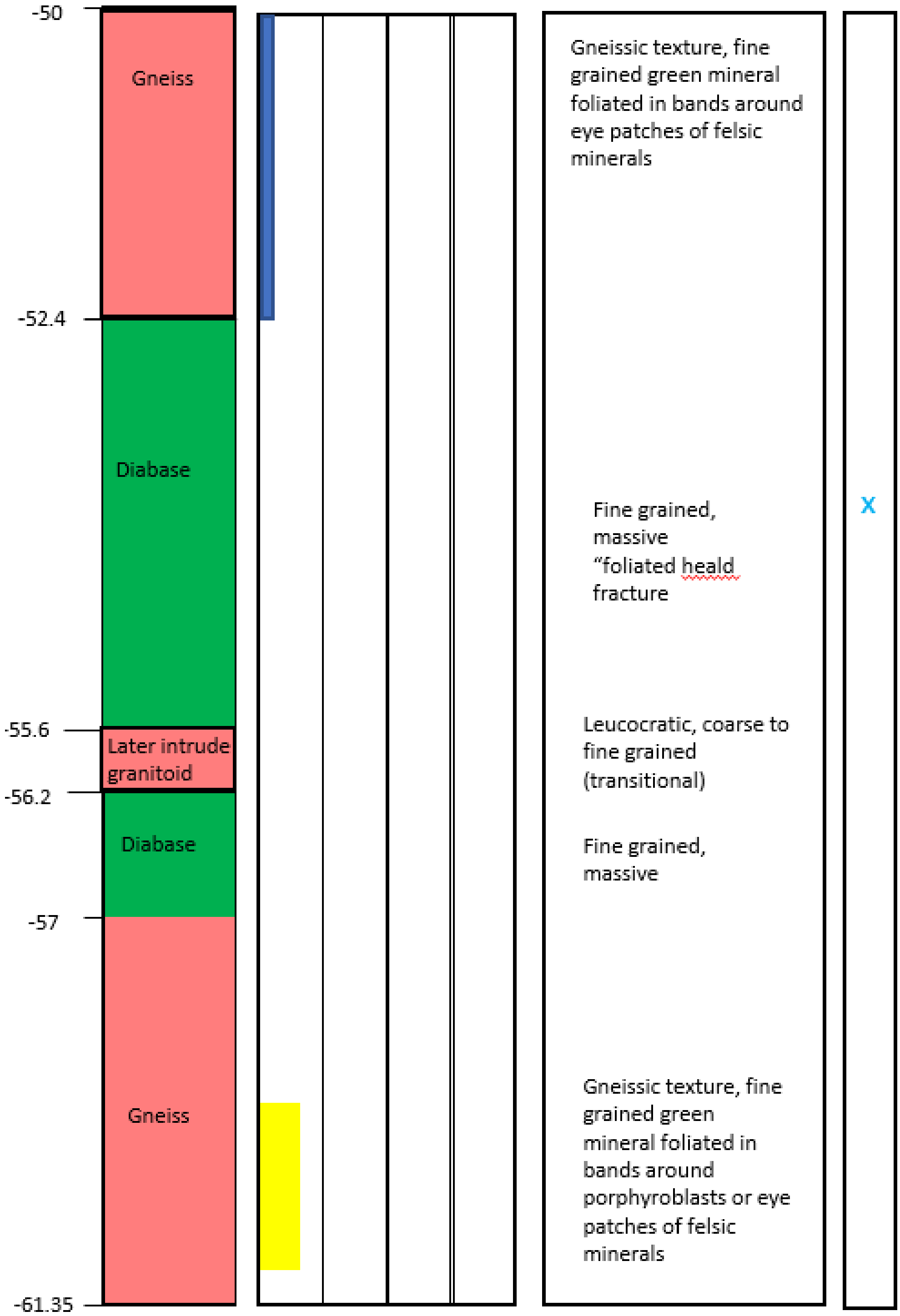
-50
Gneiss
Gneissic texture, fine grained green mineral foliated in bands around eye patches of felsic minerals
-52.4
Diabase
Fine grained, massive "foliated heald fracture
X
-55.6
Later intrude granitoid
Leucocratic, coarse to fine grained (transitional)
-56.2
Diabase
Fine grained, massive
-57
Gneiss
Gneissic texture, fine grained green mineral foliated in bands around porphyroblasts or eye patches of felsic minerals
-61.35

Chiefly gneissic rock types in Svecokarelian orogeny (2850-1870) ma

- Felsic intrusive rock
- Quartz-feldspar rich rock
- Ultramafic, mafic and intermediate intrusive rock

- Large vugs
- Small vugs
- Medium vugs

x = thin-section + chemical analysis

x = thin-section

Sample photographs

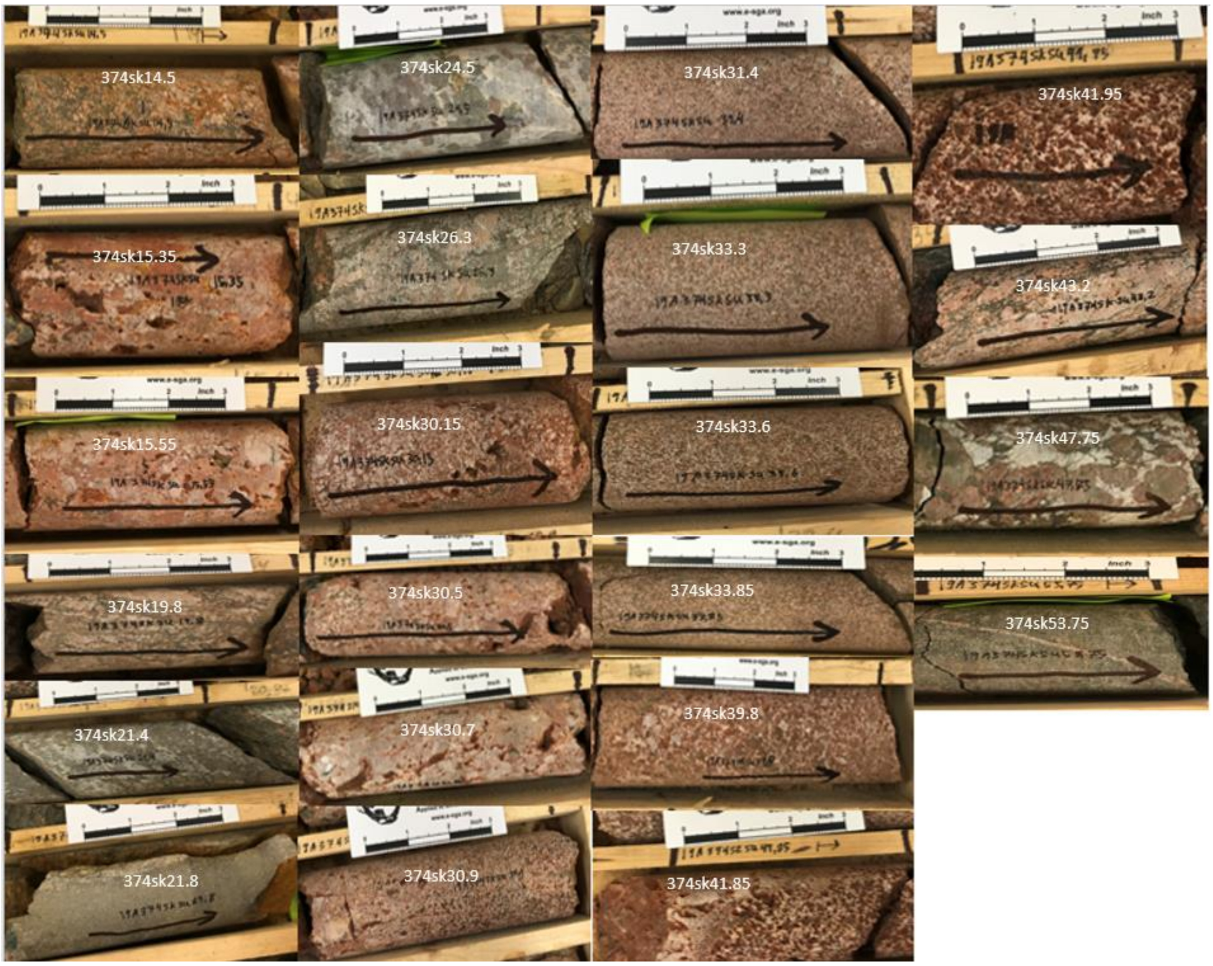

Scanned image of pieces for thin section

Thin section descriptions

Sample 374sk14.5

Mineralogy: Kfs (40%), Pl (15%), Bi/Chl (10%).

The sample is medium grained with feldspars up to 5 mm wide. It has irregular foliation bands of biotite/chlorite and it is heavily weathered and fractured containing proportions of vugs. These are commonly infilled with a red brown dusty mineral. The most common mineral in this sample is Alkali-feldspar which appears as better-preserved, anhedral grains with tartan twinning or perthite unmixing.

Grains with albite twinning can also be seen. The grains have inclusions of sericite. Plagioclase is the next most abundant mineral and is strongly altered to sericite. Within the areas of most intense sericitisation are coarser muscovite grains. Lamellae twinning cannot or barely be observed in the grains. Majority of the biotite have been altered to chlorite. They form aggregates of bands. Within the grains they have turned opaque. Inside the biotite grains zircon grains are found. The sample contains a large abundance of vugs that have irregular shapes and contain secondary mineral infill. The most common secondary mineral is goethite that have a dark red brown colour and tabular form occurring commonly in aggregates. Tooth shaped colourless low birefringence mineral also fill the vugs. These commonly have twinning and exsolution lamellae and are interpreted to be feldspar. The shape of the grains indicate that they are secondary and grew into space once the vugs had been developed. A green-yellow coloured anhedral mineral with no pleochroism or appears cleavage, II- order birefringence. Other secondary minerals include opaque minerals, micas (including muscovite).

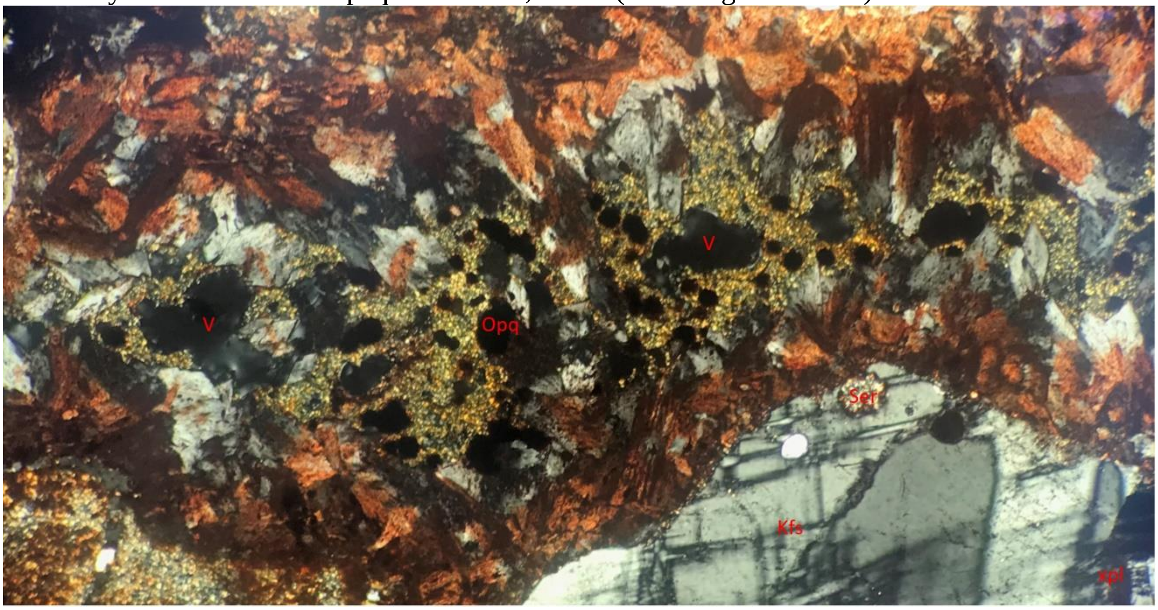

Sample 374sk15.35

Mineralogy: Kfs (25%), Pl (20%).

The sample is very coarse grained (pegmatitic) with feldspars up to 1.5 cm wide. It is heavily weathered and fractured and contains a large proportion of vugs, which are commonly infilled with secondary minerals. The most common mineral in this sample is Alkali-feldspar which occurs as well-preserved, subhedral grains with tartan twinning or perthite unmixing. The grains have inclusions of sericite. Plagioclase is the next most abundant mineral and is strongly altered to sericite. Within the areas of most intense sericitisation are coarser muscovite grains. Lamellae twinning can barely be observed in the grains. Chlorites in the sample are few and they form larger aggregates. Accessory minerals in the sample are Ti-bearing minerals and muscovite. The sample contains a large abundance of vugs that have irregular shape and contain secondary mineral infill. The most common secondary mineral is a tooth shaped colourless low birefringence mineral. These commonly have twinning and exsolution lamellae and are interpreted to be feldspar. The shape of the grains indicate that they are secondary and grew into space once the vugs had been developed. Other infill minerals are goethite that have a dark red brown colour and tabular form occurring commonly in aggregates. Other secondary infill mineral is a dark yellow coloured, anhedral with no pleochroism and II-order birefringence.

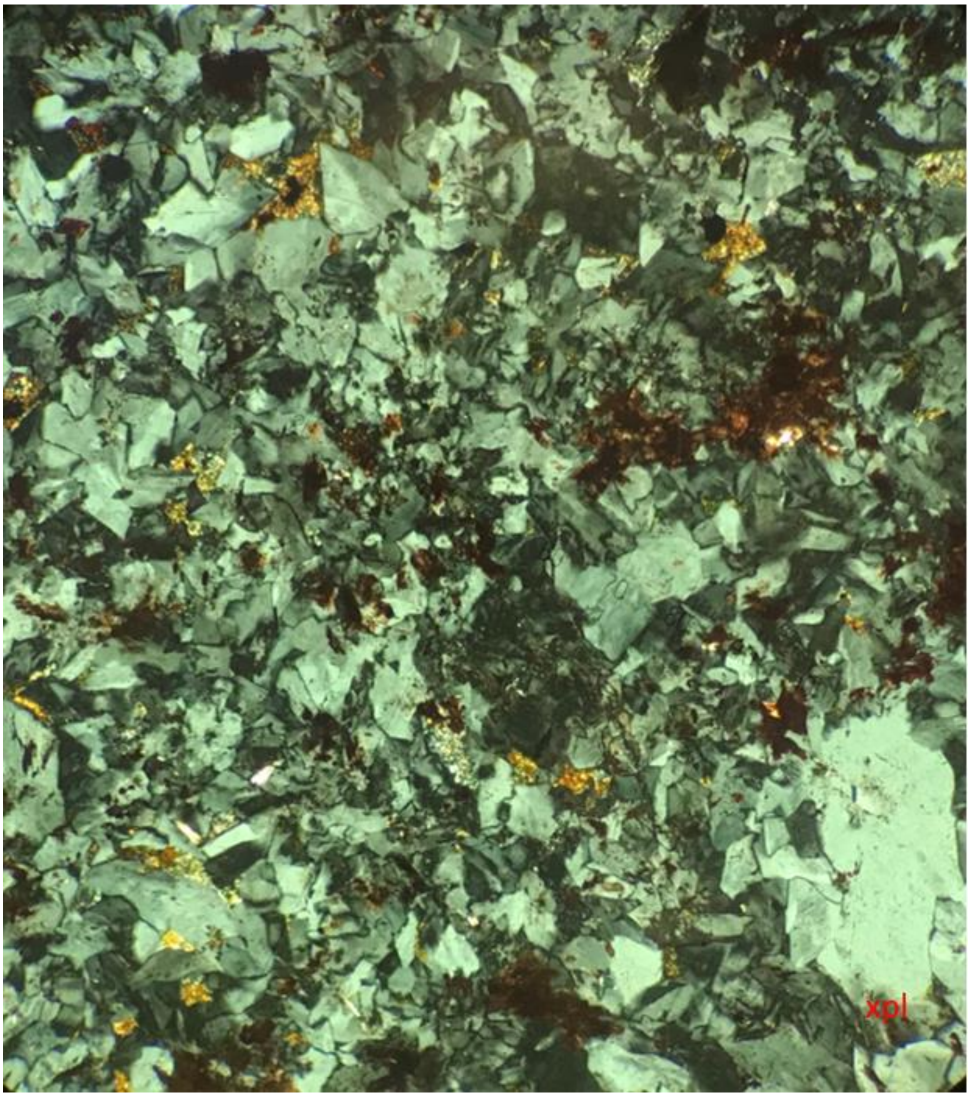

Figure 20 photo (X10) displaying secondary infill minerals in a vug.

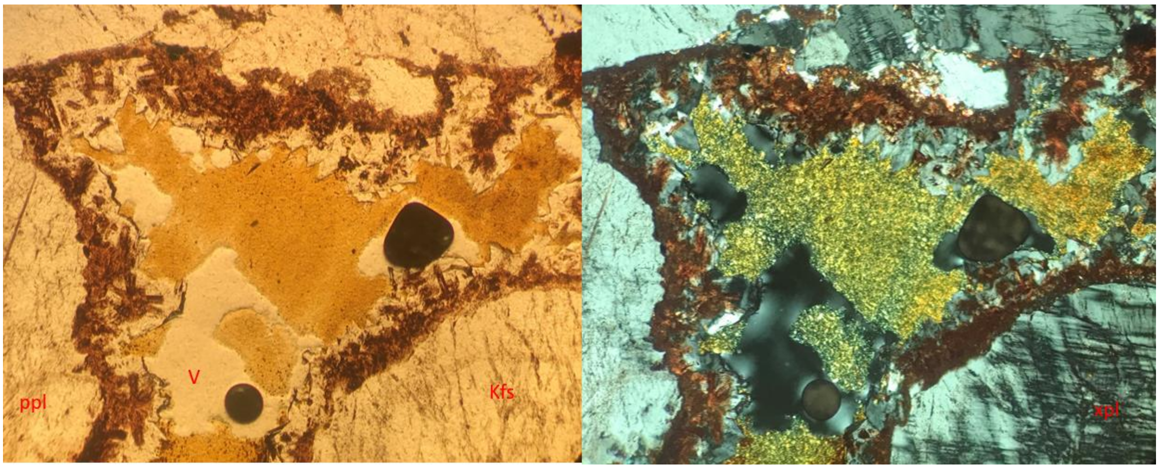

Figure 21 photo (X10) closeup on a vug that is partly filled with a dark-yellow secondary mineral.

Sample 374sk15.55

Mineralogy: Pl (45%), Kfs (30%).

The sample is very coarse grained (pegmatitic) with feldspars up to 1.5 cm wide. It is heavily weathered and fractured and contains a large proportion of vugs, which are commonly infilled with secondary minerals. The most common mineral in this sample is plagioclase which occurs as weathered, subhedral to anhedral grains that has been strongly altered to sericite. Within the areas of most intense sericitisation are coarser muscovite grains. Lamellae twinning can barely be observed in the grains. Alkali-feldspar is the next most abundant mineral which occurs as better-preserved, subhedral grains with tartan twinning or perthite unmixing. The grains have inclusions of sericite. Accessory minerals in the sample are muscovite, chlorite, Ti-bearing minerals, and opaque minerals (partly containing Fe-oxide). The sample contains a large abundance of vugs that have irregular shape and contain secondary mineral infill. The most common secondary mineral is a tooth shaped colourless low birefringence mineral. These commonly have twinning and exsolution lamellae and are interpreted to be feldspar. The shape of the grains indicate that they are secondary and grew into space once the vugs had been developed. Other infill minerals are goethite that have a dark red brown colour and tabular form occurring commonly in aggregates.

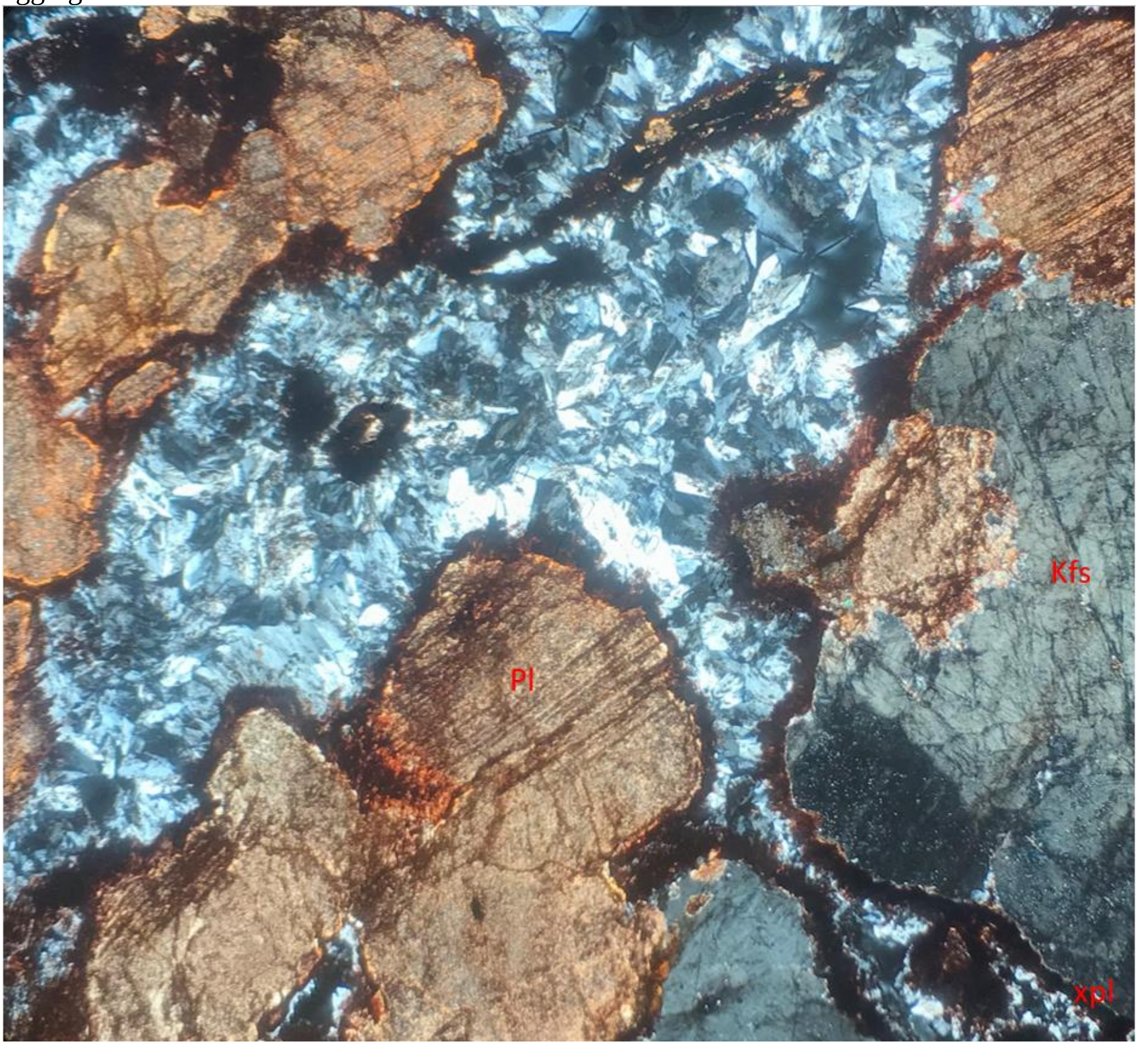

Figure 22 photo (X2.5) central in the photo a vug that has been filled with fine secondary feldspar grains.

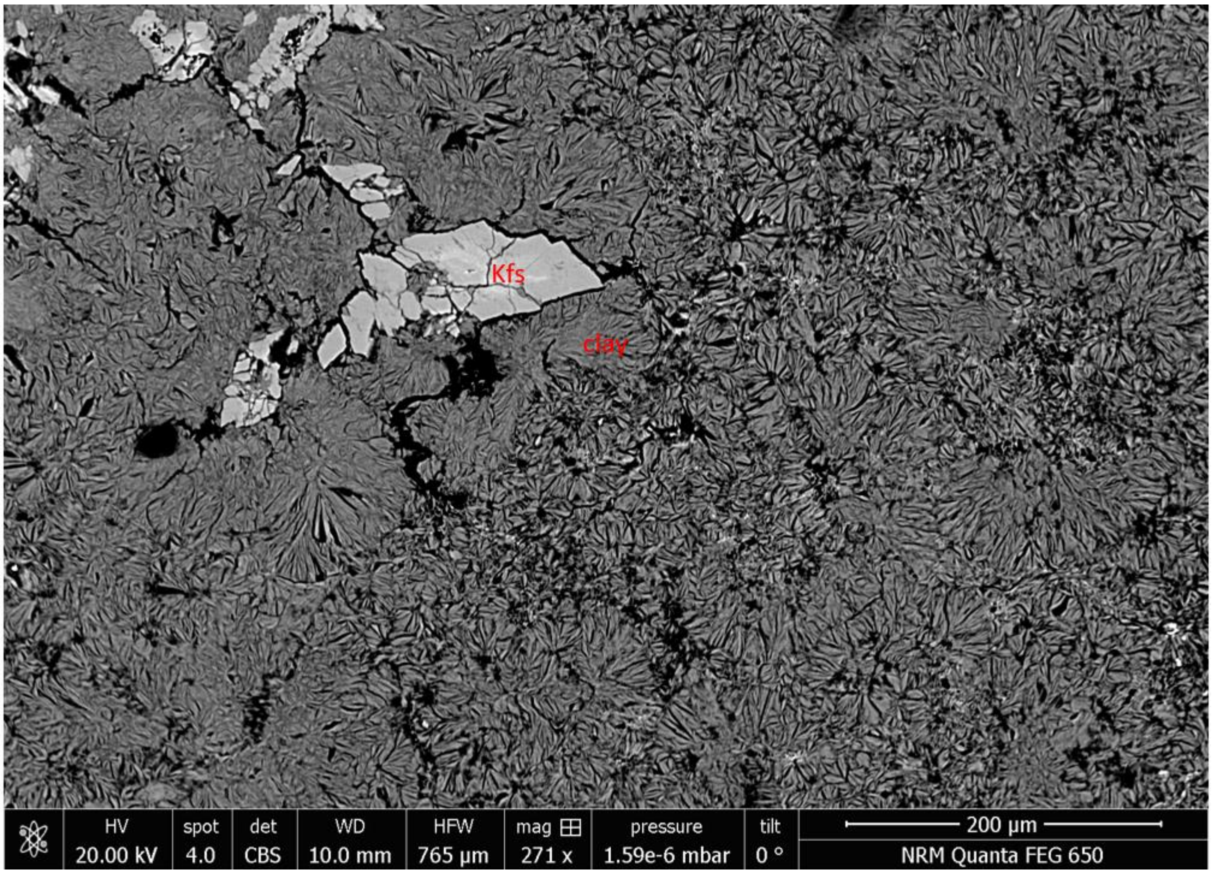

Figure 23 SEM photo over an area of a vug that are filled with a clay mineral (interpreted as Illite).

Sample 374sk19.8

Minerology: Qz (25%), Pl (15%), Kfs (10%), Chl (10%)

The sample is foliated with feldspars (plagioclase) porphyroclast up to 5 mm wide. Foliated bands of chlorite and quartz have been plastic deformed. Feldspars in the sample are weathered and fractured. The most common mineral in this sample is quartz which occurs as foliated bands that have been recrystallised into subgrains with variable shape and size and with undulose extinction. Plagioclase is the next most abundant mineral, and it forms porphyroclast in the foliation. They are strongly altered to sericite. Within the areas of most intense sericitisation are coarser muscovite grains. k-feldspar in the sample form clusters of smaller grains or bigger megacrysts. K-feldspars are well-preserved grains with tartan twinning or perthite unmixing. The grains have inclusions of sericite. Chlorites form thin aggregates of align bands between quartz bands. Within the chlorite bands inclusions of elongated recrystalised subgrains of quartz exist. Muscovite and red-brown clay mineral form thin bands adjacent to the thicker chlorite bands. One area of the sample containing black fibrous mineral resembles biotite that have exsolution Fe-Ti oxides and titanite. The sample contains large patches of intermixed chlorite and sericitisied plagioclase. Other minerals found in these patches are epidote, muscovite, opaque and Ti- bearing mineral.

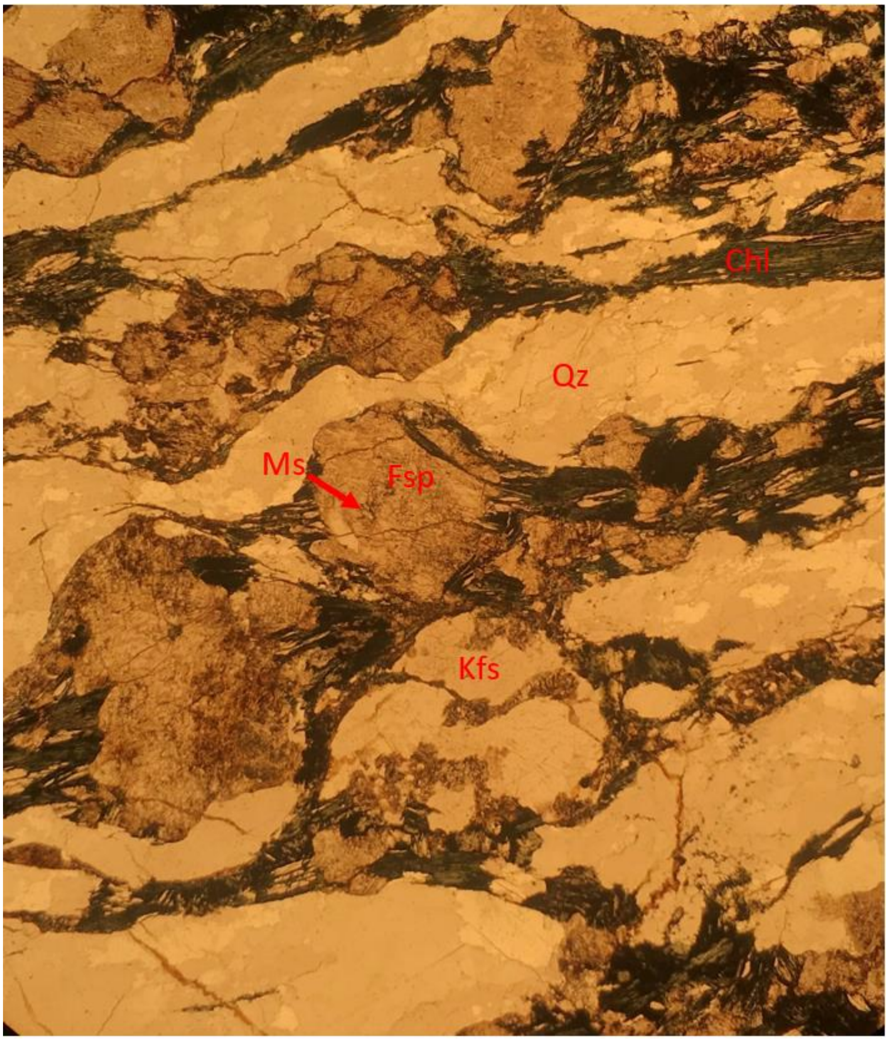

Figure 24 photo (X2.5) of a part of the thin section, displaying foliation of quartz and chlorite and larger phenocryst of feldspars (plagioclase).

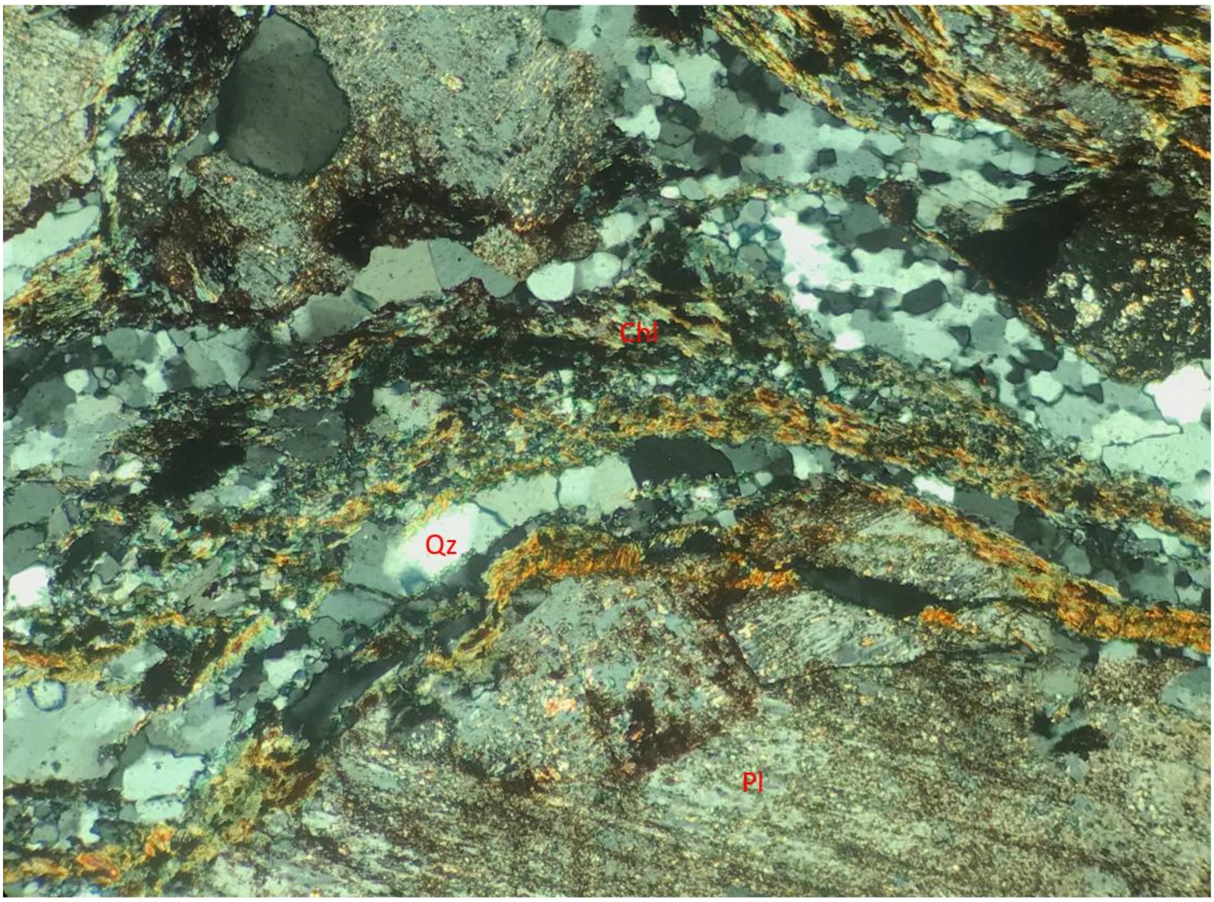

Figure 25 photo (X10) of a part of the thin section, displaying larger sericitisied plagioclase, and thin bands of recrystallized quartz and chlorite.

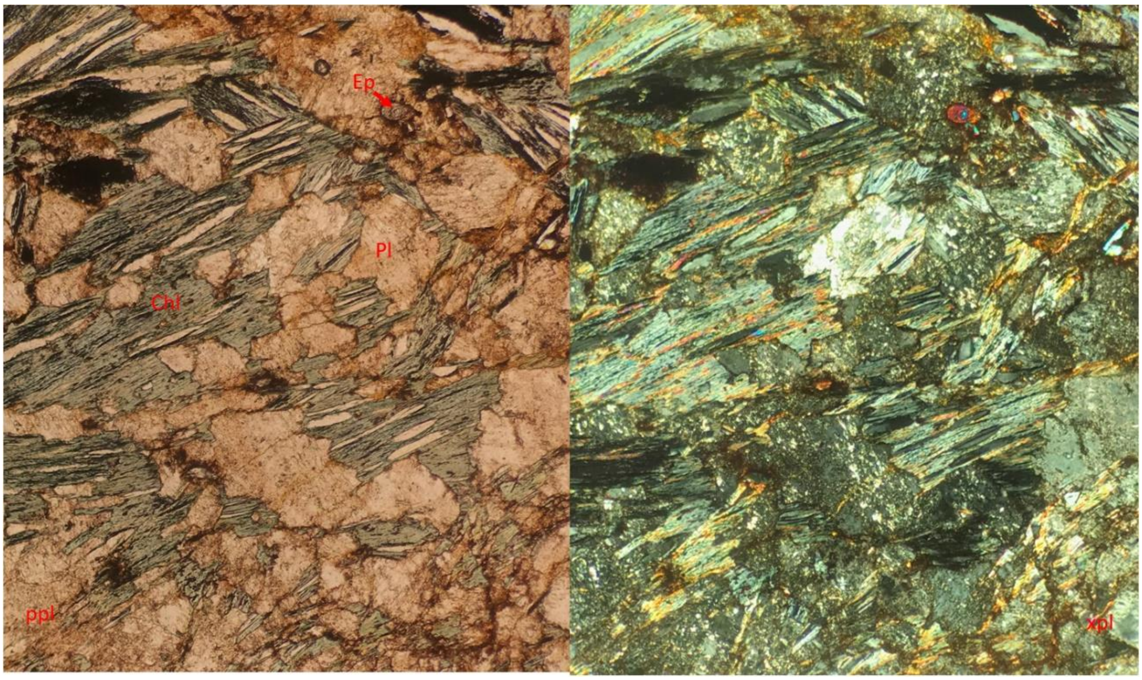

Figure 26 photo (X10) over a patch containing intermixing of plagioclase and chlorite.

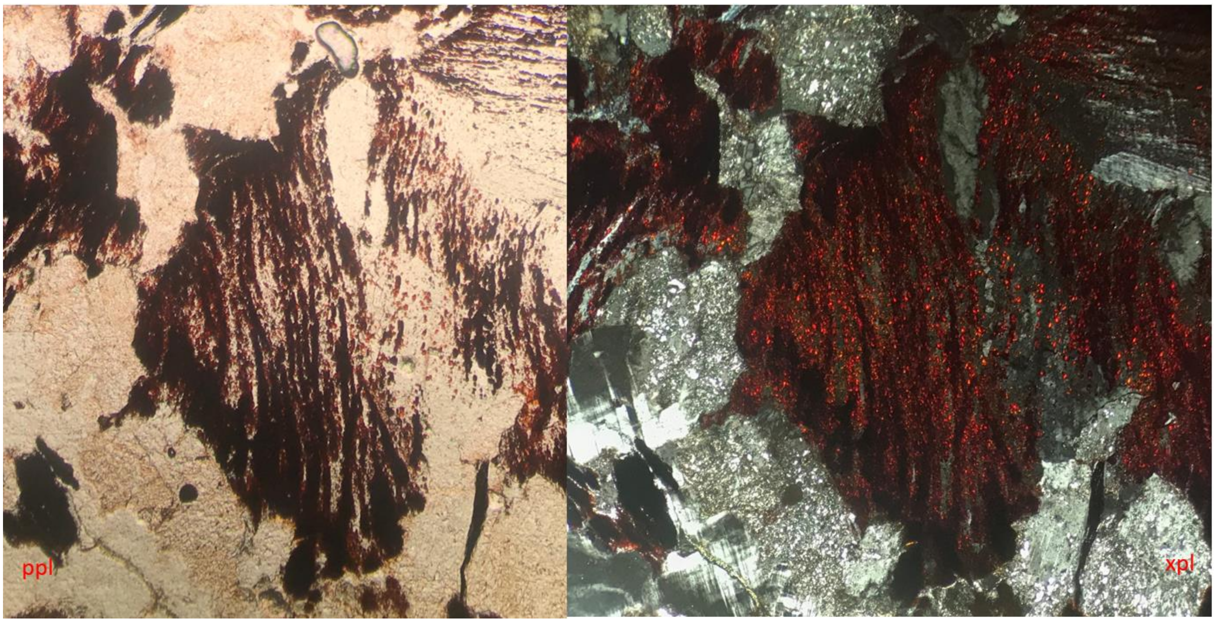

Figure 27 Biotite exsolution of Fe-Ti oxides.

Sample 374sk 21.4

Mineralogy: Fsp (35%), Bt (30%), Qz (25%)

The sample has a foliated texture with phenocrysts of feldspar up to 5 mm and large patches of ductile deformed quartz. The most common mineral in this sample is plagioclase that forms phenocrysts that are partly sericitisied. Lamellae twinning are preserved in most grains. Inclusion of single tiny muscovite grains and epidote can be seen. Biotite forms foliated bands in the sample. Minor chlorite grains can also be seen. Quartz in the sample form larger patches with recrystalised subgrains of variable shape and size and with undulose extinction. Pyrite minerals are the larger opaque minerals seen.

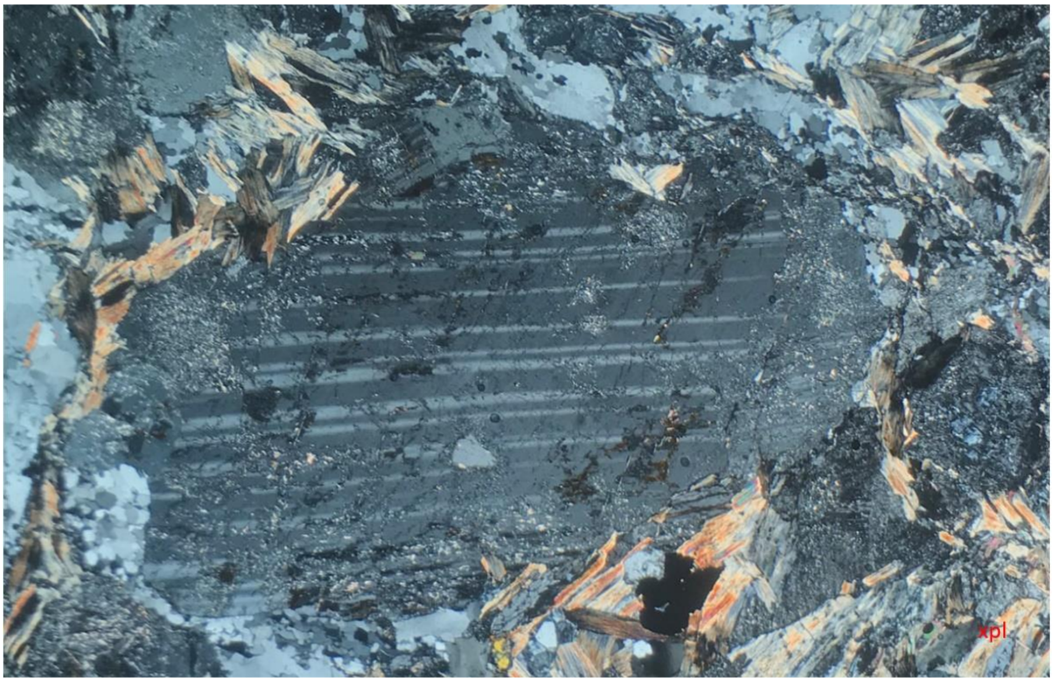

Figure 28 photo (X2.5) feldspar(albite) mineral with distinct lamellae in the centre and sericite altered on the edges.

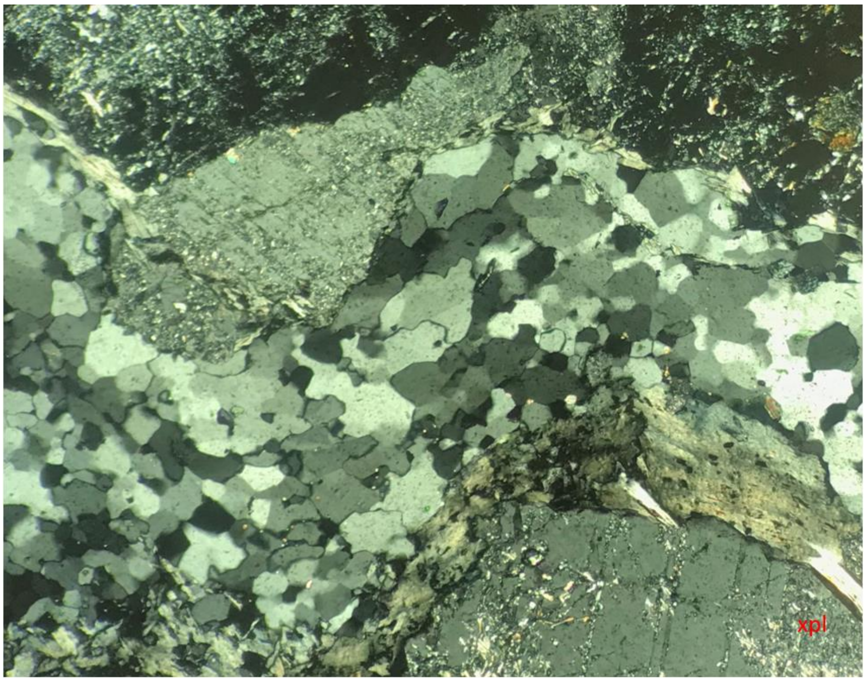

Figure 29photo (X2.5) deformed quartz that been recrystallized.

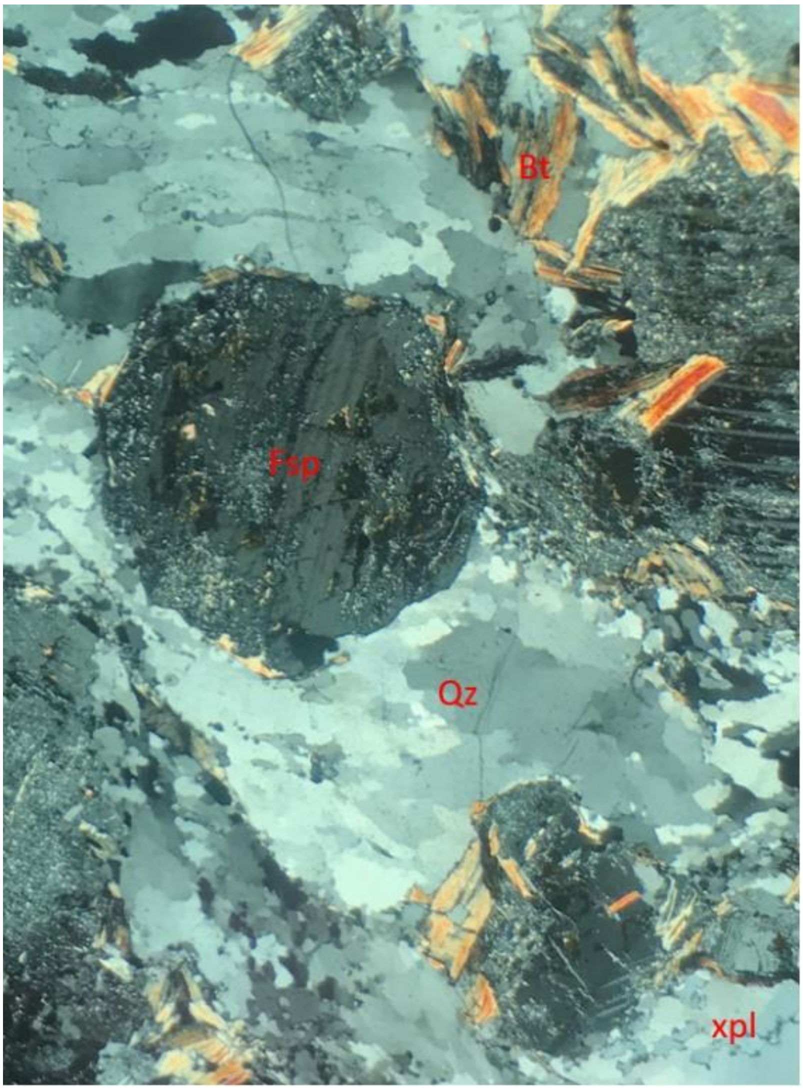

Figure 30 photo (X2.5) large Fsp surrounded by deformed and recrystallized quartz.

Sample 374sk21.8

Mineralogy: Bt/Chl (40%), Qz (30%), Fsp (30%)

The sample is fine grained with a homogenous texture with feldspar grains up to 1 mm. Quartz in the sample as undergone plastic deformation and are dynamically recrystallized. The most common mineral in this sample is biotite which occurs single grains or forming aggregates of subhedral to anhedral platy grains were the majority display chloritization. Many of the biotite have inclusions of dark deep red Ti-bearing minerals. Quartz is the next most abundant mineral, and it forms larger elongated grains which have been recrystallised subgrains with variable size and shape and show undulose extinction. Quartz grains also exists as single grains with undulose extinction. Feldspars in the sample occur as two types and have not been able to distinguish between plagioclase and alkali-feldspar. The first type is anhedral, colourless with I-order interference colour and they are strongly altered to sericite. Within the areas of most intense sericitisation are larger patches of secrete forms. The second type forms subhedral grains with lamellae twinning and they appear less weathered and only moderately altered to sericite. Accessory minerals are epidote, opaque minerals, Ti-bearing minerals

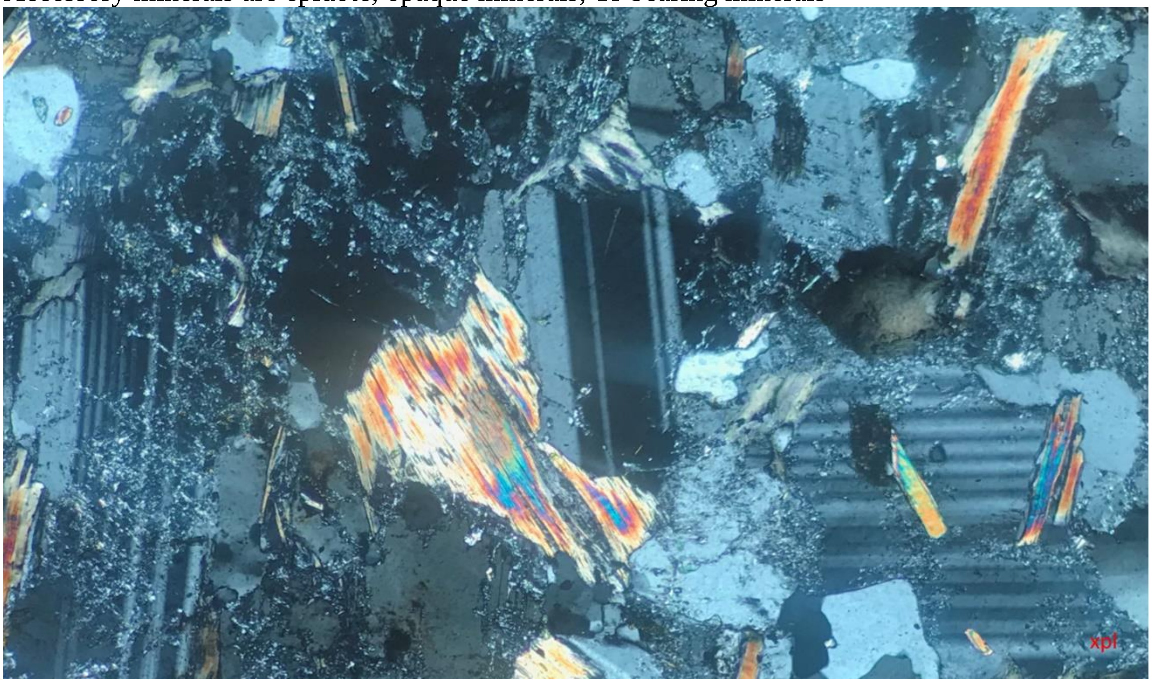

Figure 31 photo (X10) overview of minerals in the sample. Two types off feldspars, biotite with high order of interference colours are also seen in the photo.

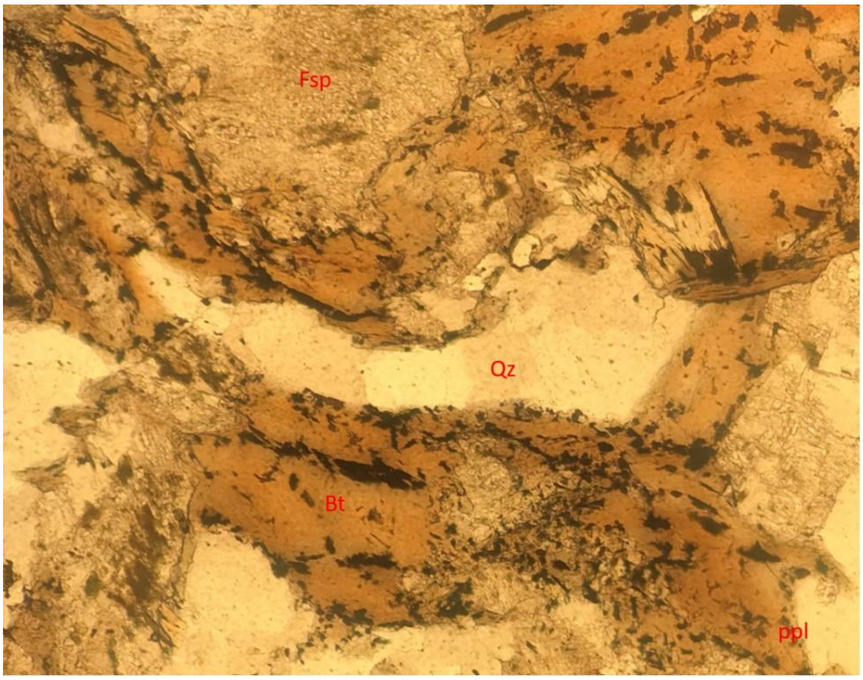

Figure 32 photo (X10) showing the dominance of biotite in the sample. Quartz and feldspar grains can also be seen.

Sample 374sk24.5

Mineralogy: Qz (60%), Pl (25%), Bi/Chl (3%)

The sample displays an intergranular texture with phenocrysts of feldspar up to 6 mm and plastic deformed quartz. Most common mineral in this sample is quartz which occur as elongated or align recrystallised grains with variable size to subgrains with undulose extinction. Plagioclase is the next most abounded mineral and is strongly altered to sericite. Within the areas of most intense sericitisation are coarser muscovite grains. Biotite is a minor mineral in this sample, and it exists as large "weathered" single grains or aggregates in sealed cracks. Some of the biotite has been altered to chlorite. Multiple sealed cracks exist through the quartz dominated parts and are filled with white micas. Accessory minerals are opaque minerals, unknown mineral with prismatic shape, colour less, zoned, first to low second order brief, 90-degree extinction.

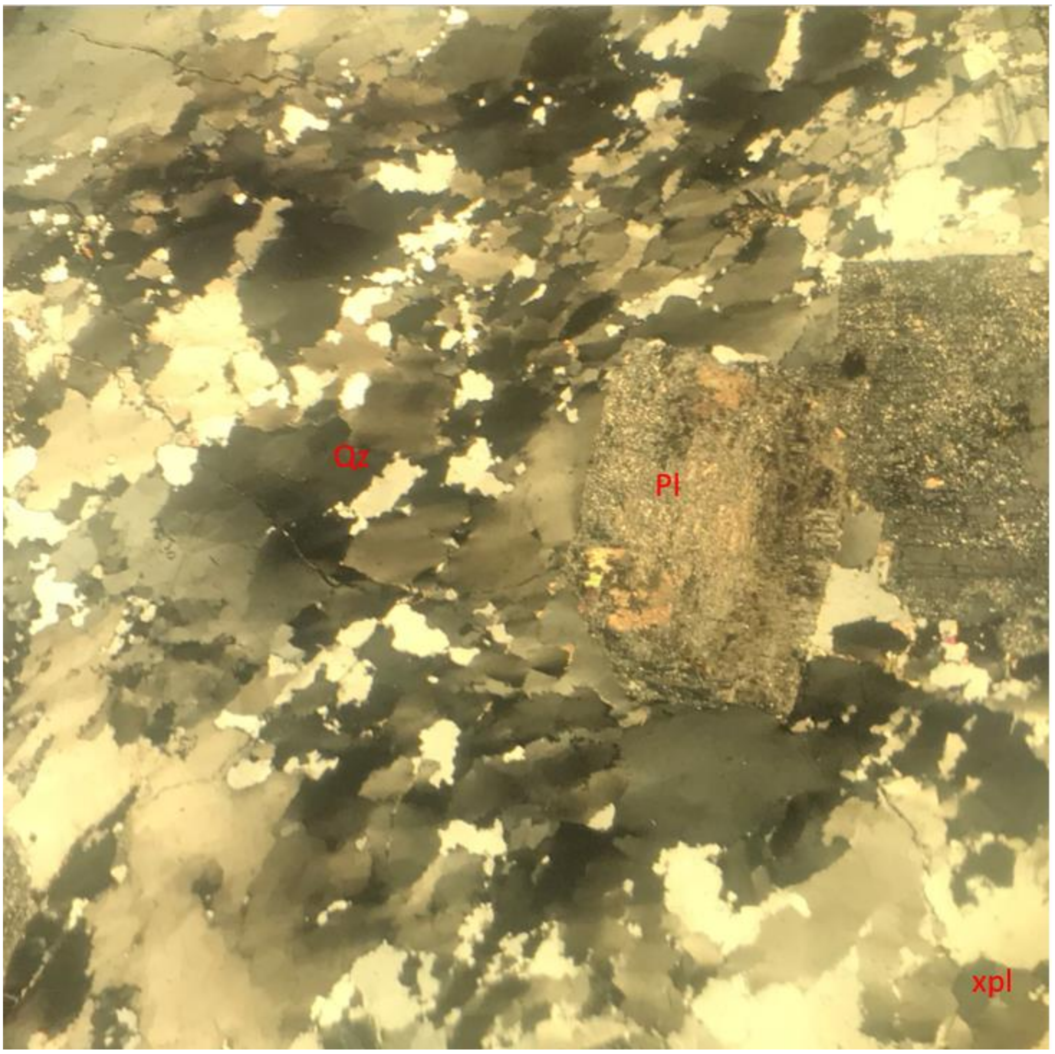

Figure 33 photo (X2.5) general minerology in the sample. Larger plagioclase grains surrounded by recrystallized quartz

Sample 374sk26.3

Minerology: Kfs (25%), Pl (20%), Qz (15%), Bi (10%)

The sample has intergranular texture with feldspar grains up to 1 cm wide. The sample is fractured and weathered. The most common mineral in this sample is k-feldspar that occurs as larger well-preserved subhedral to anhedral grains with tartan twinning or perthite unmixing. The grains have inclusions of sericite. Plagioclase is the next most abundant mineral and is strongly altered to sericite. Within the areas of most intense sericitisation are coarser muscovite grains. Lamellae twinning can barely be observed in the grains. Quartz occurs as ductile deformed elongated patches that been recrystallised to subgrains with variable shape and size and with undulose extinction. Biotite form aggregates or single grains and most of them are found adjacent to the sericitisied plagioclase. Several of the biotite grains exhibit chloritisation. Other minerals found are epidote, Ti-bearing minerals, and pyrite.

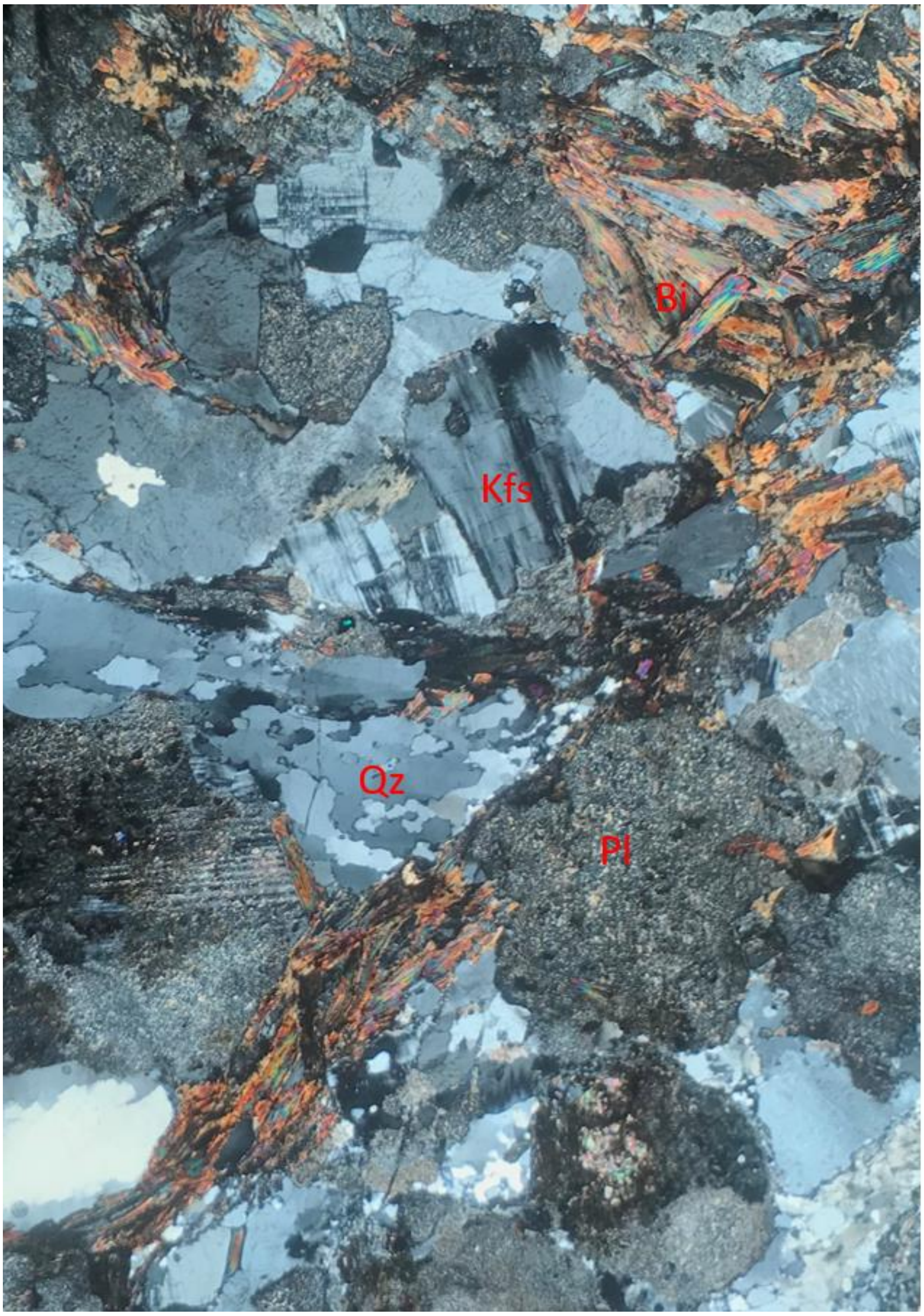

Figure 34 photo (X2.5) of a part of the thin section displaying the main minerology in the sample.

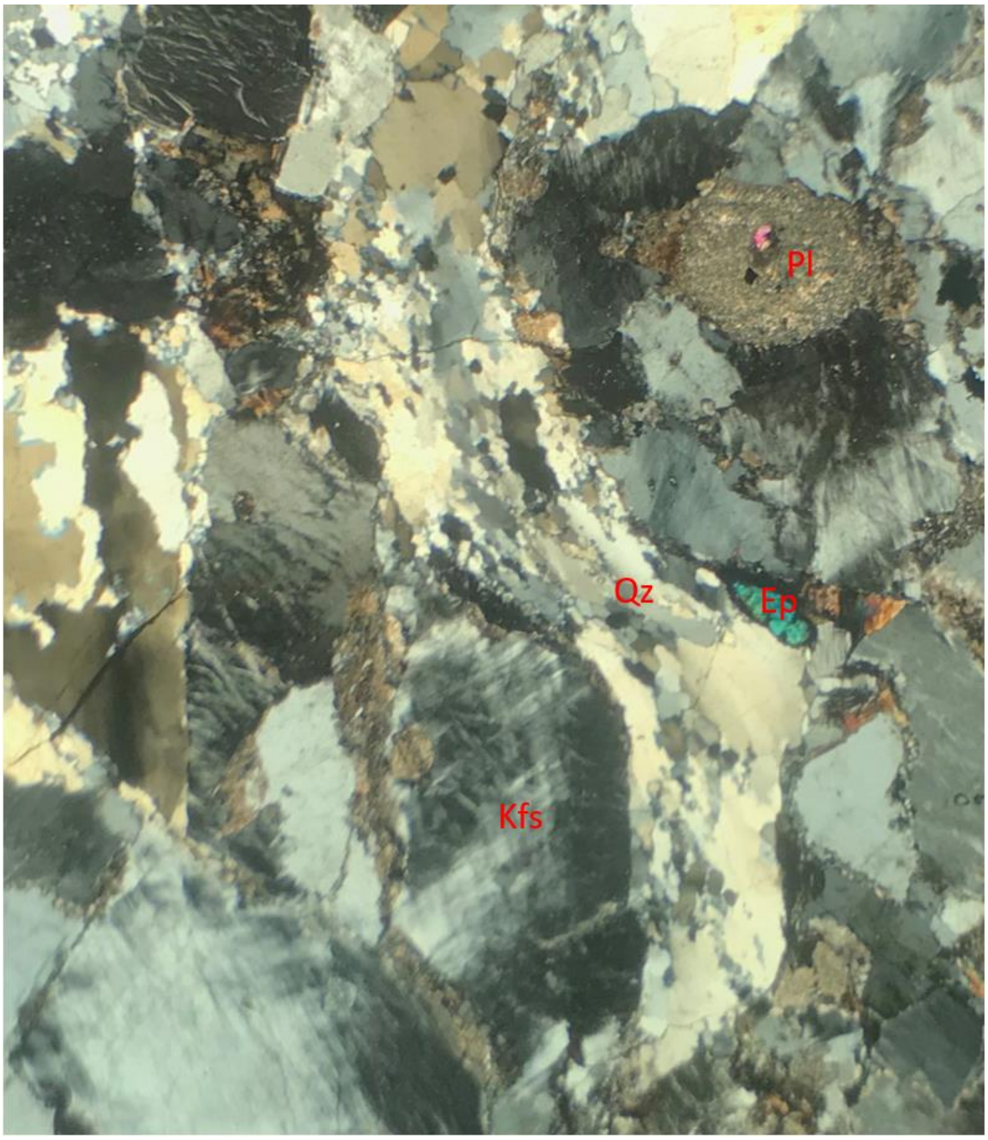

Figure 35 photo (X10) displaying intergranular texture and ductile deformed quartz that been recrystallised.

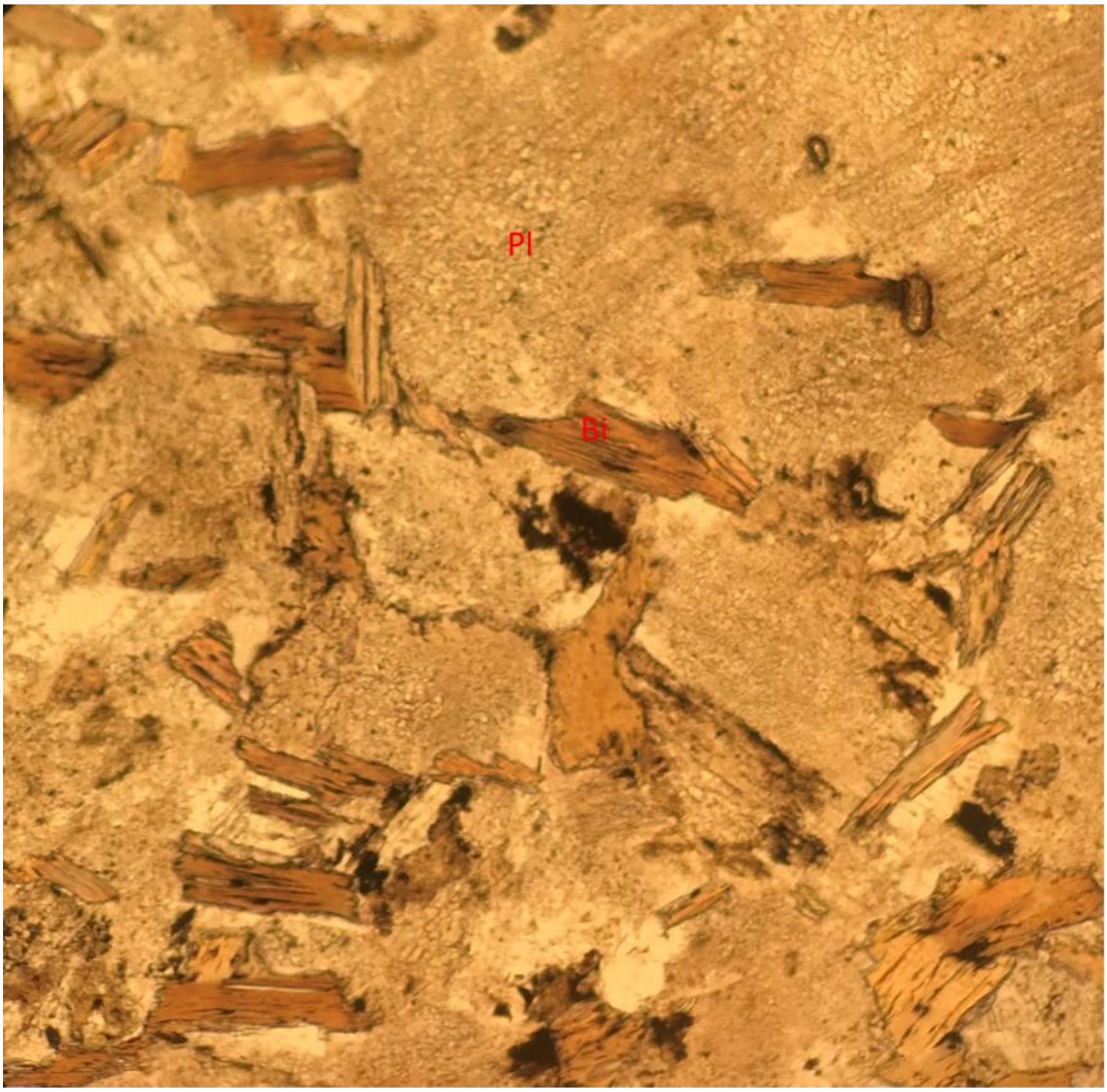

Figure 36 photo (X10) display biotite and plagioclase grains.

Sample 374sk30.15

Minerology: Secondary infill (40 %), Pl (20%), Kfs (10%).

The sample is coarse grained with feldspars up to 1 cm wide. The feldspar grains are heavily weathered and fractured. Large proportion of vugs exist in the sample and they are commonly infilled with secondary minerals. The most common minerals in the sample are the secondary infill minerals that partly fill up the pores. Most common is goethite that have a dark red brown colour and tabular form occurring commonly in aggregates. Tooth shaped colourless low birefringence mineral also fill the vugs. These commonly have twinning and exsolution lamellae and are interpreted to be feldspar. The shape of the grains indicates that they are secondary and grew into space once the vugs had been developed. other secondary infill minerals are chlorite form aggregates spread out in the sample. Most common primary mineral is Plagioclase that has been altered to sericite. Lamellae twinning can still be observed in the grains. K-feldspar grains which occurs better preserved than plagioclase form subhedral grains with tartan twinning and perthite unmixing. Minor biotite that are found in the sample has undergone chloritisation.

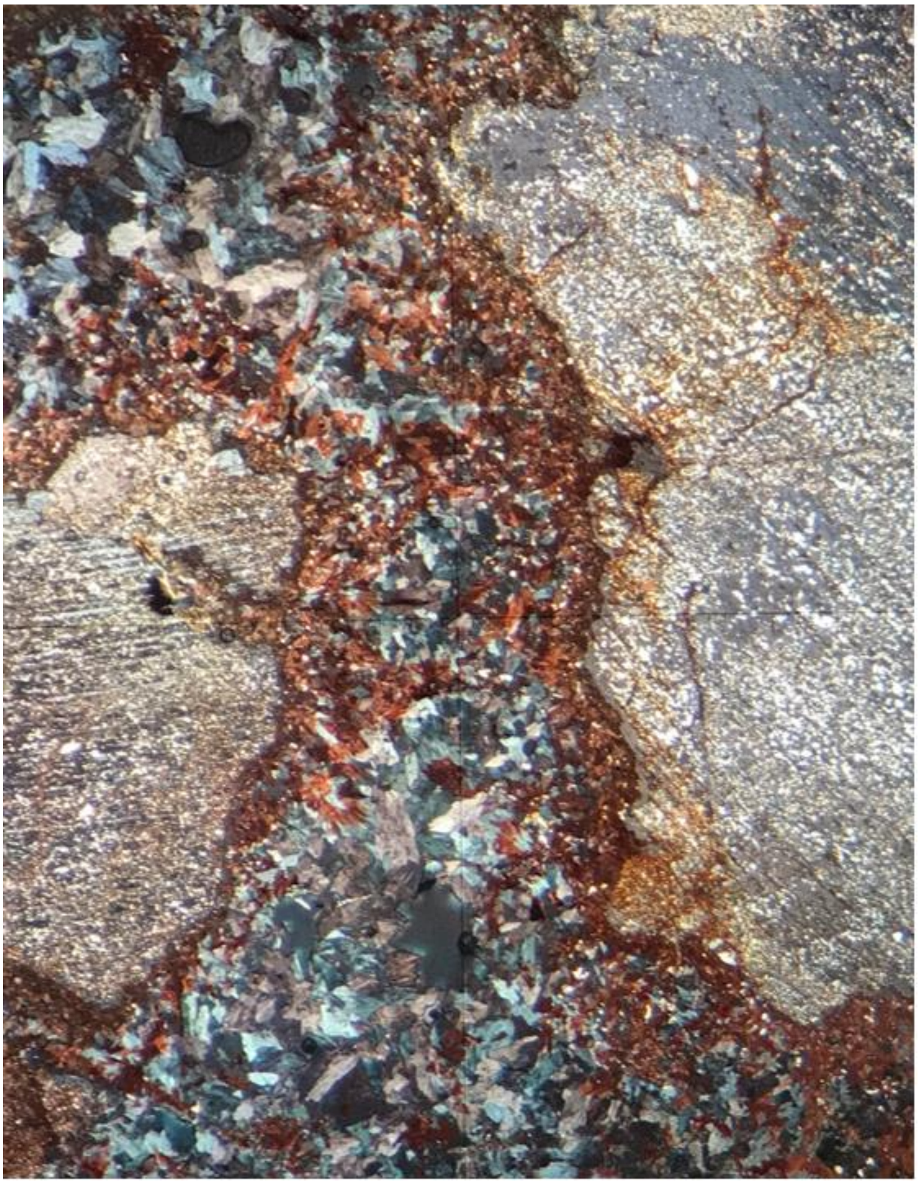

Figure 37 photo (X10), Two large plagioclase separated by secondary infill minerals.

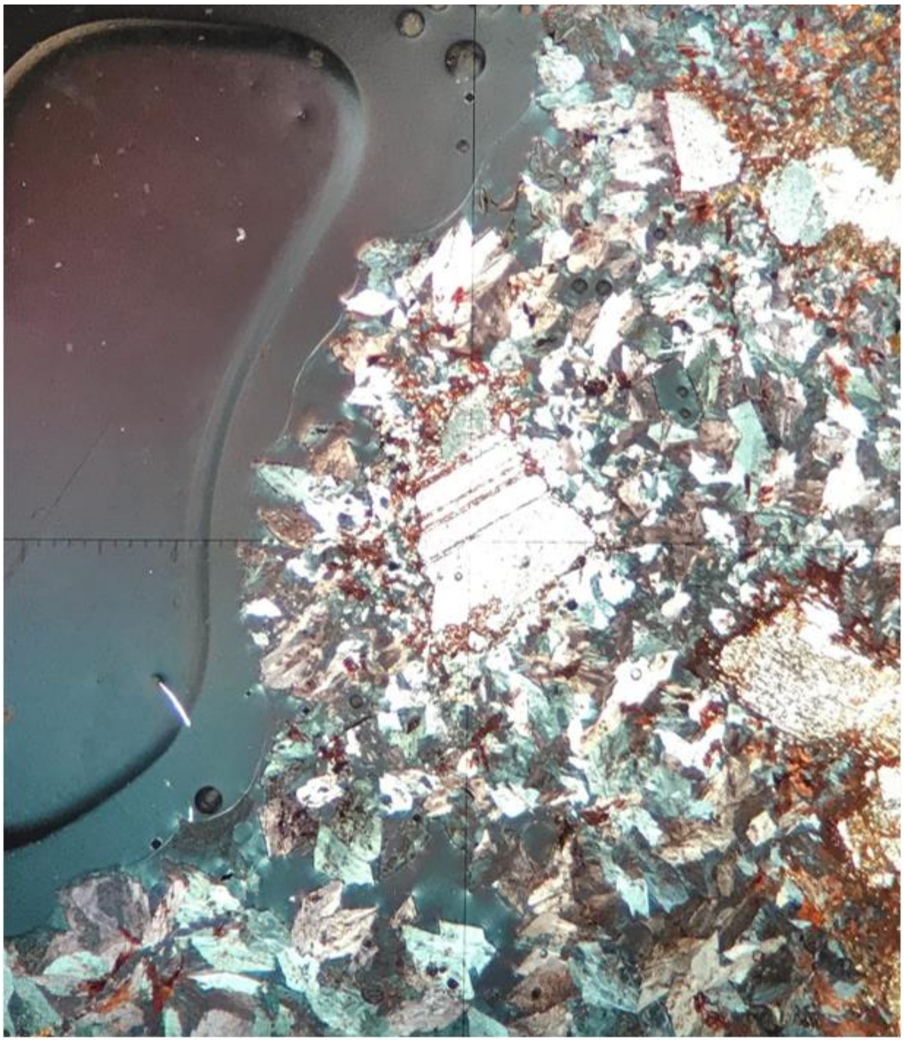
Figure 38 photo (X2.5) of a vug and secondary infill minerals

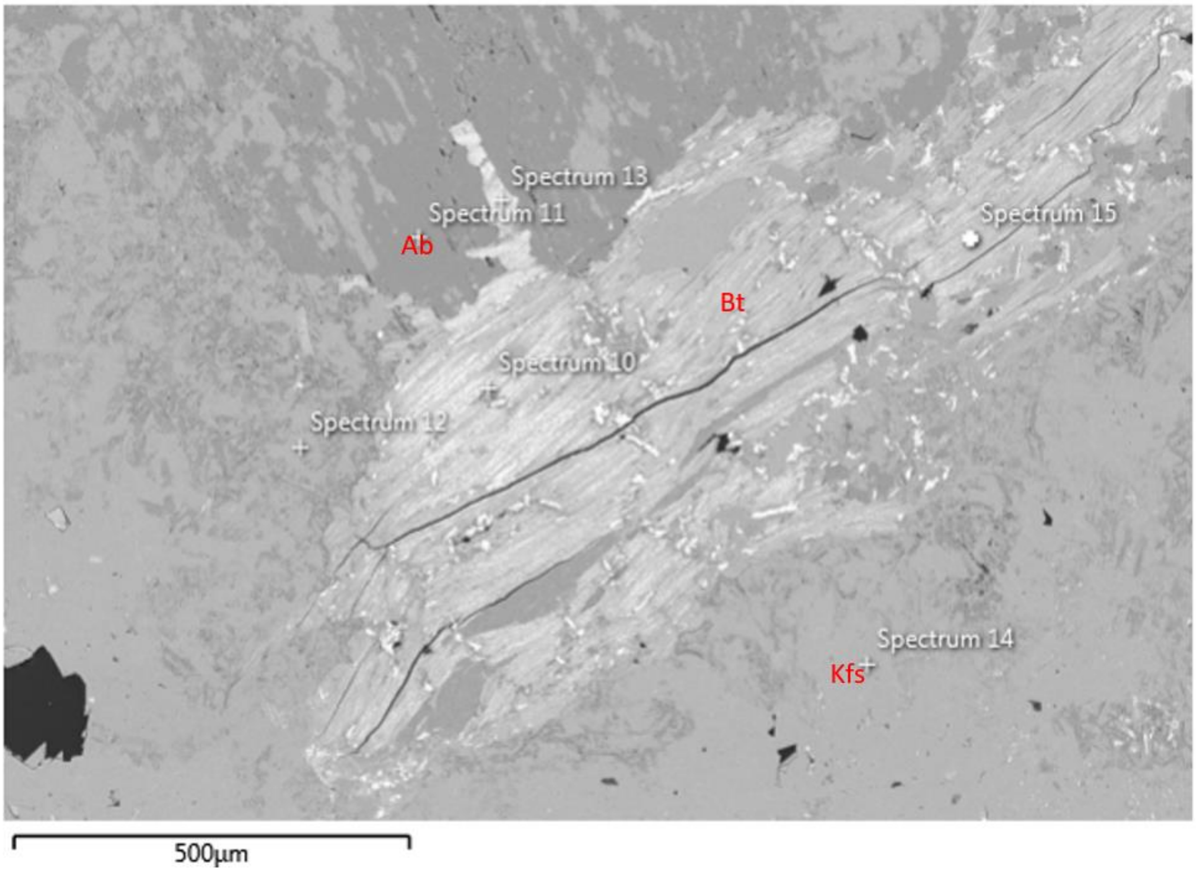

Figure 39 SEM image over a part of the thin section

Sample 374sk 30.5

Mineralogy: k feldspar (20%), plagioclase (25%)

The sample is very coarse grained with feldspars up to 1.5 cm wide. It is heavily weathered and fractured and contains large proportions of vugs, which are commonly infilled with a red brown dusty mineral. The most common mineral in this sample is Alkali-feldspar which occurs as well-preserved, euhedral to subhedral grains with pericline twinning or perthite unmixing. The grains have inclusions of sericite and are stained with Fe-oxides. Plagioclase is the next most abundant mineral and is strongly altered to sericite. Within the areas of most intense sericitisation are coarser muscovite grains. Lamellae twinning can barely be observed in the grains. Biotite forms aggregates adjacent to larger vugs. Most of the biotite has a I-order birefringence indication that they have undergone chloritisation. The sample contains a large abundance of vugs that have irregular shape and contain secondary mineral infill. The most common secondary mineral is goethite that have a dark red brown colour and tabular form occurring commonly in aggregates. Tooth shaped colourless low birefringence mineral also fill the vugs. These commonly have twinning and exsolution lamellae and are interpreted to be feldspar. The shape of the grains indicate that they are secondary and grew into space once the vugs had been developed. Other secondary minerals include chlorite, epidote, opaque minerals, micas (including muscovite). And a green-yellow coloured anhedral mineral with no pleochroism or appears cleavage, 2nd order birefringence. Titanite (and/or rutile, ilmenite) are common inclusions.

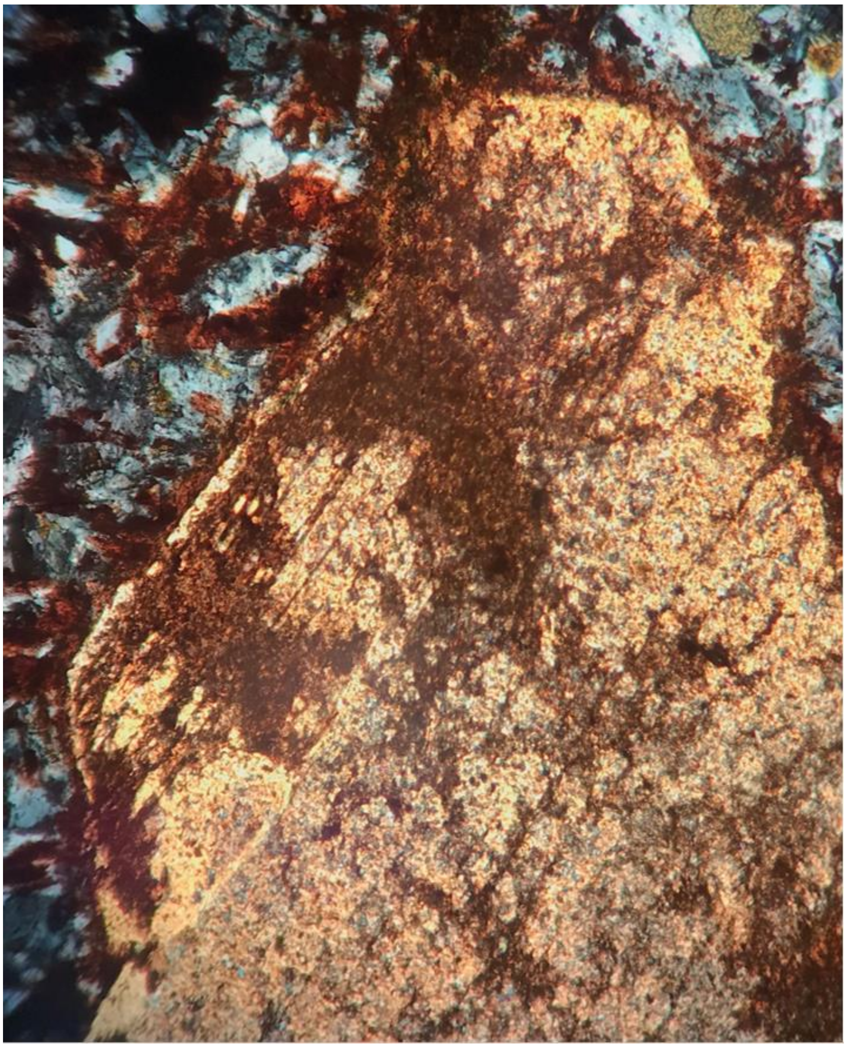

Figure 40 photo (X20) a plagioclase that has undergone sericitisation. Photo in xpl.

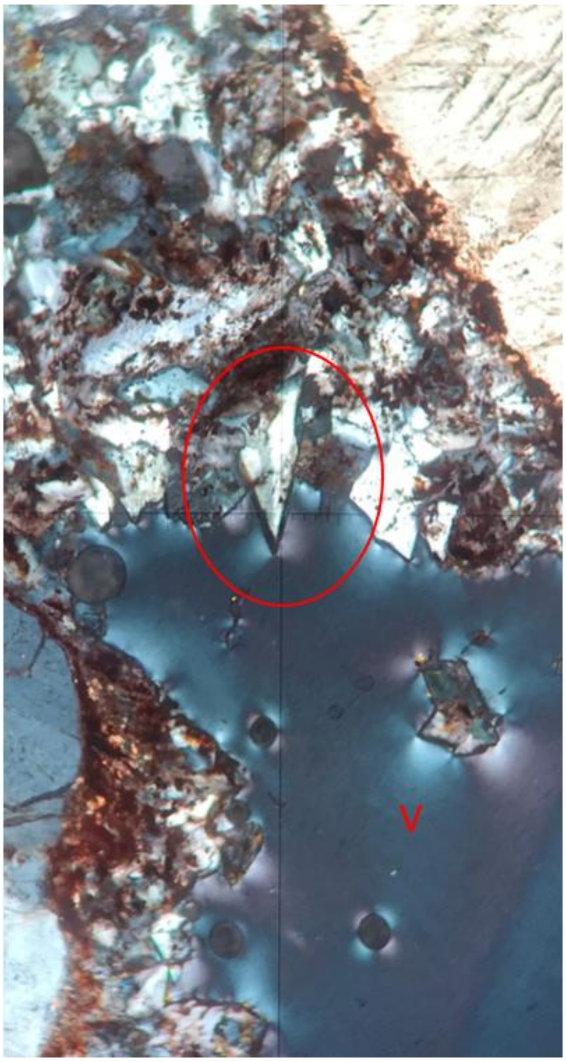

Figure 41 photo (X20) shows the vug wall where the interpreted feldspar with tooth shape. Photo in xpl.

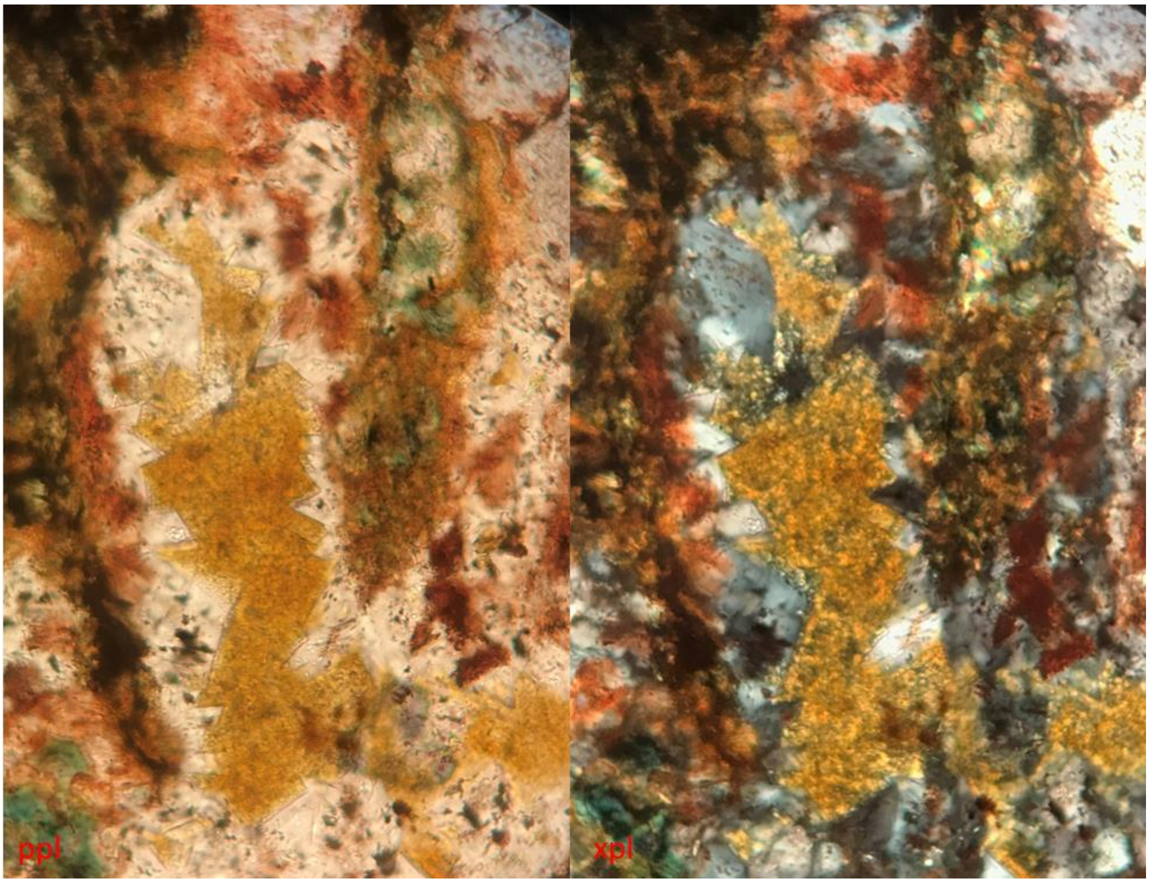

Figure 42 Photo(X20) display secondary infill minerals. In the middle the green-yellow coloured mineral. Also seen is the red-brown coloured clay mineral and small interpreted feldspars.

Sample 374sk30.7

Mineralogy: Kfs (70%), Pl (2%)

The sample is very coarse grained and completely dominated by alkali-feldspars with grains up to 1 cm wide. It is heavily weathered and fractured (brecciated) and contains vugs that exist inside the large feldspars and in boundaries between grains. The vugs are commonly infilled with a red brown dusty mineral. Coarse alkali-feldspar which occurs as well-preserved, euhedral to subhedral grains with perthite texture. The grains have inclusions of sericite and are stained with Fe-oxides. Plagioclase exist as minor grains that are strongly altered to sericite. Lamellae twinning can barely be observed in the grains. Common accessory mineral is titanite (and/or rutile, ilmenite). The sample contains a large abundance of vugs that have irregular size and shape and contain secondary mineral infill. The most common secondary mineral is goethite that have a dark red brown colour and tabular form occurring commonly in aggregates. Tooth shaped colourless low birefringence mineral also fill the vugs. These commonly have twinning and exsolution lamellae and are interpreted to be feldspar. The shape of the grains indicates that they are secondary and grew into space once the vugs had been developed. Opaque (Fe-oxide) are also common infills.

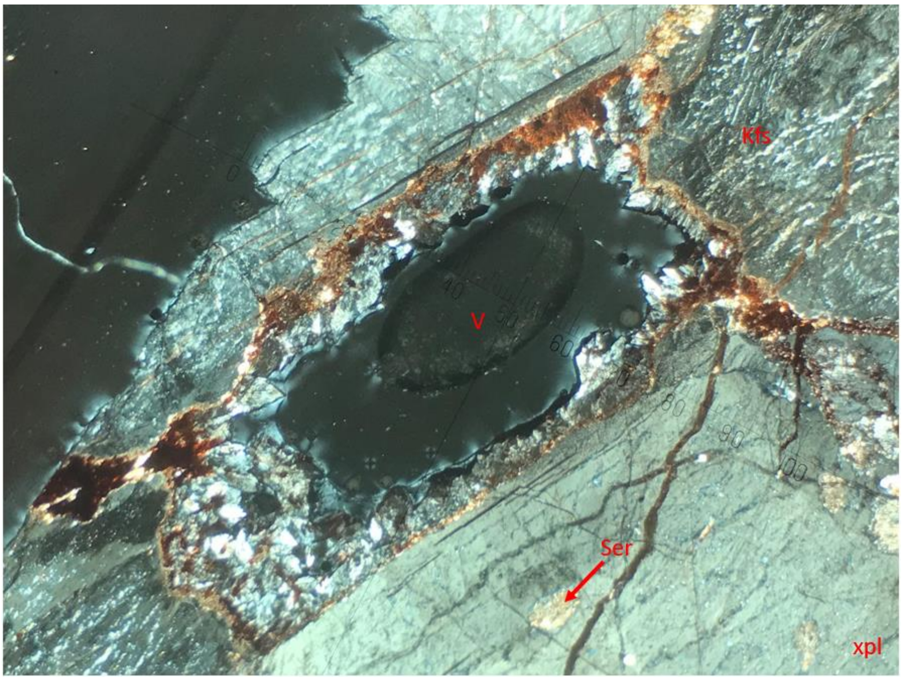

Figure 43 photo (X10) of a vug with mineral infill on the edges notes the tooth shape of those low birefringence minerals.

Sample 374sk30.9

Mineralogy: Kfs (25%), Pl (15%), Opq (10%), Qz (2%)

The sample has an inequigranular, clastic texture with feldspars up to 5 mm wide. It is heavily weathered and fractured and contains a large proportion of vugs, which are commonly infilled with a red brown dusty mineral. The most common mineral in this sample is k-feldspar which occur well-preserved, subhedral to anhedral grains with tartan twinning unmixing. The grains have inclusions of sericite. Plagioclase is the next most abundant mineral and is strongly altered to sericite. Within the areas of most intense sericitisation are coarser muscovite grains. Lamellae twinning can barely be observed in most of the grains. Biotite has been chloritised and muscovite grains can be seen inside the grains. In the black mass grains of euhedral muscovite is seen. Aggregates of chlorite are common secondary infill. The sample contains a large abundance of vugs that have irregular shapes and contain secondary mineral infill. The most common secondary mineral is goethite which has a dark red brown colour and tabular form occurring commonly in aggregates. Aggregates of chlorite are common secondary infill in fractures. Other secondary minerals in fractures include micas (muscovite), clay minerals, opaque minerals (containing non-mature haematite) and quartz.

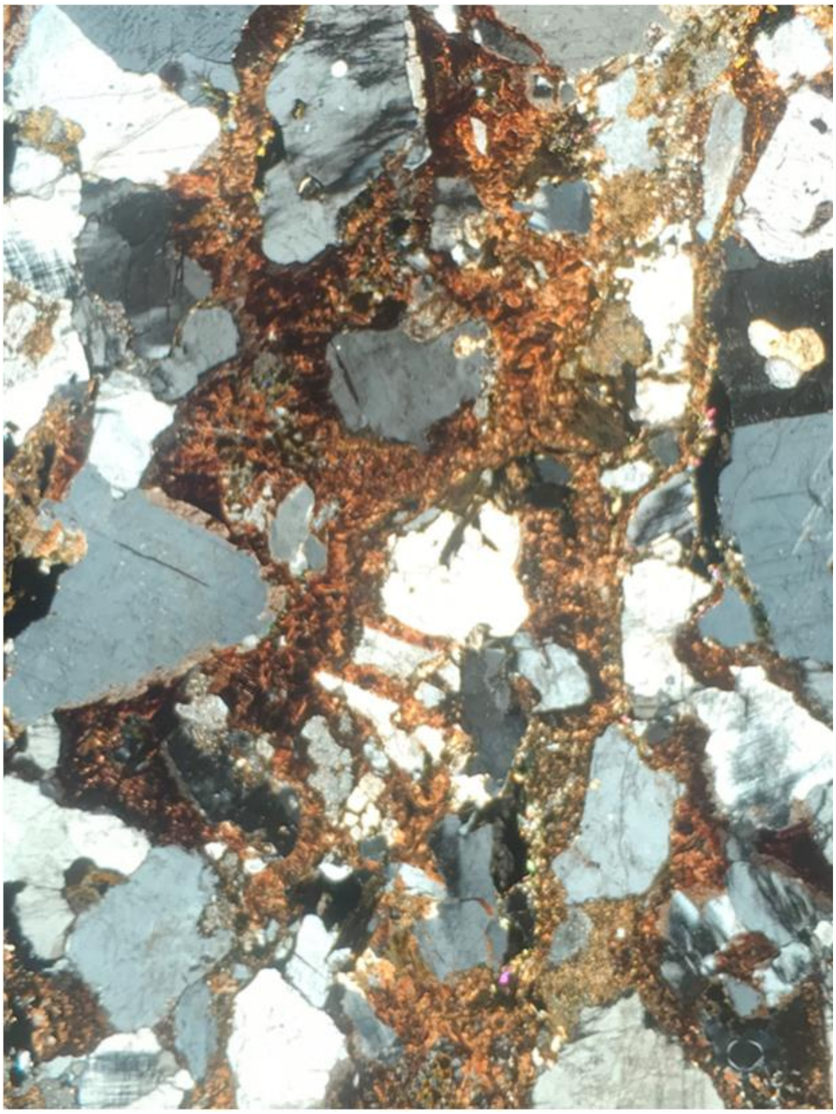

Figure 44 photo (X2.5) of a section of the thin section. Larger grains of feldspars and finer "matrix" or mostly red brown clay, but also muscovite, biotite, and chlorite.

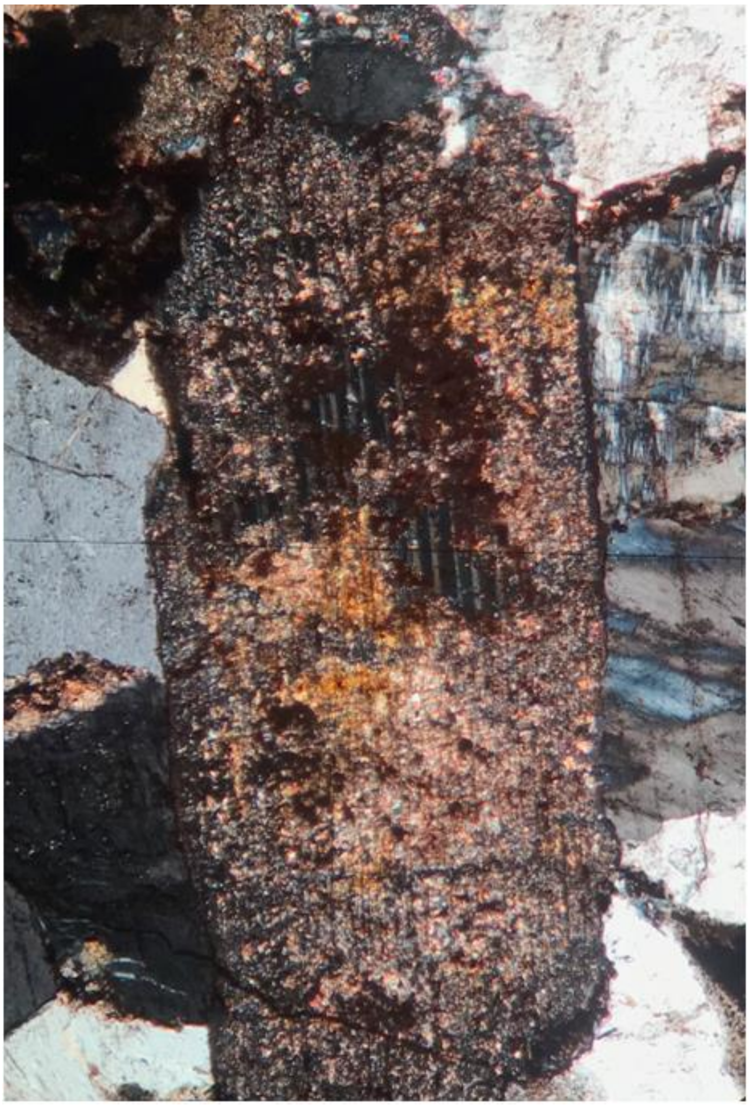

Figure 45 plagioclase grain that been sericitisied, lamellae twinning can still be seen in the middle.

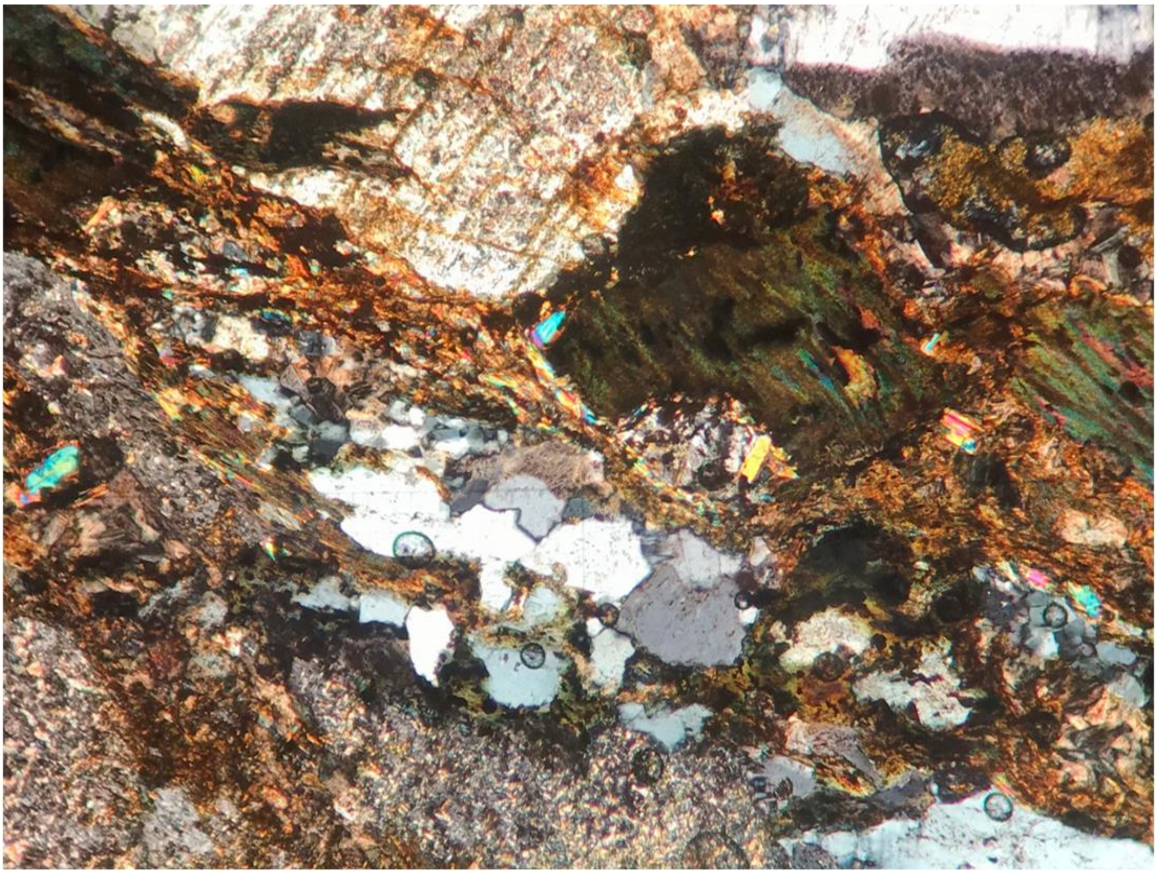

Figure 46 photo of a part of the thin section showing miner quartz grains surrounded by finer muscovite and chlorite. larger chlorites can also be seen and sensitised plagioclase.

Sample 374sk31.4

Mineralogy Kfs (30%), Pl (25%), Qz (15%), Bt (7 %)

The sample is fine grained with an intergranular texture with feldspars up to 5 mm wide. It is weathered and alkali-feldspars are coarser than other minerals in the sample. The sample contains almost no vugs. The most common mineral in the sample is k-feldspar occurs as well-preserved, subhedral to anhedral grains with tartan twinning or perthite unmixing. The grains have inclusions of sericite. Plagioclase is the next most abundant mineral and is strongly altered to sericite and stained with fine grained Fe-oxide. Within the areas of most intense sericitisation are coarser muscovite grains. In some plagioclase grains lamellae twinning can clearly be observed. Quartz forms patches or veins with recrystalised subgrains of variable size and shape. They do not display undulose extinction. Biotite in the sample has a dark appearance due to exsolution of Fe-Ti oxides forming Ti-oxides inside the grains possibly rutile. Muscovite can be observed as tiny grains inside or next to several of the biotite grains. Associated with the biotite grains are a green-yellow coloured anhedral mineral with no pleochroism or cleavage and 2nd order birefringence. Inside these minerals tiny opaque minerals occurs. These are interpreted that have being formed when biotite breaks down.

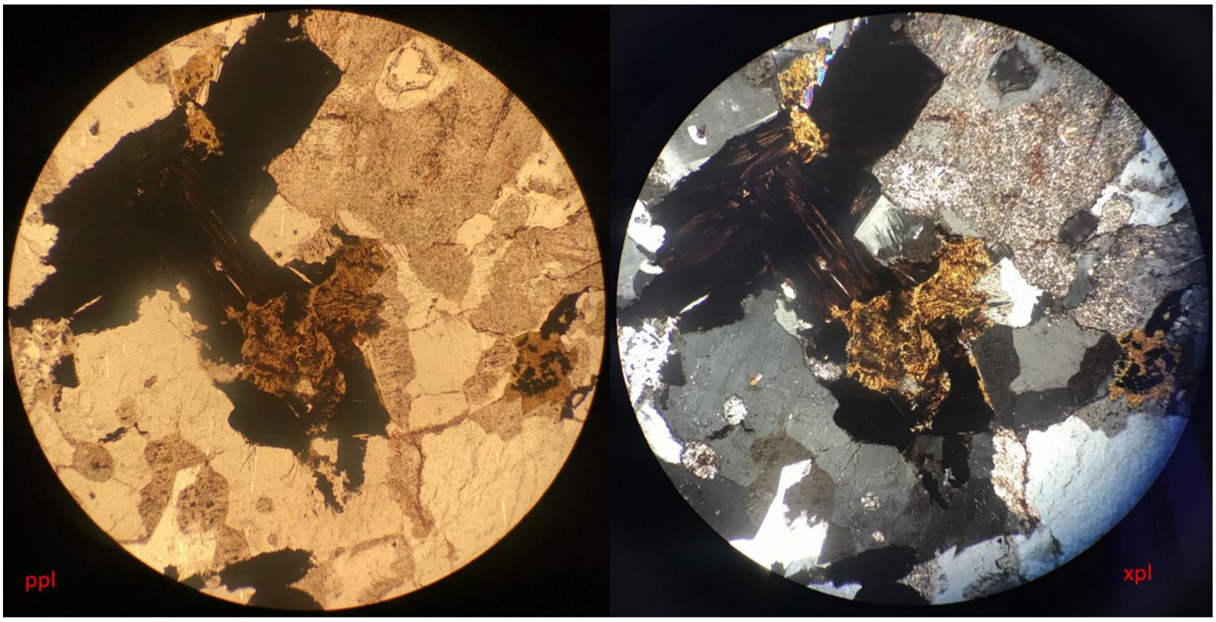

Figure 47 photo (X10) biotite grains (black) and in the middle a green-yellow clay mineral presumed to have been formed from the biotite.

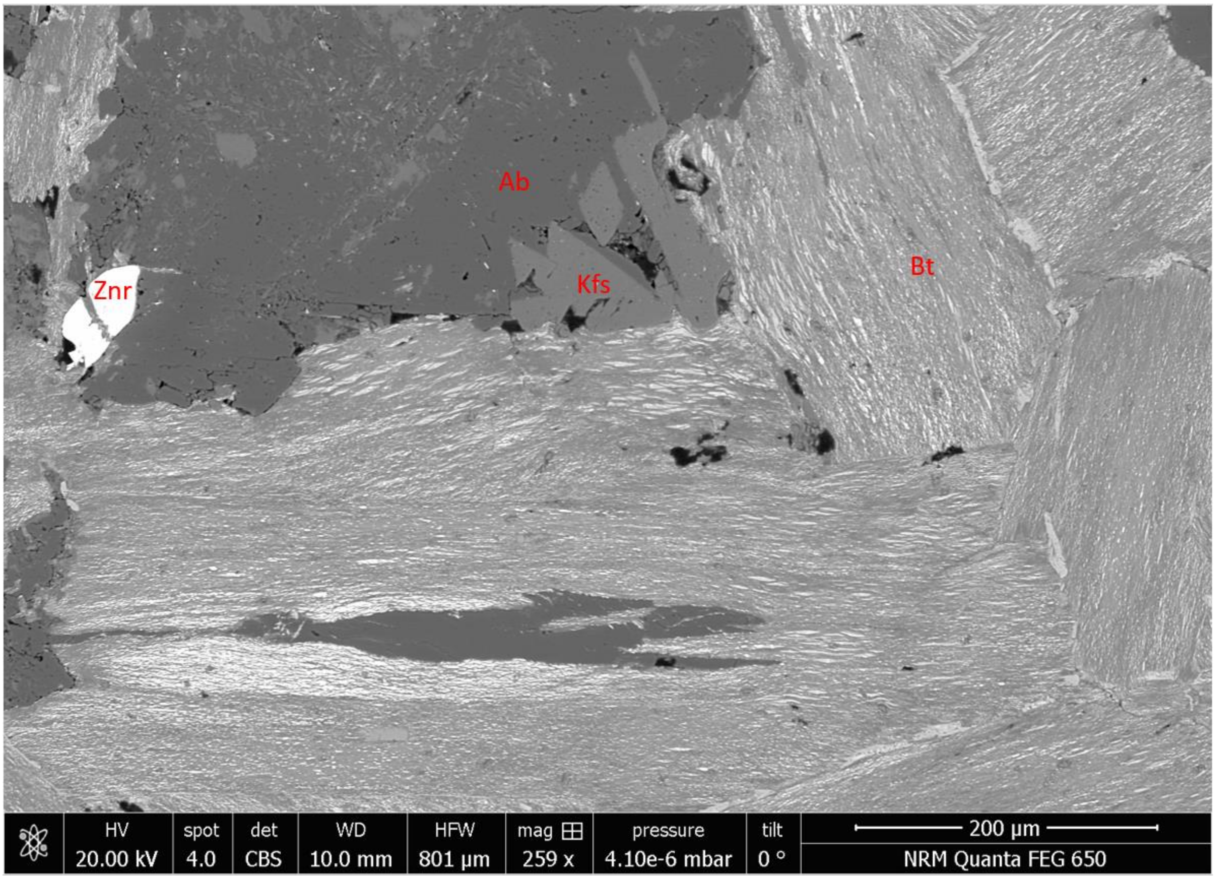

Figure 48 SEM photo of a part of the thin section.

Sample 374sk33.3

Mineralogy: Qz (25%), Pl (20%), Kfs (15%), Opq (5%)

The sample is a fine-grained homogenous texture with feldspars up to 3 mm wide. It is weathered and displays elongated. Alkali-feldspars are coarser than other minerals in the sample. The sample contains sporadically placed vugs. The most common mineral in this sample is quartz that form patches or veins of recrystalised subgrains with variable size and shape. Plagioclase is the next most abundant mineral and is strongly altered to sericite and stained with Fe-oxide. Within the areas of most intense sericitisation are coarser muscovite grains. In some grains lamellae twinning can clearly be observed while in others its barley seen. Alkali-feldspar which occurs as well-preserved, euhedral to subhedral grains with tartan twinning or perthite unmixing. The grains have inclusions of sericite. Black minerals are seen in the sample and resemble biotite as a result of exsolution of Fe-Ti oxides and titanite. Tiny euhedral muscovite can be spotted in several of the back spots. Opaque minerals with variable size and shape containing non-mature haematite. Other accessory minerals are titanite and zircon. The sample contains a small amount of vugs that have variable size and shape and certain contain secondary mineral infill. The most common secondary mineral is a green-yellow coloured anhedral mineral with no pleochroism or appears cleavage, 2nd order birefringence. Adjacent to the vugs mineral forming saw pattern or tooth shape.

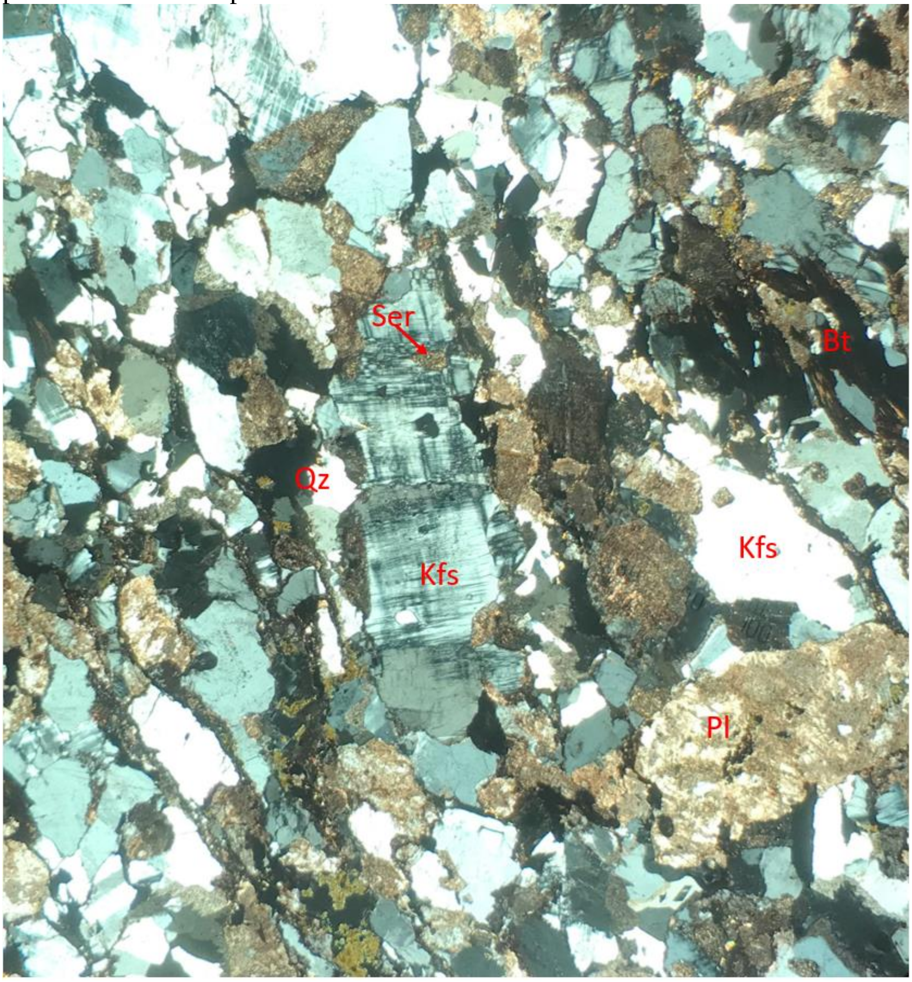

Figure 49 photo (2.5) general minerology in the sample.

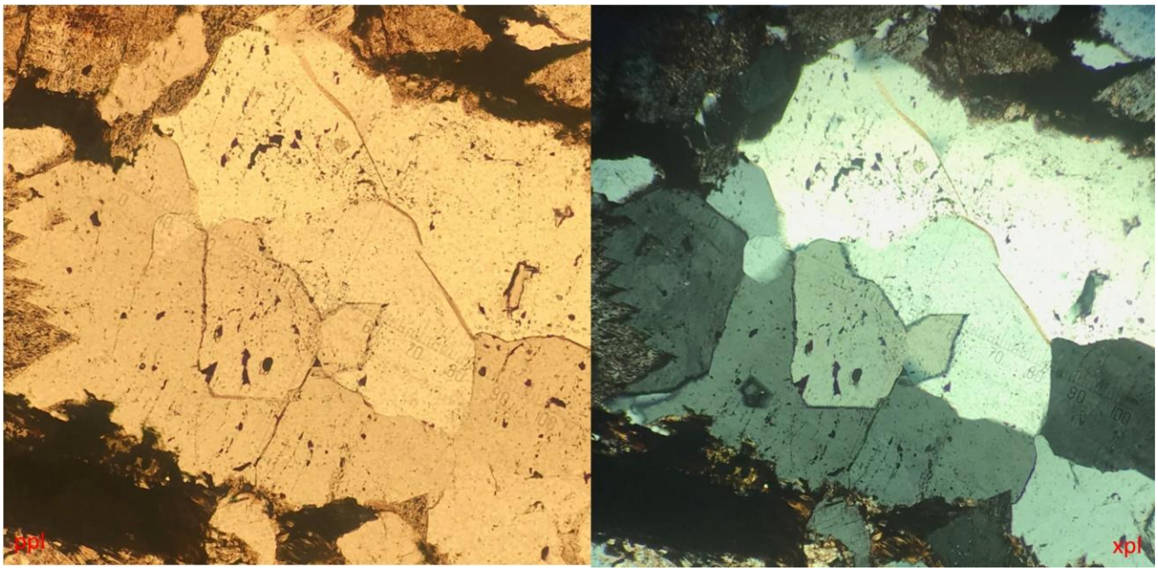

Figure 50 photo (X10) showing recrystallized quartz.

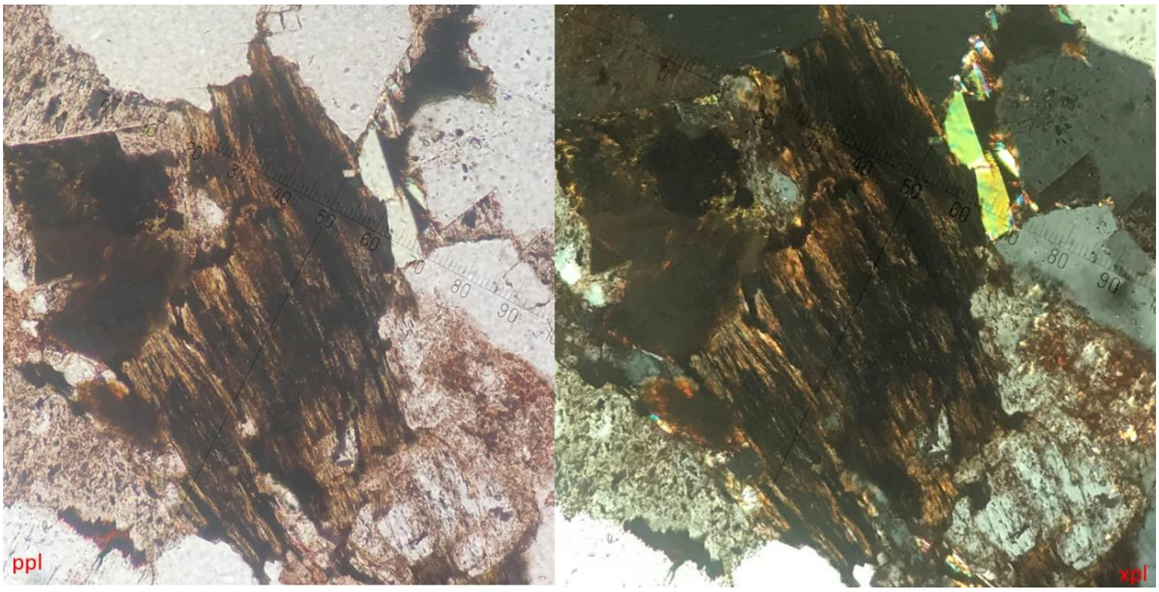

Figure 51 photo (X20) anhedral biotite. To upper right two euhedral micas.

Sample 374sk33.6

Mineralogy: Kfs (20%), Pl (20%), Qz (15%), Bi/Opq (10%)

The sample is fine grained with a homogenous texture with feldspars up to 1 mm wide. It is weathered and the sample contains sporadically placed vugs. The most common minerals in this sample are k-feldspars and plagioclase. K-feldspars which occur as well-preserved, euhedral to subhedral grains with tartan twinning or perthite unmixing. The grains have inclusions of sericite. Plagioclase minerals are strongly altered to sericite and stained with Fe-oxide. Within the areas of most intense sericitisation are coarser muscovite grains. In some grains lamellae twinning can clearly be observed while in others its barley seen. Quartz form patches or veins with variable grain size and shape of recrystalised subgrains. Biotite is common in the sample and has a dark appearance due to exsolution of Fe-Ti oxides and titanite. Tiny euhedral muscovite can be spotted in several of these black zones of biotite. Other accessory minerals are titanite Ti-bearing minerals and zircon. The sample contains small amount of vugs with variable size and shape. On the vug walls secondary minerals growth a green-yellow coloured anhedral mineral with no pleochroism or appears cleavage and overgrowth tooth shape feldspars stained with Fe-oxides.

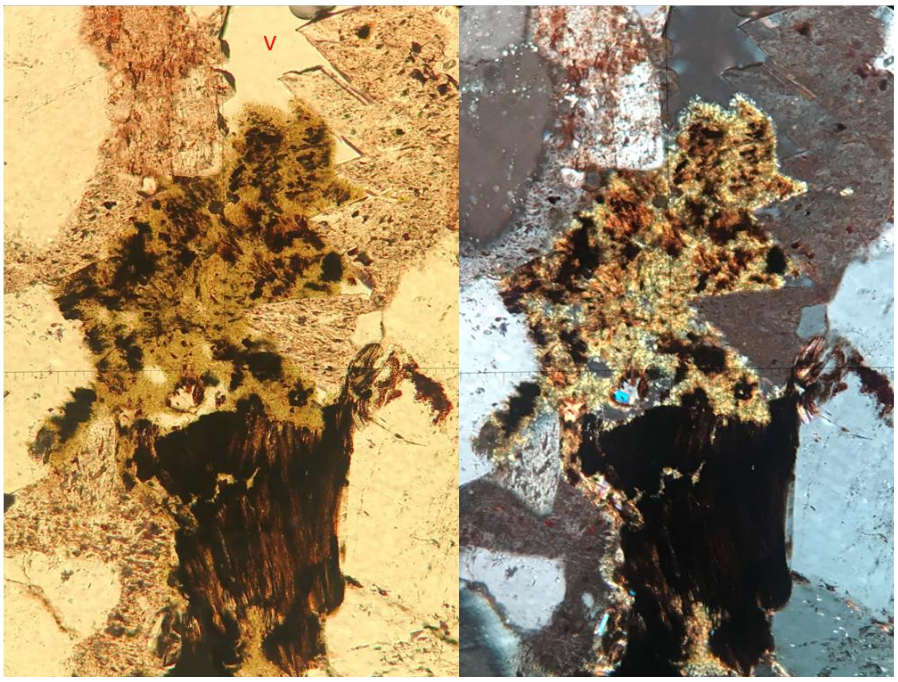

Figure 52 photo (X10) showing in the middle a secondary infill green-yellow coloured mineral. Under the green-yellow mineral, a biotite and on top a vug. Note the brown-grey tooth shape mineral that point into the vug. Left photo in ppl, right photo in xpl.

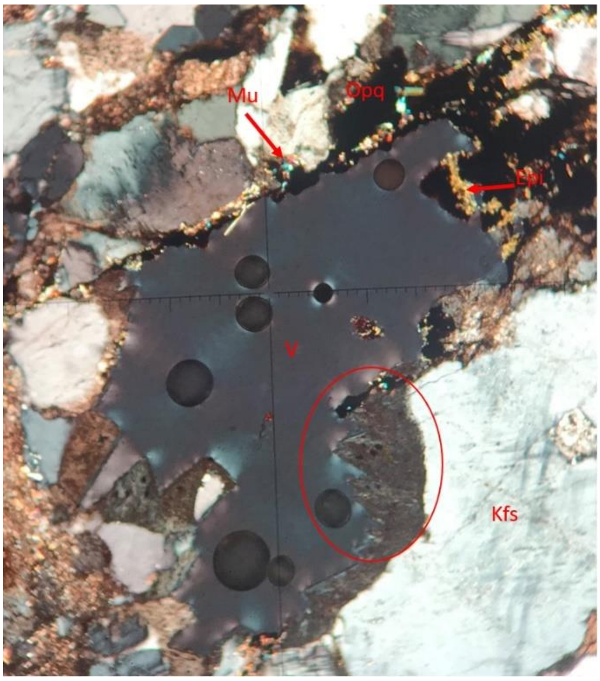

Figure 53 photo (X10) a vug and on the wall a k-feldspar that is overgrowth with a tooth shape mineral interpreted to be feldspar (adularia). Photo in xpl.

Sample 374sk33.85

Mineralogy: Kfs (15%), Pl (10%), Bi (5%)

The sample is fine grained with a homogenous texture with feldspars up to 3 mm wide. The overall sense is that the sample is minor foliated with the appearance of larger feldspar being elongated and point in the same direction. Vugs are relatively common compared with other samples of fine grained granitoids. Quartz is uncommon as only a few grains were noted in the sample. The most common mineral in this sample alkali-feldspar occurs as well-preserved, subhedral to anhedral grains with tartan twinning or perthite unmixing. The grains have inclusions of sericite. Larger feldspar grains adjacent to vugs has edges overgrowth of secondary minerals. Plagioclase is the next most abundant mineral and is strongly altered to sericite. Within the areas of most intense sericitisation are coarser muscovite grains. Plagioclase stained with Fe oxides are common. Lamellae twinning can barely be observed in the grains. Biotite in the sample are anhedral, common forming aggregates and are dark brown to black. Grains with greenish tint to them exist also. Adjacent tiny muscovite grains are common to the biotite. Opaque areas interlink with biotite aggregates exist throughout the sample. Those areas are partly containing tiny grains of Fe-oxides. Green-yellow coloured anhedral mineral with no pleochroism or appears cleavage, 2[nd] order birefringence is common secondary infill mineral. Fine red-brown coloured mineral with tabular form forming aggregates most likely albite.

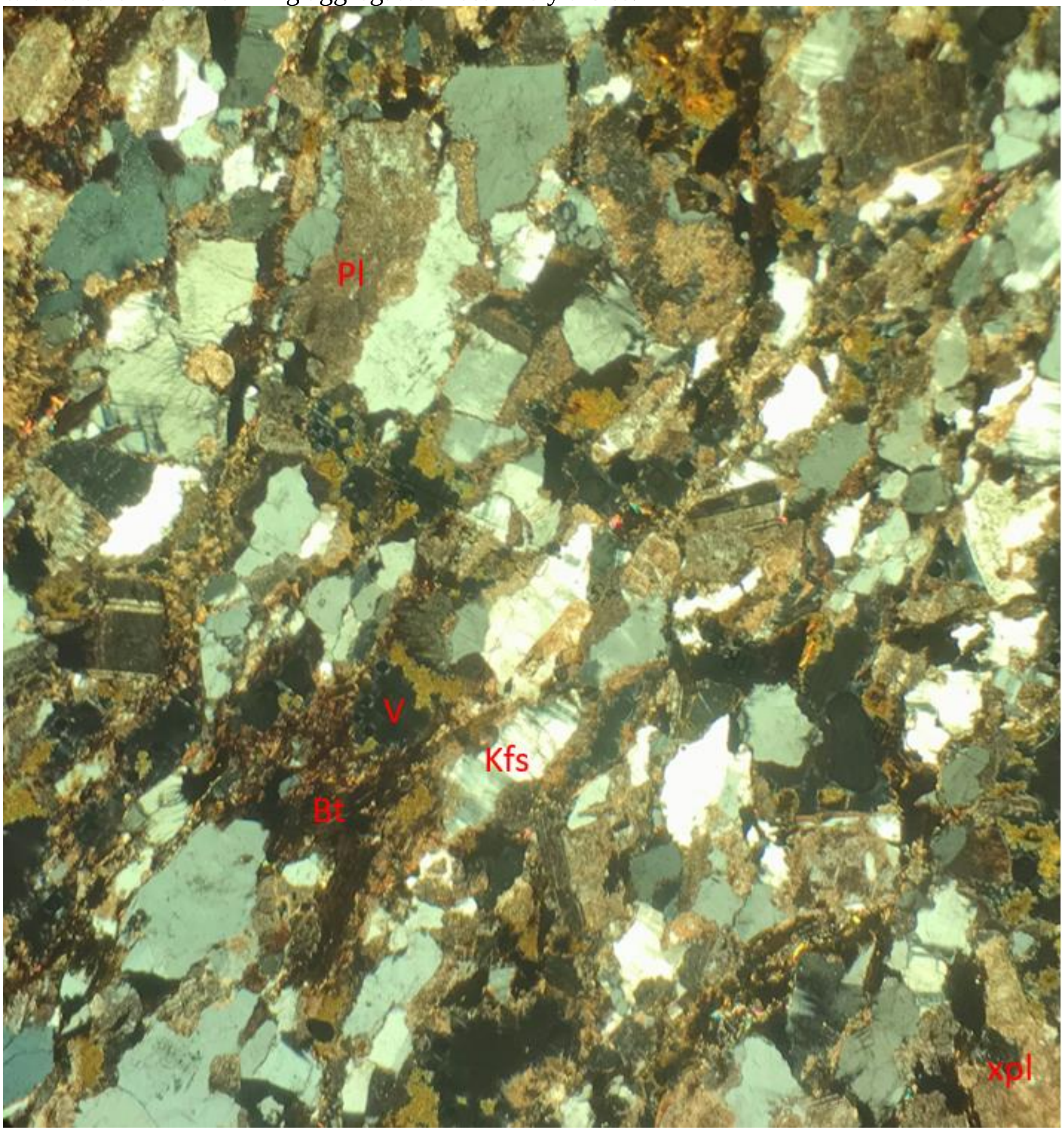

Figure 54 photo (X2.5) overall minerology of the sample. larger feldspar grains with an overall direction.

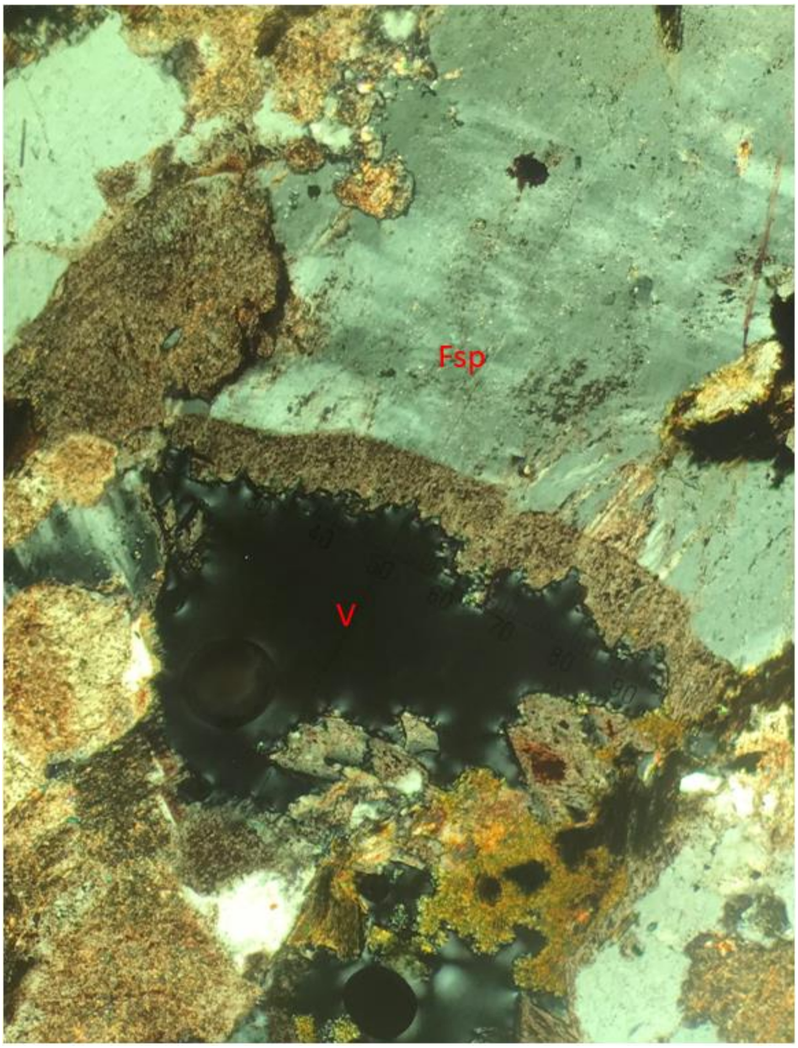

Figure 55 photo (X10) in centre a vug and north side a large feldspar grain with mineral overgrowth on the edge.

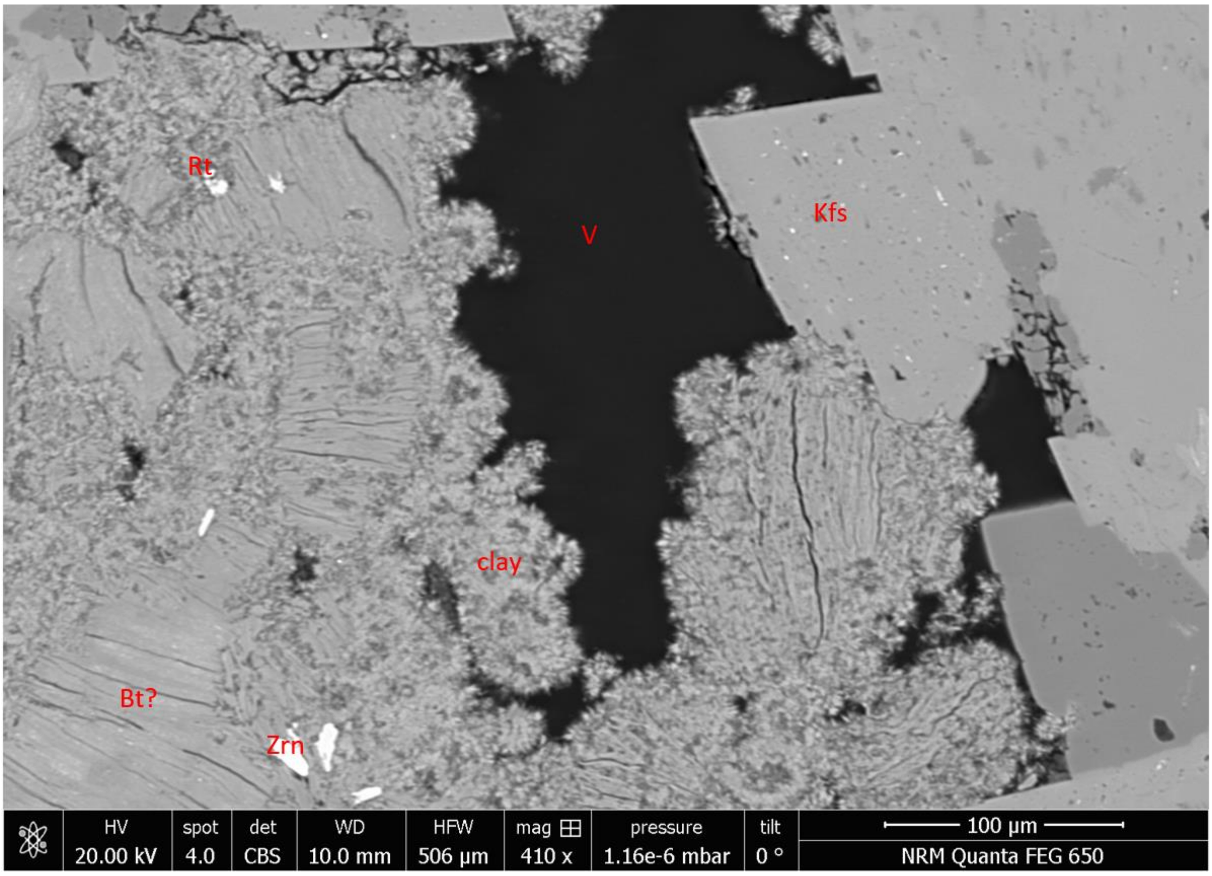

Figure 56 SEM photo. Vug in the middle and biotite that are breaking down to clays.

Sample 374sk39.8

Mineralogy: Kfs (30%), Pl (20%), Bt (5%)

The sample is medium grained with feldspars up to 5 mm wide. It is heavily weathered and fractured and contains proportions of vugs in variable size and shape. The walls of the vugs have an infill of a red brown dusty mineral. The most common mineral in this sample is Alkali-feldspar which occurs as well-preserved, subhedral to anhedral grains with tartan twinning or perthite unmixing. The grains have inclusions of sericite. Plagioclase is the next most abundant mineral and is strongly altered to sericite. Within the areas of most intense sericitisation are coarser muscovite grains and are stained with Fe-oxides. Lamellae twinning can barely be observed in the grains. Biotite is minor and forms anhedral grains that are spread out in the sample. Most of the biotite grains are black and only weak pleochroism is seen in the browner to greener part of the grains, and they show low II-order interference colours only in the non-black parts of the grains. Accessory minerals are epidote, Ti-bearing minerals, chlorite, and opaque minerals. The sample contains a large abundance of vugs that have irregular shape, and several contain secondary mineral infill on the walls. The most common secondary mineral is goethite that have a dark red brown colour and tabular form occurring commonly in aggregates. Tooth shaped colourless low birefringence minerals also fill the vugs wall. These commonly have twinning and exsolution lamellae and are interpreted to be feldspar. The shape of the grains indicate that they are secondary and grew into space once the vugs had been developed.

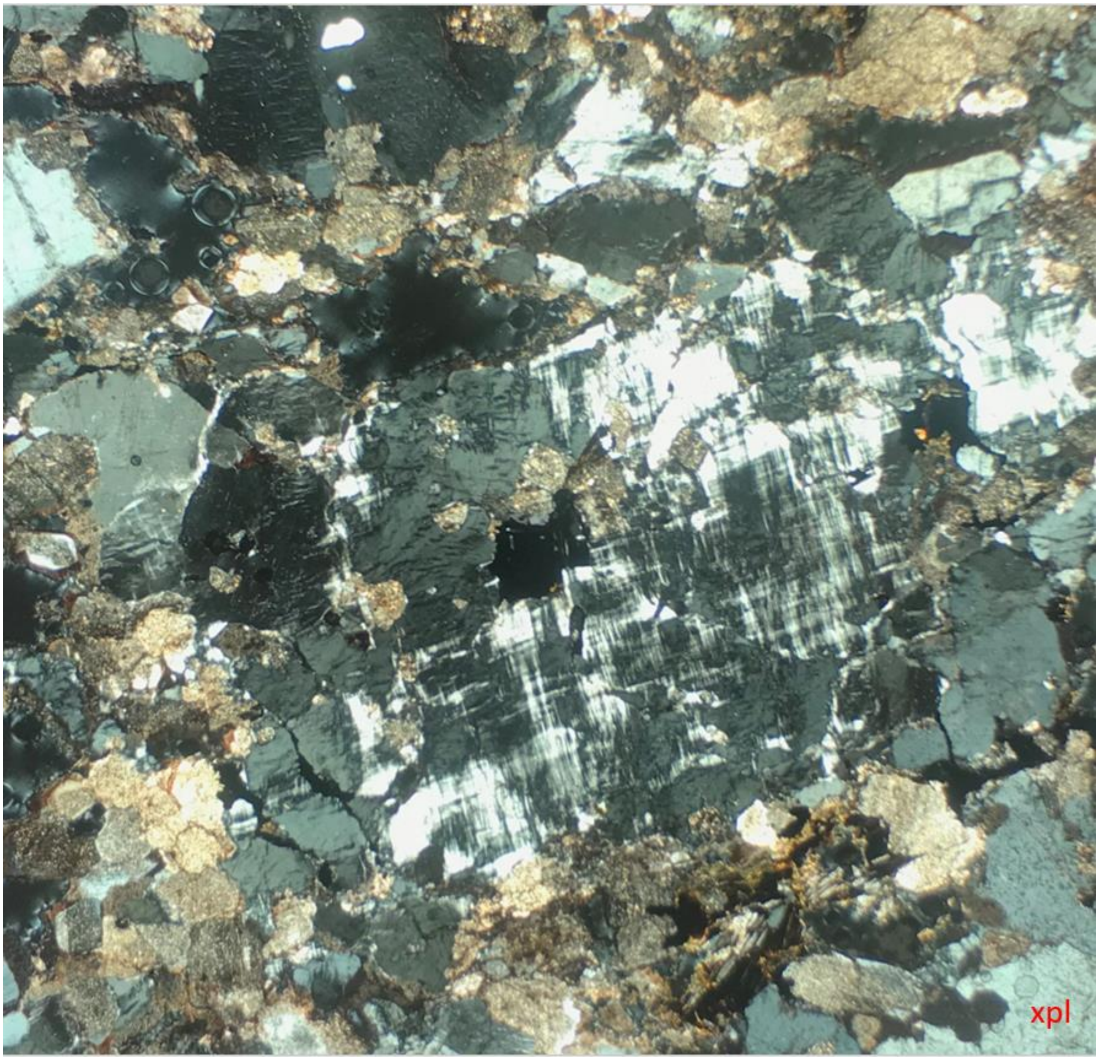

Figure 57 photo (X2.5) overview of the minerology in the sample. larger better-preserved k-feldspar with tartan twinning, smaller sericite plagioclase, and vugs of variable sizes.

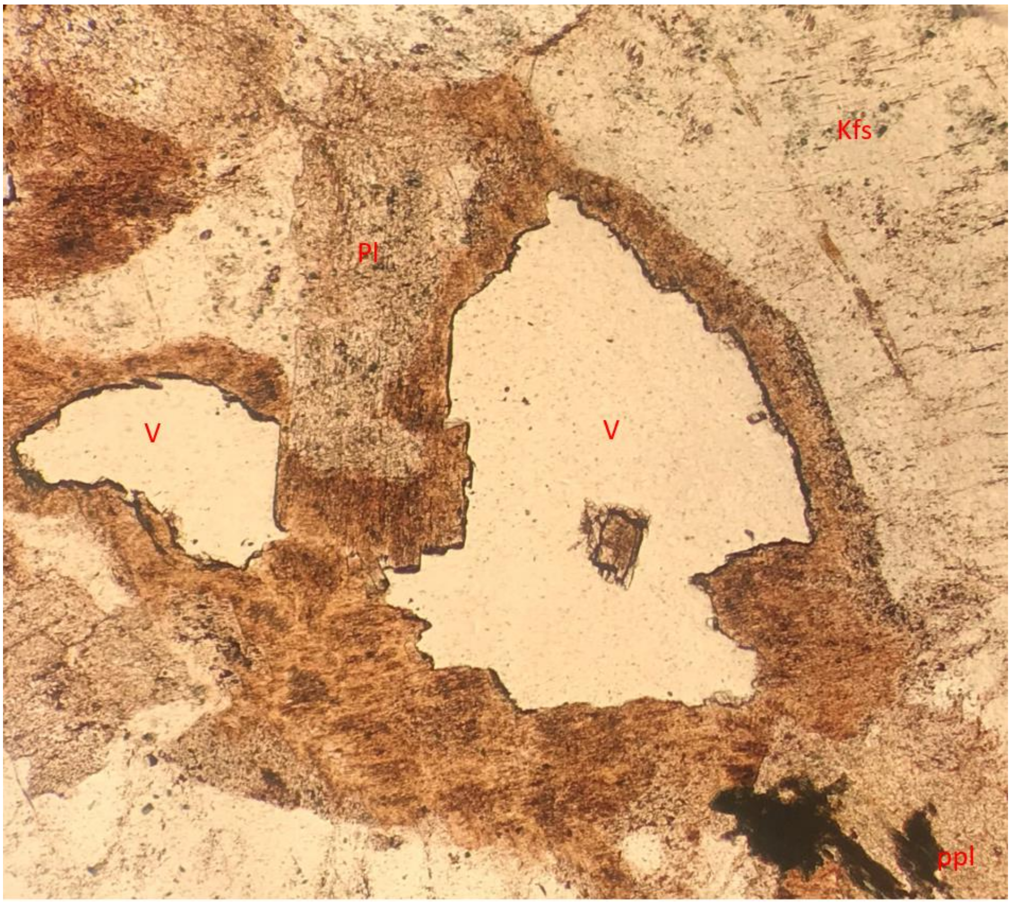

Figure 58 photo (X10) vug in the centre sounding by feldspars with overgrowth of secondary mineral.

Sample 374sk41.85

Minerology: Pl (20%), Kfs (15%).

The sample as an intergranular texture with feldspars up to 1 cm wide. It is heavily weathered and consists of both open fractures and sealed ones. A large proportion of vugs also exist, which commonly have infilled rims with a red brown dusty mineral. The most common mineral in this sample is plagioclase which occurs as anhedral grains that either are strongly altered to sericite or have clear lamellae twinning with sericite inclusions. Plagioclases tend to also be stained with Fe-oxide. K-feldspar, which is the next most abundant, occurs as better preserved subhedral to anhedral grains with tartan twinning or perthite unmixing. The grains have inclusions of sericite. Other minerals are black fibrous minerals with irregular shape and size, usually muscovite grains are present in the back mass or adjacent to it. An unidentifiable mineral has been observed which has the following properties; it is opaque with an elongated shape, with relic of feldspar inside the main body. The sample contains a large abundance of vugs that have irregular shape. Walls of the vugs contain secondary mineral infill. The most common secondary mineral is goethite which has a dark red brown colour and tabular form occurring commonly in aggregates. Minor colourless low birefringence minerals also fill the walls. These commonly have twinning and exsolution lamellae and are interpreted to be feldspar (adularia). The shape of the grains indicate that they are secondary and grew into space once the vugs had been developed.

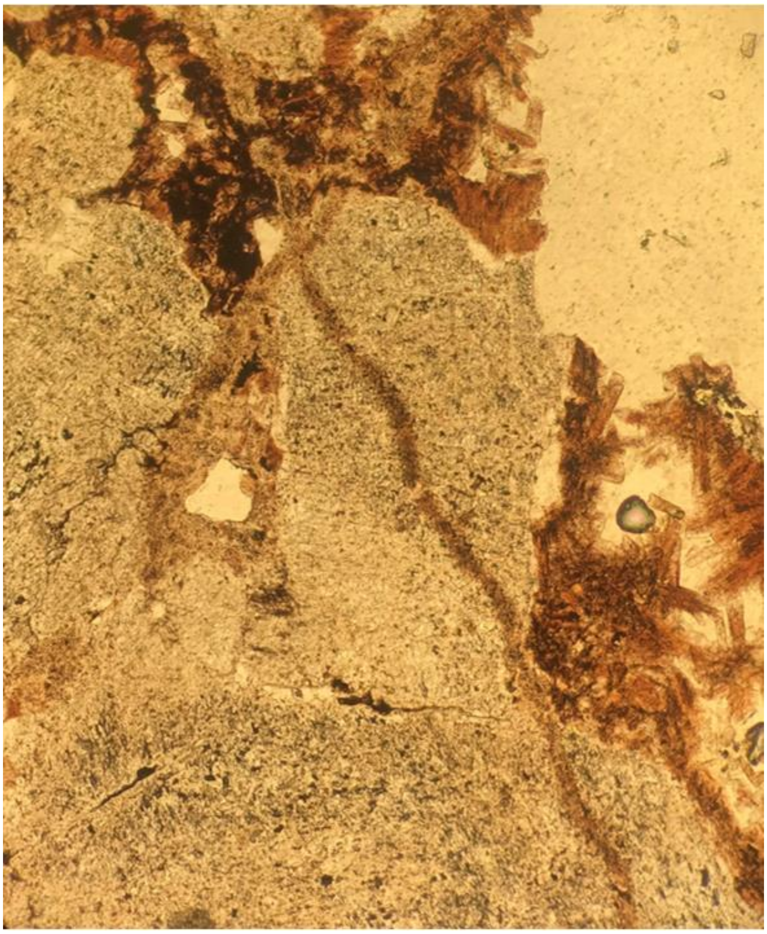

Figure 59 photo (X10) sericite plagioclase with a sealed fractured crossing the grain.

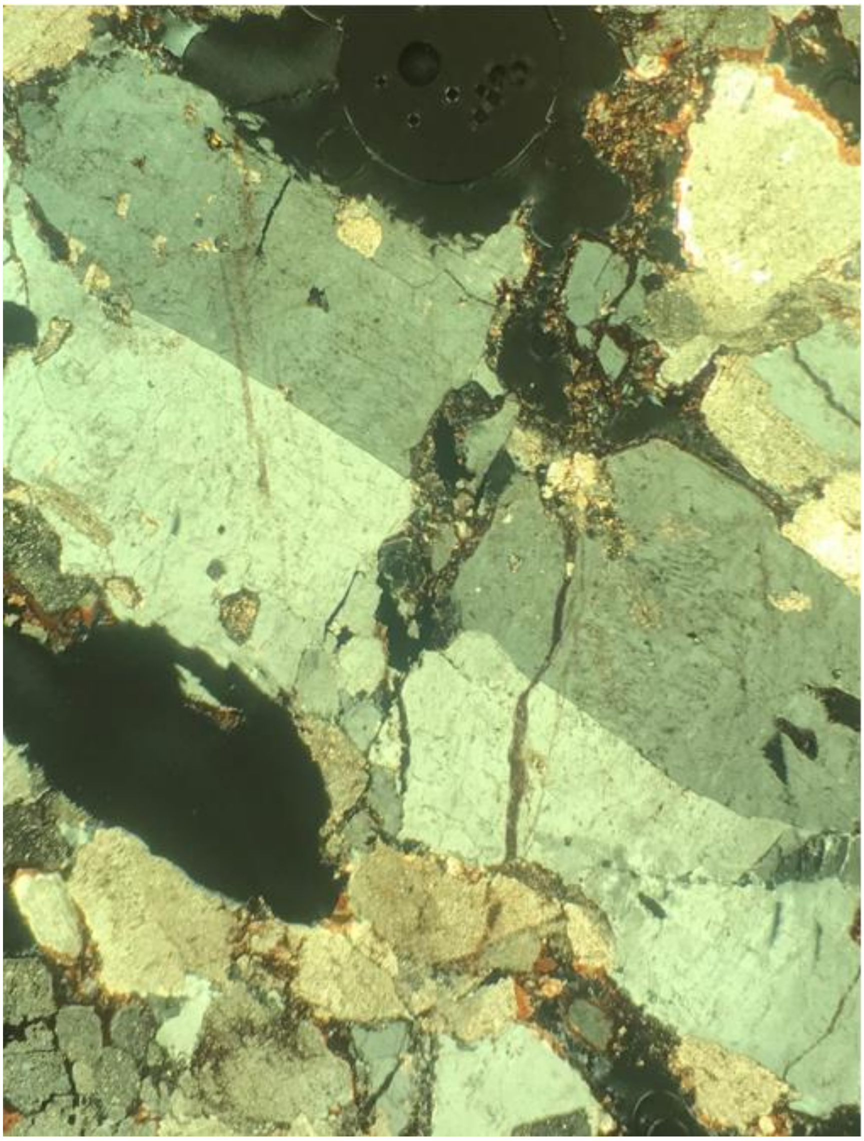

Figure 60 photo (X2.5) large k-feldspar grain that has been fractured in the middle.


Figure 61 photo (X20) black fibrous mineral, tiny muscovite is present on the south edge.

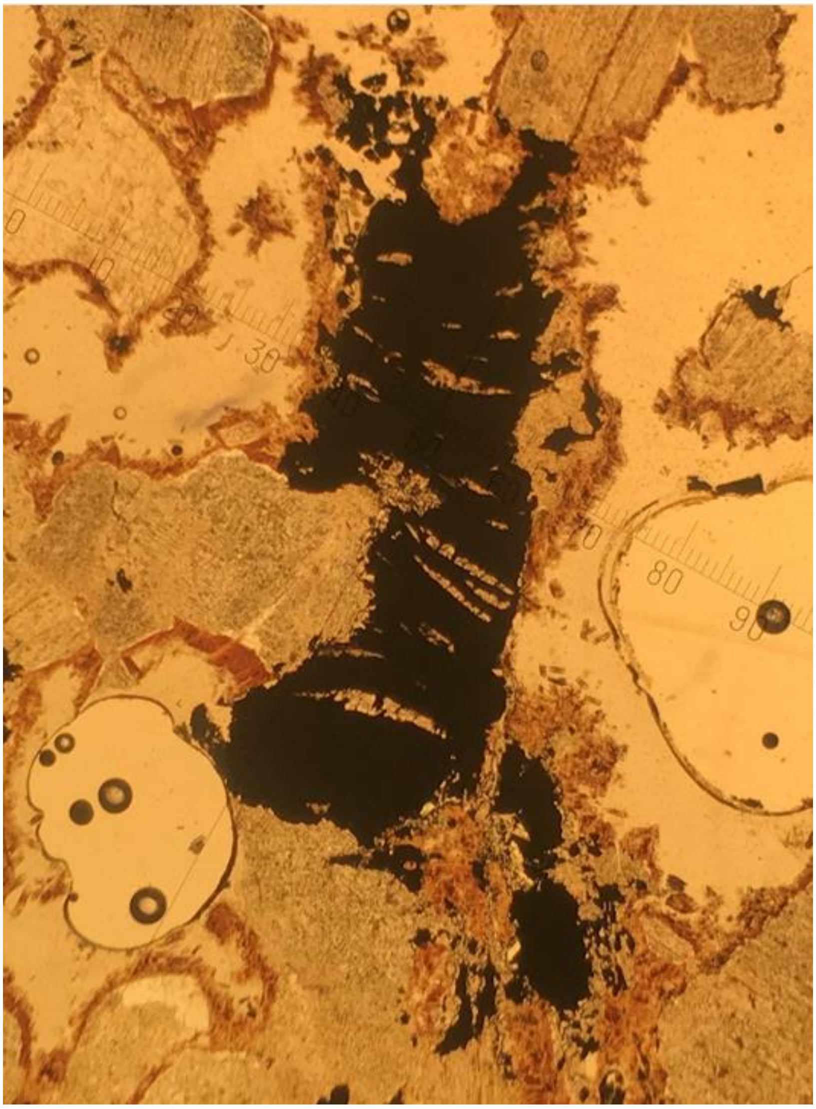

Figure 62 photo (X2.5) opaque mineral, with tiny rests of feldspars inside.

Sample 374sk 41.95

Mineralogy: Kfs (35%), Pl (30%), BK mineral (7%)

The sample has variable grain sizes with k-feldspars up to 7 mm wide. It is heavily weathered and fractured and contains a large proportion of vugs, which are not infilled with minerals. The most common mineral in this sample is Alkali-feldspar which occurs as larger better-preserved, subhedral to anhedral grains with tartan twinning or perthite unmixing. The grains have inclusions of sericite. Plagioclase is the next most abundant mineral and is strongly altered to sericite. Within the areas of most intense sericitisation are coarser muscovite grains. Lamellae twinning can barely be observed in the grains. The sample contains a large amount of anhedral black minerals with variable size and shapes. Muscovite can be seen inside or on the edges of this black mineral. Accessory minerals are epidote and Ti-bearing minerals. The sample contains a large abundance of vugs that have irregular shape that do not contain any mineral infill.

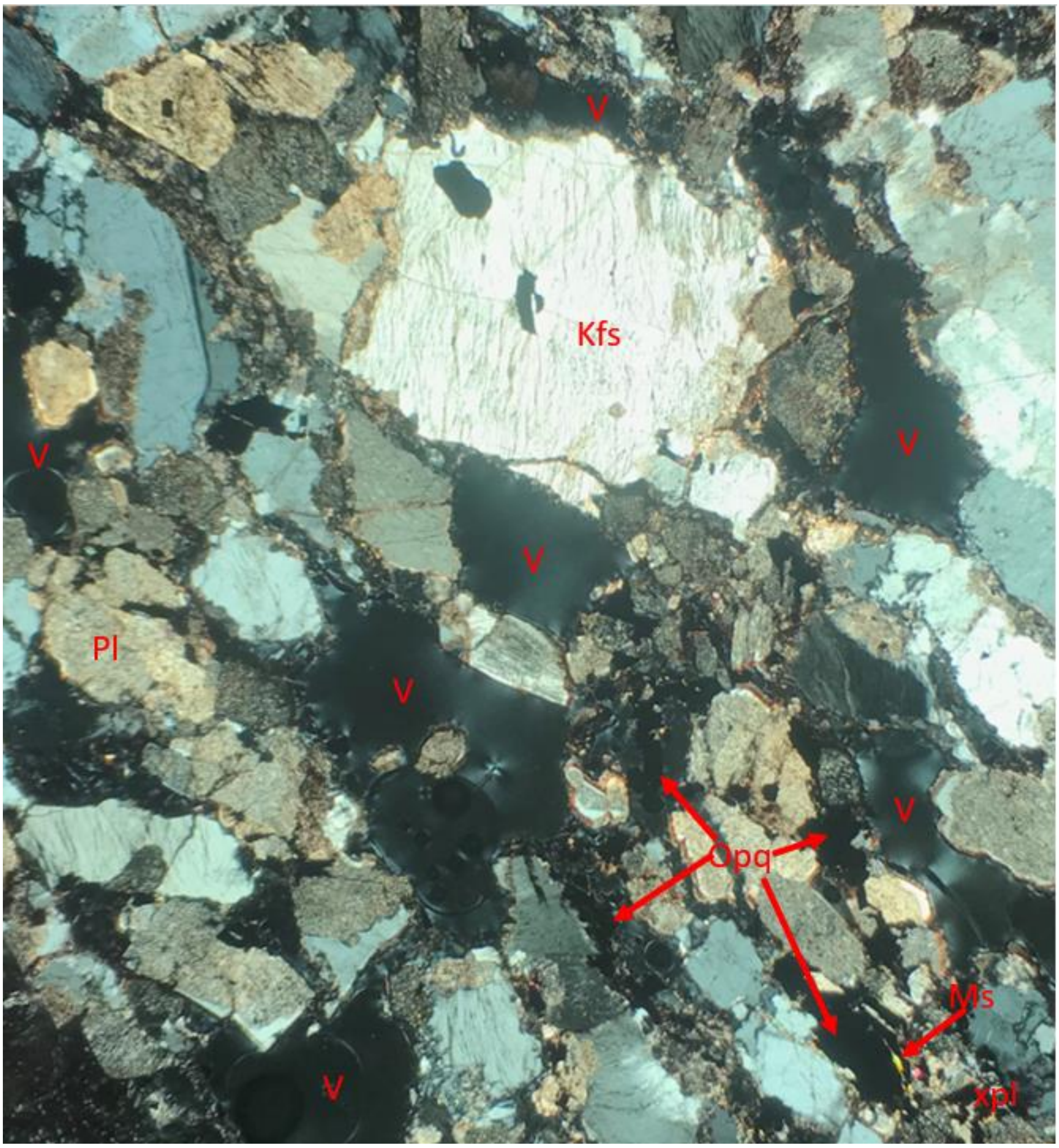

Figure 63 photo (X2.5) general minerology in the sample.

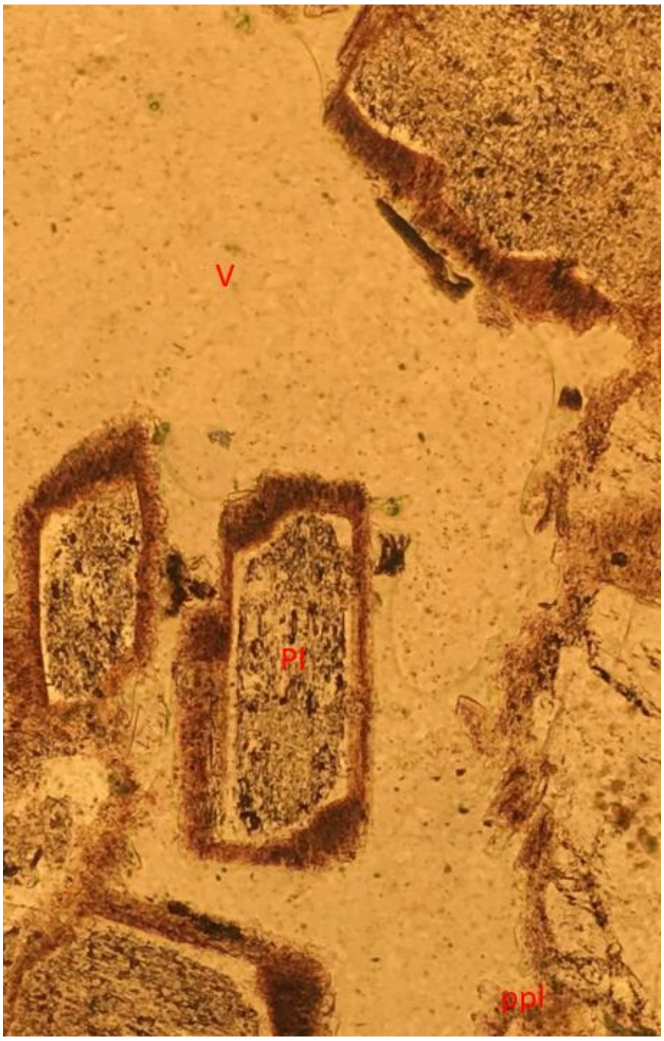

Figure 64 Photo (X10) a vug in the sample with plagioclase grains that has its red edges presumably albite.

Sample 374sk43.2

Mineralogy: Kfs (30%), Pl (20%), Bi (15%), Qz (10%).

The sample is generally equigranular apart from some coarser feldspar grains that can be up to 8 mm wide. Bands of biotite aggregates occurs. The sample is weathered and minor vugs appear sporadically. The most common mineral in this sample is Alkali-feldspar which occurs as well-preserved, subhedral to anhedral grains with tartan twinning or perthite unmixing. The grains have inclusions of sericite. Plagioclase is the next most abundant mineral and larger grains is strongly altered to sericite compared with smaller grains they are less altered. Larger plagioclases are stained with Fe-oxides. Biotite and minor chlorite form foliated bands and aggregates in the sample. Quartz grains exist in patches of variable size through the sample or as thin veins, individual grains do not display undulose extinction. Ti-bearing minerals are also seen in the sample. Vugs in the sample are few and rarely have mineral infill. Feldspars closest to the vugs have been overgrown with new feldspars, presumably adularia. Goethite exists between feldspars grain boundaries and as sealed cracks in feldspars and as infill on the wall of the vugs. Anhedral epidote as a secondary infill between grains can be seen as well.

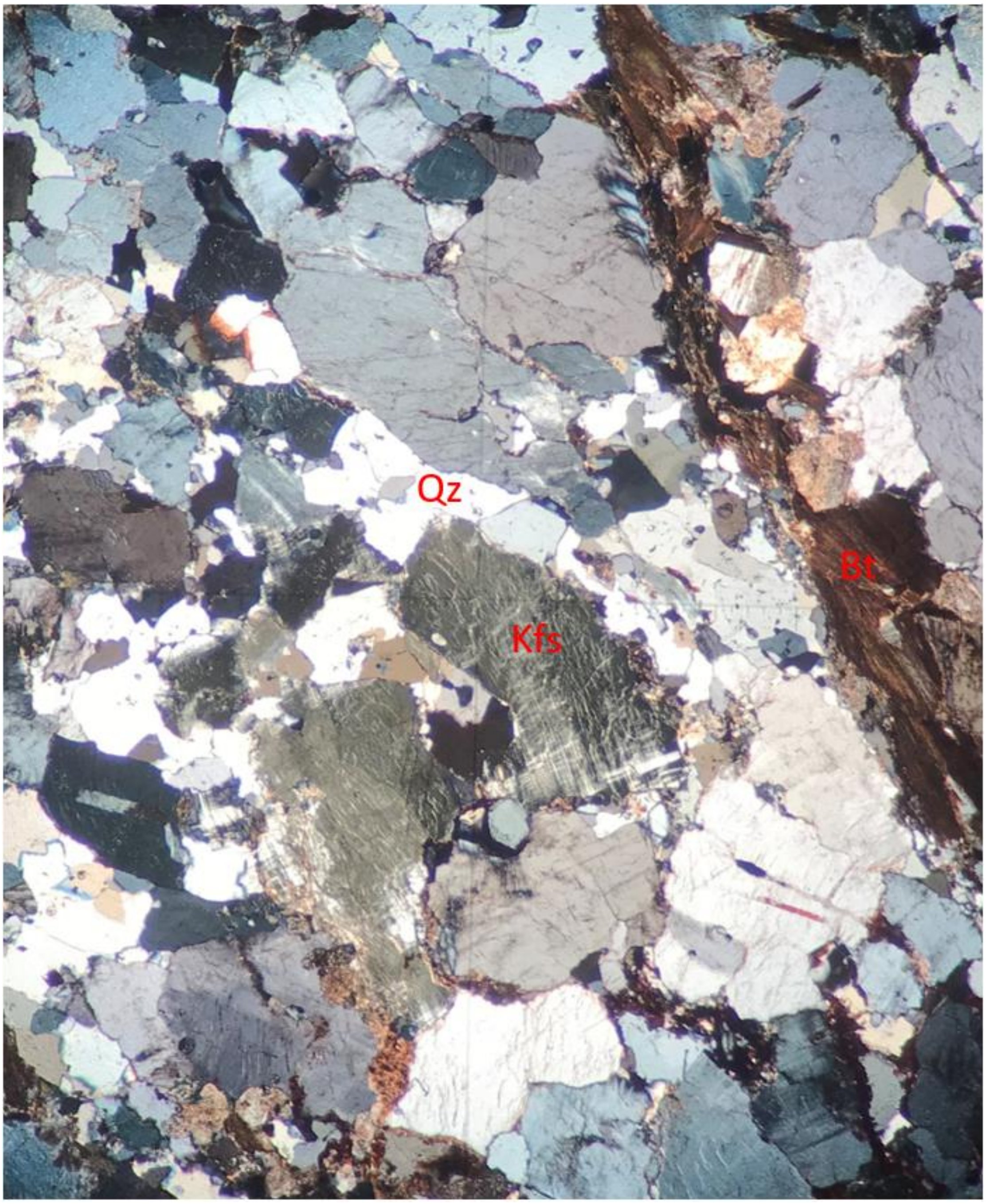

Figure 65 photo (X2.5) over a part of the thin section displaying some of the minerology

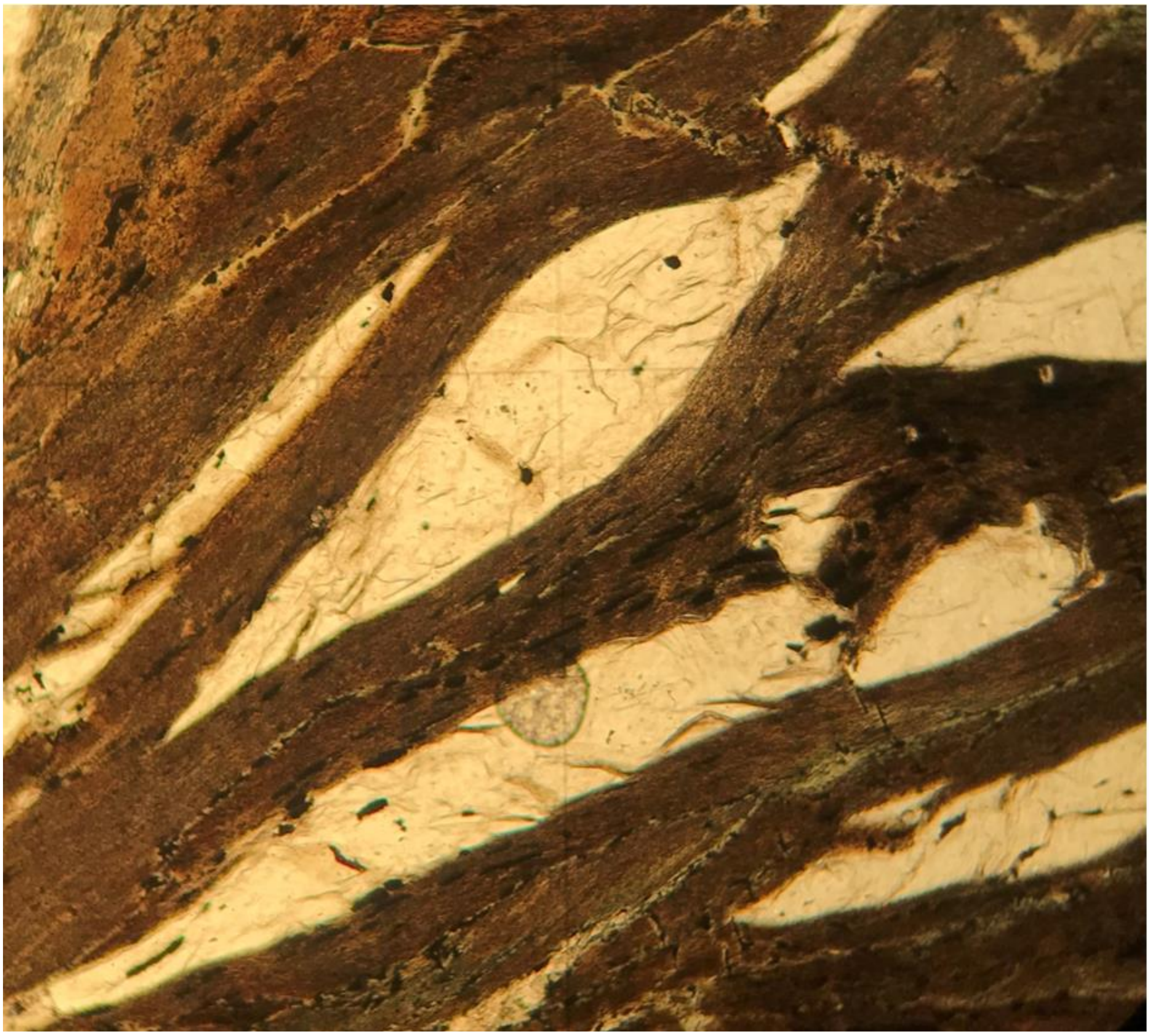

Figure 66 photo (X10) deformed biotite grains around a (feldspar/quartz) mineral.

Sample 374sk47.75

Mineralogy: Fsp (60%), Qz (20%), Bt (10%)

The sample is coarse grained with feldspars up to 8 mm wide. It is heavily weathered and fractured and contains sealed cracks which are commonly infilled with an opaque/black mineral. The most common mineral in this sample is plagioclase-feldspar which forms larger subhedral to anhedral interlocking grains that are altered to sericite. Within the areas of most intense sericitisation are coarser muscovite grains. Grains are commonly stained with Fe-oxides. Lamellae twinning can be observed in the grains. Quartz is the next most abounded mineral. It forms large patches or veins of subgrains of variable size and shape that have been recrystallised and have undulose extinction. Biotite forms aggregates or clusters pervasive through the sample. Several of the biotite has been chloritised. Accessory minerals: opaque minerals and epidote. Numerous of sealed cracks occur in the sample. Most of them have a black mineral infill that are weak dark red brown towards the edges. Other infill minerals are quartz, micas, and chlorite.

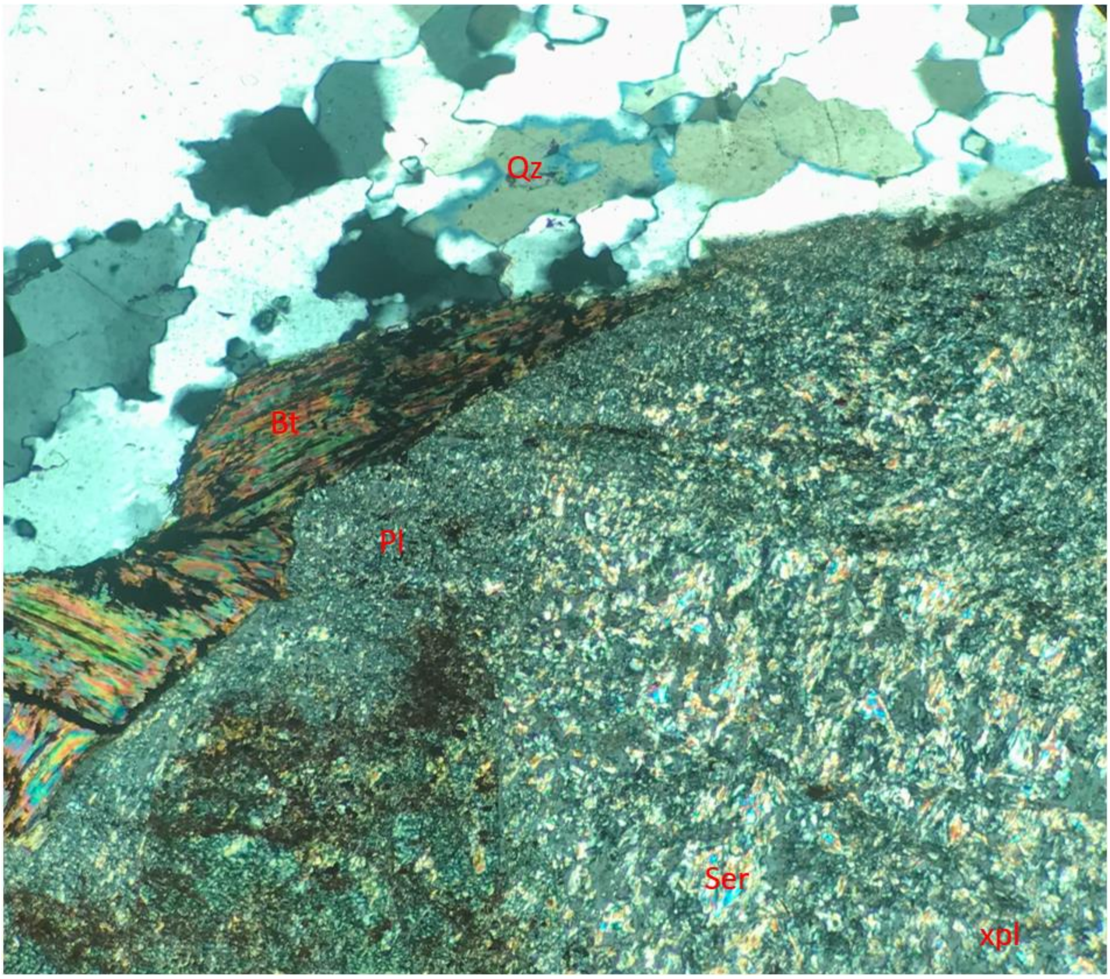

Figure 67 photo (X10) main minerology, note the large plagioclase that is altered to sericite.

Sample 374sk53.75

The sample is fine grained with grains up to 2 mm wide. It is heavily weathered and deformed with grains display interlocking boundary. The most common mineral in this sample are green minerals. Amphiboles are extremely weather and most of the grains has been altered to chlorite. Chlorites appear both as alteration from amphibole minerals and as euhedral minerals. Plagioclases are complete sericitisied, and some plagioclases are stained with Fe-oxides. A quartz vein is crossing the sample and it consists of subgrains with undulose extinction. Accessory minerals are epidote, calcite, apatite, Ti-bearing minerals, and opaque minerals.

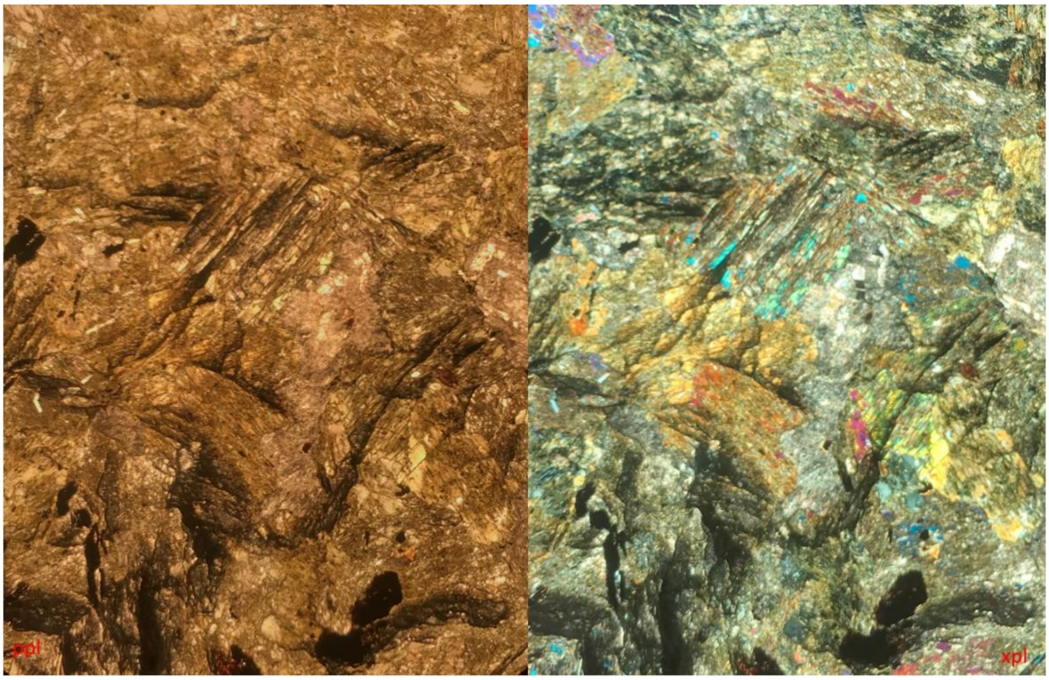

Figure 68photo (X10) displaying the general minerology in the sample.

Point counting

Down below follows the full tables from each sample that has been point counted. They contain; sample name, step length used for that sample, number of counts done and the total amount of counted lines. P = individual counting points done, % = what percentage that correspond to. 1σ is the standard error (eq. 2) for the point count based on Plas and Tobi (1965). 2σ to get the 95% confidence interval.

$$1\sigma_{mineral\ X} = \sqrt{\frac{mode_{mineral\ X}(\%)*(100-mode_{mineral\ X}(\%))}{number\ of\ total\ counts}} \quad (2)$$

374sk30.15						
steplength (mm)	*count*	*total lines*	p	%	1σ	2σ
2	157	9				
Kfs			24	15.3	2.9	5.7
Pl			41	26.1	3.5	7.0
Vug			11	7	2.0	4.1
Vug + infill			73	46.5	4.0	8.0
Bt			0	0	0.0	0.0
Chl			8	5.1	1.8	3.5
Qz			0	0	0.0	0.0
Secondary minerals			0	0	0.0	0.0
Other minerals			0	0	0.0	0.0

374sk30.5						
steplength (mm)	*count*	*total lines*	p	%	1σ	2σ
2	136	8				
Kfs			18	13.2	2.9	5.8
Pl			48	35.3	4.1	8.2
Vug			5	3.7	1.6	3.2
Vug + infill			65	47.8	4.3	8.6

Bt			0	0	0.0	0.0
Chl			0	0	0.0	0.0
Qz			0	0	0.0	0.0
Secondary minerals			0	0	0.0	0.0
Other minerals			0	0	0.0	0.0

374sk30.7						
steplength (mm)	*count*	*total lines*	p	%	1σ	2σ
2	193	11				
Kfs			164	85	2.6	5.1
Pl			1	2.1	1.0	2.1
Vug			4	2.1	1.0	2.1
Vug + infill			23	11.9	2.3	4.7
Bt			0	0	0.0	0.0
Chl			0	0	0.0	0.0
Qz			0	0	0.0	0.0
Secondary minerals			1	0.5	0.5	1.0
Other minerals			0	0	0.0	0.0

374sk30.9						
steplength (mm)	*count*	*total lines*	p	%	1σ	2σ
1	585	18				
Kfs			261	44.6	2.1	4.1
Pl			65	11.1	1.3	2.6
Vug			29	5	0.9	1.8
Vug + infill			84	14.4	1.5	2.9
Bt			11	1.9	0.6	1.1
Chl			0	0	0.0	0.0
Qz			0	0	0.0	0.0
Secondary minerals			111	19	1.6	3.2
Other minerals			24	4.1	0.8	1.6

374sk31.4						
steplength (mm)	*count*	*total lines*	p	%	1σ	2σ
1	446	15				
Kfs			159	35.7	2.3	4.5
Pl			122	27.4	2.1	4.2
Vug			1	0.2	0.2	0.4
Vug + infill			2	0.4	0.3	0.6
Bt			19	4.3	1.0	1.9
Chl			0	0	0.0	0.0
Qz			59	13.2	1.6	3.2
Secondary minerals			42	9.4	1.4	2.8
Other minerals			42	9.4	1.4	2.8

374sk33.3						
steplength (mm)	*count*	*total lines*	p	%	1σ	2σ

1	755	25				
Kfs			201	26.6	1.6	3.2
Pl			142	18.8	1.4	2.8
Vug			22	2.9	0.6	1.2
Vug + infill			30	4	0.7	1.4
Bt			44	5.8	0.9	1.7
Chl			0	0	0.0	0.0
Qz			129	17.1	1.4	2.7
Secondary minerals			85	11.3	1.2	2.3
Other minerals			102	13.5	1.2	2.5

374sk33.6						
steplength (mm)	*count*	*total lines*	p	%	1σ	2σ
1	581	19				
Kfs			169	21.3	1.7	3.4
Pl			124	21.3	1.7	3.4
Vug			12	2.1	0.6	1.2
Vug + infill			22	3.8	0.8	1.6
Bt			14	2.4	0.6	1.3
Chl			0	0	0.0	0.0
Qz			93	16	1.5	3.0
Secondary minerals			86	14.8	1.5	2.9
Other minerals			62	10.7	1.3	2.6

374sk33.85						
steplength (mm)	*count*	*total lines*	p	%	1σ	2σ
1	661	20				
Kfs			205	31	1.8	3.6
Pl			154	23.3	1.6	3.3
Vug			38	5.7	0.9	1.8
Vug + infill			82	12.4	1.3	2.6
Bt			41	6.2	0.9	1.9
Chl			0	0	0.0	0.0
Qz			3	0.5	0.3	0.5
Secondary minerals			73	11	1.2	2.4
Other minerals			65	9.8	1.2	2.3

SEM

SEM data is provided on request.

Stockholms universitet
SE-106 91 Stockholm
Telefon: 08 – 16 20 00
www.su.se